January 2013

The Translational Machinery as a Target for Radiosensitization

Thomas John Hayman

University of South Florida, thayman@health.usf.edu

Follow this and additional works at: http://scholarcommons.usf.edu/etd

Part of the Oncology Commons

www.manaraa.com

The Translational Machinery as a Target for Radiosensitization

by

Thomas J. Hayman

A dissertation submitted in partial fulfillment
of the requirements for the degree of
Doctor of Philosophy
Department of Molecular Medicine
College of Medicine
University of South Florida

Co-Major Professor: Philip J. Tofilon, Ph.D.
Co-Major Professor: Robert J. Deschenes, Ph.D.
Michael J. Barber, D.Phil.
Srikumar P. Chellappan, Ph.D.
Peter G. Medveczky, M.D.

Date of Approval:
May 15, 2013

Keywords: eIF4E, S6K, mTOR, mRNA Translation, Radiosensitization

ACKNOWLEDGMENTS

I would like to thank my advisor Dr. Phil Tofilon for the scientifically rigorous training that he has provided me over the past several years. This training will provide an excellent foundation for my continuing scientific career. Secondly, I would like to thank the other members of my lab, as their discussions and guidance have been extremely valuable to me. Furthermore, I would like to thank the Radiation Oncology Branch at the National Cancer Institute for providing me with a great environment to learn and grow as a scientist. The University of South Florida Morsani College of Medicine has been vital in helping me to achieve the goal of obtaining a Ph.D. My family's support has truly been a blessing and has allowed me to persevere. Lastly, I would like to thank Ashley Loveless, who has been my foundation throughout this journey.

TABLE OF CONTENTS

LIST OF TABLES

LIST OF FIGURES

ABSTRACT

Current approaches aimed at improving the efficacy of radiation as a cancer treatment modality involve the development and application of molecularly targeted radiosensitizers, a strategy that requires a thorough understanding of the fundamental processes comprising the cellular radioresponse. Recent data indicating that radiation modifies gene expression primarily through translational control rather than transcriptional events suggests that mRNA translation contributes to cell survival after irradiation. The overall goal of this project is to determine whether the regulatory/rate-limiting components of the translational machinery provide targets for tumor cell radiosensitization. The majority of translation in mammalian cells occurs in a cap-dependent manner and is highly dependent on eIF4E. As such, we investigated a regulatory role for eIF4E in cellular radiosensitivity. eIF4E knockdown enhanced the radiosensitivity of tumor but not normal cells. eIF4E knockdown inhibited the dispersal of radiation-induced γH2AX foci. Furthermore, radiation was found to increase the binding of >1000 unique mRNAs to eIF4E, many involved in DNA replication, recombination, and repair. S6 kinase 1 (S6K1), also an important regulatory component of the translational machinery, enhances the translation of specific mRNA subpopulations, independent from eIF4E, and mediates ribosome biogenesis. The role of S6K1 in determing cell survival after radiation was determined in several tumor cell lines

and one normal cell line. S6K1 knockdown enhanced the radiosensitivity of all 3 tumor lines. In contrast S6K1 knockdown had no effect on the cellular radiosensitivity of the one normal line tested. The mechanistic target of rapamycin (mTOR) is a critical kinase in the regulation of gene translation and has been suggested as a potential target for radiosensitization. Importantly, it plays a major role in regulating eIF4E availability as well as S6K1 activity. The radiosensitizing activities of the allosteric mTOR inhibitor rapamycin with that of the ATP competitive mTOR inhibitor PP242 were compared. Based on immunoblot analyses, whereas rapamycin only partially inhibited mTORC1 activity and had no effect on mTORC2, PP242 inhibited the activity of both mTOR containing complexes. In the two tumor cell lines evaluated, PP242 treatment 1h before irradiation increased radiosensitivity, whereas rapamycin had no effect. PP242 had no effect on the cellular radiosensitivity of a normal lung fibroblast line. PP242 exposure did not influence the initial level of γH2AX foci after irradiation, but did significantly delay the dispersal of radiation-induced γH2AX foci. Finally, PP242 administration to mice bearing U251 xenografts enhanced radiation-induced tumor growth delay. A next generation analog of PP242, INK128, is currently undergoing analysis in clinical trials. Given our data showing ATP-competitive mTOR inhibition is a strategy for tumor radiosensitization as well as the fact that radiotherapy is a primary treatment modality for locally advanced pancreatic ductal adenocarcinoma, the effects of INK128 on pancreatic cancer radiosensitivity were determined. In three pancreatic cancer cell lines addition of INK128 immediately after radiation resulted in radiosensitization. Consistent with the effects of PP242 on other cell lines, INK128 exposure did not influence the initial level of γH2AX foci after irradiation, but did significantly delay the dispersal of radiation-

induced γH2AX foci. Furthermore, in pancreatic tumor xenografts INK128 inhibits mTOR activity as well as cap-complex formation in a time-dependent manner. Lastly, INK128 treatment significantly prolonged the radiation-induced tumor growth delay of pancreatic tumor xenografts. In summary, the data provided in this thesis have begun to characterize the role of the translational machinery in determining the cellular response to radiation.

CHAPTER 1:

Introduction

It is estimated in 2013 that there will be approximately 1.6 million non-skin cancers diagnosed in North America (cancer.org), of which approximately 75% of these patients will receive radiotherapy at sometime during their treatment course. As radiotherapy continues to be a primary treatment modality for the majority of patients undergoing cancer therapy, the development of strategies to improve its efficacy could benefit a large number of patients. This has led to an emphasis upon the development of molecularly targeted radiosensitizers, a strategy that requires a thorough understanding of the mechanisms mediating cellular radioresponse. Along these lines, radiation-induced post-translational modifications of existing proteins (e.g. phosphorylation and ubiquitination) have been the subject of extensive investigation. These modifications have been linked causally to cellular radiosensitivity and play important roles in the DNA damage response (DDR) and signal transduction pathways. As such, these modifications have provided a rich source of potential targets for radiosensitization. Additionally, as radiation has previously been shown to induce changes in the transcription of numerous genes, the modulation of gene expression has also been thought to play a role in the cellular radioresponse. That is, similar to prokaryotes radiation-induced changes in gene expression in mammalian cells may constitute a protective or adaptive response against radiation-induced cell death. As such, it has been generally thought that defining the inducible genes as well as the mechanisms governing their expression may provide not

1

only novel insight into the fundamental radioresponse, but may also lead to the identification of targets for radiation sensitizers.

To examine the radiation-induced control of gene expression numerous studies have published results of various analyses of total cellular mRNA (e.g. northern, RT-PCR and microarray) in a number of normal cells and tissue as well as for tumor cell lines grown both *in vitro* and *in vivo* (1-6). However, comparison of these changes in the transcriptome reveals few commonly affected genes among the cell types evaluated or even among tumor cell lines originating from tumors of identical histologic origin. In addition, whereas these analyses accurately reflect changes in mRNA abundance, the radiation-induced changes in mRNA levels do not correlate with changes in the corresponding protein product. While there are exceptions involving individual genes (2), the majority of radiation-induced changes in mRNA abundance have not been extended to the protein level. Along these lines, Skanderová et al. directly compared radiation-induced proteins with their corresponding mRNAs and reported no correlation for the 10 proteins evaluated (7). As protein expression is the functional and operational end product of gene expression, the lack of correlation between radiation-induced changes in mRNA abundance and protein expression, as well as the established heterogeneity among the cell lines, it is difficult to assign a functional consequence to radiation-induced gene expression. Consistent with the aforementioned findings Birell et al. showed that after irradiation of yeast, there was little to no relationship between radiation radiation-induced transcriptional changes and survival after irradiation (8).

A fundamental assumption of these analyses is that radiation-induced changes in gene expression are primarily the result of modifications in transcription. However, in

2

addition to transcription, numerous post-transcriptional processes contribute to the control of gene expression. In contrast to prokaryotic cells, mammalian transcription and translation are not directly coupled, with each event confined to separate cellular compartments (nucleus versus cytoplasm; Figure 1). Consistent with this uncoupling, there is a poor correlation between changes in mRNA abundance and protein expression in eukaryotic cells exposed to a number of types of stress (9-12). Furthermore even under basal growth conditions the agreement between mRNA and protein expression profiles was shown to be at best 65% in a study paneling the NCI-60 cell lines (13). Accounting for the discrepancy between the transcriptome and the proteome is translational control (14-16), which has been shown to play an important role in regulating gene expression during such fundamental processes as embryogenesis (17), T-cell activation (18), growth factor signaling (19), and tumorigenesis (20).

More recent studies have begun to define the effects of radiation on translational control (21-22). The initiation of translation involves the recruitment of mRNAs to polyribosomes (polysomes), and as such the association of a given mRNA with polysomes can then be used as an indicator of translational activity (15). To perform global profiling of mRNAs undergoing translation (the translatome) these studies employed microarray analysis of polysome-bound mRNA after radiation in a several cell lines and these results were compared to radiation-induced changes in the transcriptome. A study from our laboratory initially focused on the U87 glioma cell line and showed that radiation affects ~10 fold more genes at the translational level than on the transcriptional level (22). Furthermore, there was no overlap between genes affected translationally and transcriptionally in U87 cells (22). Important with regards to functional consequence, a

3
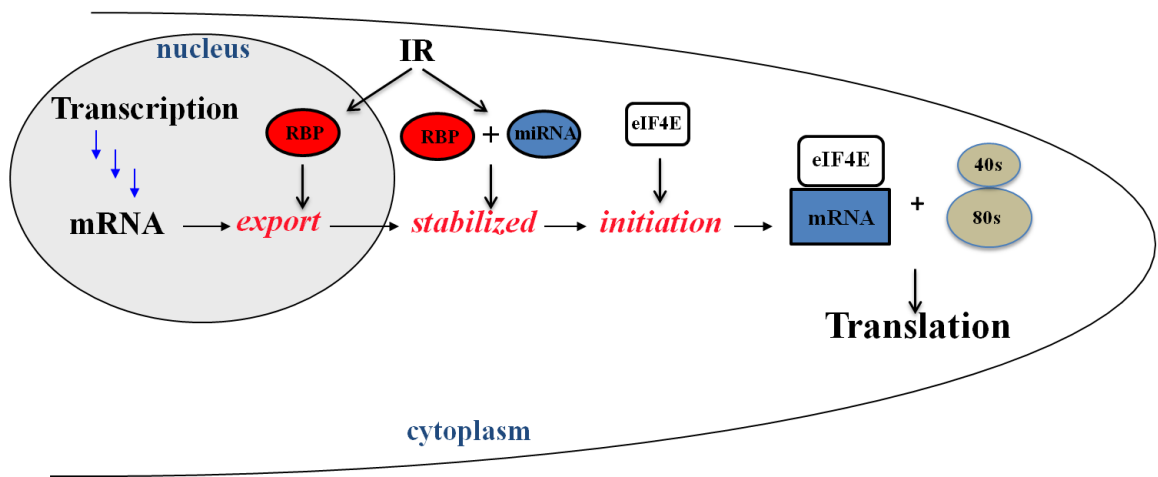
Figure 1: Post-transcriptional regulation and radiation.

correlation between radiation-induced changes in polysome-bound mRNAs and changes in the corresponding protein product was established, with 14/16 proteins evaluated showing consistent changes in translational activity and protein expression (22). It was then further shown that radiation-induced changes in translation were similar among 3 glioma cell lines, in contrast to radiation-induced changes in the transcriptome (22).

A second study published by our laboratory extended the results of the previously mentioned study by profiling radiation-induced translational changes in a panel of 18 cell lines, comprised of both tumor and normal cell lines (21). In contrast to changes in the transcriptome, radiation-induced translational changes clustered according to the tissue of origin (e.g. pancreatic carcinoma cell lines versus glioma cell lines). Network analyses showed that the mRNAs affected at the translational level belonged to distinct functional categories and were not a random collection of genes (21). Furthermore, many of these functional categories appeared to histology-specific. Importantly, as the potential to exploit differences in tumor and normal cells is of critical importance for therapeutic application, many of the changes were exclusive to tumor or normal cells (21). Consistent with our results another laboratory has recently published analysis of polysome-bound mRNA and has shown radiation to affect the translation of numerous mRNAs that are functionally related (23). Although translational control of gene expression appears to be a component of the cellular radioresponse, whether specific molecules of the translational machinery are determinants of the cellular radiosensitivity has yet to be determined, and is the subject of this thesis.

There are numerous processes involved in the post-transcriptional control of gene expression (e.g. mRNA splicing, export, stability, and translation initiation) (24). Each of

these processes can operate independently to regulate gene expression at the post-transcriptional level. RNA-binding proteins (RBPs), of which there are > 700 in humans, play important roles in the regulation of each of the post-transcriptional processes (24). Clearly, the mechanisms mediating the translational control of gene expression are extremely complex with each step/event subject to regulation by environmental signals including potentially radiation. In fact, radiation has been shown to influence the components of the post-transcriptional gene expression infrastructure as well as the signaling pathways involved in their regulation (25-27). These processes, for the most part, culminate in translation initiation and ribosome binding, the final and rate limiting steps in mRNA translation (Figure 1) (28). Among the proteins regulating translation initiation are eIF4E and S6K (29). Furthermore, the mechanistic target of rapamycin (mTOR), which plays a major role in determining gene translation in response to environmental and oncogenic stress, regulates the availability of eIF4E and activity of S6K (29). Thus, to determine whether radiation-induced translation control of gene expression influences radiosensitivity, these specific components of the translational machinery were the focus of this thesis.

CHAPTER 2:

Methods

Cell lines and treatments: MDA-MB-231 (breast adenocarcinoma), A549 (lung adenocarcinoma) DU145 (prostate adenocarcinoma), and MRC9 (normal lung fibroblasts) were obtained from American Type Culture Collection (ATCC). U251 (glioma) cells were obtained from the Division of Cancer Treatment and Diagnosis Tumor Repository (DCTD), National Cancer Institute (NCI). Miapaca-2, Panc1, and PSN1 (all pancreatic cancer cell lines) were kind gifts from Dr. Deborah Citrin's laboratory. The cell lines were maintained in DMEM (MDA-MB-231 and U251), RPMI (A549, Miapaca-2, Panc1, and PSN1), or MEM (DU145 and MRC9) media supplemented with 10% FBS (Invitrogen, Carlsbad CA). ATCC employs short tandem repeat DNA fingerprinting, karyotyping, and cytochrome C oxidase to authenticate cell lines. Primary human mammary epithelial cells (HMEC) were obtained from GIBCO in 2010 and maintained in complete Mammary Epithelial Growth Medium (Lonza). All cells were cultured less than 6 months after resuscitation. Cell cultures were maintained in an atmosphere of 5% CO_2/95% air at 37°C. Ribavirin (Sigma-Aldrich), PP242 (Sigma-Aldrich or Chemdea) and rapamycin (EMD-Biochemicals) were dissolved in dimethyl sulfoxide. Cell cultures were irradiated using a 320 X-ray source (Precision XRay Inc.) at a dose rate of 2.3 Gy/min.

siRNA Transfection*: A pool of four siRNA duplexes (SMARTpool) targeted to eIF4E or S6K1 and a non-targeted siRNA pool (scramble) were purchased from

Dharmacon Inc (Lafayette, CO). Transfection with the respective siRNA pool was carried out with cell cultures at 60-70% confluency using Dharmafect 1 transfection reagent (Dharmacon) per manufacturer's protocol. All experiments were carried out 72 h post transfection.

Clonogenic Survival Assay: To evaluate radiosensitivity, cells were plated at clonal density in 6-well plates, allowed to attach, followed by the specified drug and/or radiation treatment protocol. 10 to 14 days after seeding, plates were stained with 0.5% crystal violet, the number of colonies determined, and the surviving fractions were calculated. Radiation survival curves were generated after normalizing for the cytotoxicity induced by eIF4E knockdown, S6K1 knockdown, rapamycin, PP242, or INK128 treatment alone. Dose enhancement factor defined as the ratio of the dose of radiation required to reduce surviving fraction to 0.1 in untreated cells to the dose of radiation required to reduce surviving fraction to 0.1 in treated cells. Data presented are the mean ± SEM from at least 3 independent experiments.

Immunoblotting and antibodies: Cells were lysed in 50mM Tris-HCl (pH 7.5), 150mM NaCl, 2mM EDTA, 2mM EGTA, 25mM NaF, 25mM β-glycerophosphate, 0.2% Triton X-100, 0.3% NP-40, and 0.1mM sodium orthovanadate (for cytoplasmic proteins), or 50mM Tris-HCL (ph 8.0), 1% SDS, and 10mM EDTA (for nuclear proteins); supplemented with 1x phosphatase inhibitor cocktails II and III (Sigma-Aldrich), and 1x HALT protease inhibitor cocktail (Thermo Scientific) for 15 minutes on ice. Total protein was quantified using BCA protein assay (Thermo Scientific); separated by SDS-PAGE; transferred to PVDF (Millipore) and probed with the indicated antibodies. Bands were visualized using Pierce ECL Western Blotting Substrate (Thermo Scientific). Anti-

eIF4E, anti-CHK1, anti-4E-BP-1, anti-phospho-eIF4E S209, anti-phospho-4E-BP-1 T37/46, anti-phospho-4E-BP-1 S65, anti-AKT, and anti-phospho-AKT s473 antibodies were purchased from Cell Signaling Technology. Anti-β-actin and anti-eIF4G antibodies were obtained from Sigma-Aldrich and BD Biosciences, respectively. Anti-Rad51 and anti-Rad17 antibodies were purchased from Santa Cruz Biotechnologies. Donkey-anti-rabbit and sheep-anti-mouse Horseradish Peroxidase conjugated secondary antibodies were purchased from GE Healthcare.

Cell Cycle Analysis: Cell cycle phase distribution was determined by flow cytometric analysis. Cells were trypsinized, fixed with 70% ethanol, stained with Guava Cell Cycle Reagent (Millipore), and analyzed with the Guava EasyCyte flow cytometer (Millipore).

Apoptotic Cell Death: Cells undergoing apoptosis were quantified according to annexin V staining (Annexin V Apoptosis Detection Kit, BD Biosciences). Briefly, for each treatment condition cells were resuspended in 1x Annexin V Binding Buffer and incubated with Annexin V-Cy5 antibody in the dark at room temperature. Hoechst 33258 was added for live/dead discrimination and samples analyzed by flow cytometry (BD Biosciences LSRII flow cytometer).

Immunofluorescent analysis of γH2AX foci: To visualize foci, cells, grown in chamber slides, were fixed with 4% paraformaldehyde, permeabilized with 0.1% Triton X-100, and blocked with 1% bovine serum albumin (BSA) in PBS containing 5% goat serum. The slides were incubated with antibody to phospho-H2AX (Millipore) followed by incubation with goat-anti-mouse-Alexa488 (Invitrogen) and mounted with Prolong

9

gold anti-fade reagent containing 4', 6-diamidino-2-phenylindole (Invitrogen) to visualize nuclei. Cells were analyzed on a Zeiss upright fluorescent microscope.

Mitotic Catastrophe: Cells, grown in chamber slides, were fixed with a 10% neutral buffered formalin solution and incubated with antibody to α-tubulin (Sigma-Aldrich) followed by incubation with goat anti-mouse with Alexa-488 antibody and mounted with Prolong gold anti-fade reagent containing 4', 6-diamidino-2-phenylindole. Cells with nuclear fragmentation, defined as the presence of two or more distinct nuclear lobes within a single cell were classified as being in mitotic catastrophe.

Cap-Binding Assay: eIF4F cap complex formation was measured using m^7-GTP batch chromatography (30). Briefly, cells were lysed in 20mM Tris-HCl (pH 7.4), 150mM NaCl, 1mM EDTA, 1mM EGTA, 1mM β-glycerophosphate, 1mM sodium orthovanadate, 1% Triton X-100, 0.2mM PMSF, 1x phosphatase inhibitor cocktails II and III (Sigma-Aldrich), and 1x HALT protease inhibitor cocktail (Thermo Scientific) for 15m on ice. 400µg of lysate were pre-cleared for 1h at 4°C then incubated with m^7-GTP Sepharose 4B beads (GE Healthcare) overnight at 4°C. Beads were washed three times with lysis buffer; bound protein was eluted, denatured, and then separated using SDS-PAGE followed by immunoblotting for eIF4G and eIF4E.

RIP-Chip and Microarray Analysis: The RIP-Chip kit and anti-eIF4E antibody were obtained from MBL International (Woburn, Ma); the procedure was performed in biological triplicate according to manufacturer's protocol. Briefly, 10^7 cells were washed followed by lysis and isolation of the cytoplasmic fraction, which was then pre-cleared with Protein-A sepharose beads at 4°C for 1h. The lysates were then split into equal parts; half was incubated with eIF4E conjugated Protein-A sepharose beads and half was

10

incubated with IgG conjugated Protein-A sepharose beads (negative control). The RNA associated with each type of bead was then eluted and isolated.

The isolated RNA was amplified using GeneChip 3' IVT Express Kit (Affymetrix) and hybridized to GeneChip Human genome U133A 2.0 array chips (Affymetrix) per manufacturer's protocol. Using Affymetrix Expression Console, Mas5 normalization was performed on all data sets. An expression cutoff of $p \leq 0.05$ was implemented to filter all data. The negative control expression values (IgG) were subtracted from their respective sample counterparts on a probeset basis; the three replicates were then averaged. Probesets that had fold increase ≥ 1.5 (radiation to control) or went from an expression value less than or equal to 0 before radiation to positive expression value after radiation (not bound to bound) were then further analyzed by Ingenuity Pathway Analysis (IPA). IPA curates a database that is defined by interactions reported in the literature. Gene lists are uploaded to IPA and network analysis was performed. The IPA analysis was performed using the IPA database available in October-December 2011. The data have been deposited in NCBI's Gene Expression Omnibus (31) and are accessible through GEO Series accession number GSE36179.

In vivo Tumor Growth Delay: Eight to ten-week-old female athymic nude mice (NCr *nu/nu*; NCI Animal Production Program, Frederick, MD) were used in these studies. Animals are caged in groups of 5 or less and fed animal chow and water ad libitum. A single cell suspension of U251 (10^7 cells), Miapaca-2 (5×10^6 cells), or PSN1 (5×10^6 cells) was injected subcutaneously into the right hind leg. When tumors grew to a mean volume of approximately 210 mm^3 (U251) or 180 mm^3 (PSN1) mice were

11

randomized into four groups: vehicle treated controls (5% N-Methylpyrrolidone, 15% Polyvinylpyrrolidone, and 80% water), drug treated (PP242 or INK128), radiation (at dose specified for specific experiment), or drug/radiation combination. The treatment protocols are described in detail in the results sections of their respective chapters. Radiation was delivered locally using a Pantak X Ray source with animals restrained in a custom designed lead jig. To obtain tumor growth curves, perpendicular diameter measurements of each tumor were measured 2 to 3 times per week with a digital caliper and volumes were calculated using a formula *(L x W^2) / 2*. Data are expressed as mean ± SEM tumor volume. Each experimental group contained between 5-7 mice. All animal studies were conducted in accordance with the principles and procedures outlined in the NIH Guide for Care and Use of Animals.

CHAPTER 3:

Translation Initiation Factor eIF4E is a Target for Tumor Cell Radiosensitization

Note to Reader

Portions of the results have been previously published (Hayman TJ, Williams ES, Jamal M, Shankavaram UT, Camphausen K, and Tofilon PJ (2012). Translation initiation factor eIF4E is a target for tumor cell radiosensitization. *Cancer Res* **72**, 2362-2372.) and are utilized with permission of the publisher. Eli Williams helped design and complete experiments; Muhammad Jamal helped with data acquisition; Uma Shankavaram assisted with bioinformatics analysis; Kevin Camphausen and Philip Tofilon helped to design and oversee project.

Abstract

A core component in the cellular response to radiation occurs at the level of translational control of gene expression. Because a critical element in translation control is the availability of the initiation factor eIF4E, which selectively enhances the cap-dependent translation of mRNAs, we investigated a regulatory role for eIF4E in cellular radiosensitivity. eIF4E knockdown enhanced the radiosensitivity of tumor cell lines but not normal cells. Similarly, pharmacological inhibition of eIF4E with ribavirin also enhanced tumor cell radiosensitivity. In tumor cells eIF4E attenuation did not affect cell cycle phase distribution or radiation-induced apoptosis, but it delayed the dispersion of radiation-induced γH2AX foci and increased the frequency of radiation-induced mitotic

catastrophe. Radiation did not affect 4E-BP1 phosphorylation or cap-complex formation but it increased eIF4E binding to >1000 unique transcripts including many implicated in DNA replication, recombination and repair. Taken together, our findings suggest that eIF4E represents a logical therapeutic target to increase tumor cell radiosensitivity.

Introduction

In eukaryotic cells the majority of translation occurs in a cap-dependent manner, which involves eIF4E binding to the 7-methyl guanosine (m^7G) cap on the 5' end of an mRNA resulting in the recruitment of eIF4G and eIF4A to form the eIF4F initiation complex and subsequently ribosome binding (32). This process is a final and rate-limiting step in translation initiation and is highly dependent on the availability of eIF4E. Elevated levels of eIF4E preferentially enhance the translation of mRNAs with long, highly structured 5' untranslated regions (UTRs), which tend to encode proteins related to cell proliferation and survival such as c-myc, Bcl2, FGF-2, and survivin (33-34). Moreover, eIF4E also promotes the nucelocytoplasmic shuttling of select mRNAs such as cyclin D and ornithine decarboxylase (ODC) with their increased cytoplasmic levels leading to increased translation (33-34). Thus, via at least 2 mechanisms eIF4E plays a critical role in the regulating gene translation.

At the cellular level elevated eIF4E has been implicated in oncogenesis (35). Overexpression of eIF4E has been shown to drive the malignant transformation of primary human mammary epithelial cells (36) and immortalized rodent cells (37) with ectopic expression of eIF4E in animal models increasing the incidence of a variety of tumor types (38). Evaluation of biopsy and surgical specimens indicates that eIF4E expression is frequently elevated in a number of human cancers including breast,

14

prostate, head and neck, and lung (33, 39). Increased eIF4E levels have also been associated with malignant progression (40) as well as poor therapeutic outcome (41-42). Finally, in preclinical models inhibition of eIF4E activity results in cytotoxicity for tumor but not normal cells (42-43). Given eIF4E's function in the translational control of gene expression and data suggesting that it contributes to the neoplastic phenotype, we have defined the consequences of eIF4E knockdown on the radiosensitivity of tumor and normal cell lines. The data presented here indicate loss of eIF4E activity selectively enhances tumor cell radiosensitivity through an inhibition of DNA double strand break repair. In addition, radiation is shown to significantly increase the number of mRNAs

Results

To determine whether eIF4E plays a role in determining radiosensitivity 3 tumor lines (MDA-MB-231, breast carcinoma; DU145, prostate carcinoma; A549, lung carcinoma) and 2 normal cell lines (HMEC mammary epithelial and MRC9 lung fibroblasts) were evaluated using the clonogenic survival assay. Each cell line was treated with siRNA specific to eIF4E or non-targeted siRNA; 72h after transfection cultures seeded at clonal density for survival analysis. As shown in Figure 2A, siRNA to eIF4E reduced eIF4E protein levels significantly when compared to non-targeted siRNA. The effects of eIF4E knockdown alone on the survival of each cell line are shown in Figure 2B. eIF4E knockdown significantly reduced clonogenic survival of all three tumor lines. As compared to the tumor cells, eIF4E knockdown induced significantly less cytotoxicity in the normal cell lines. These results are consistent with previous reports showing that tumor cells are more dependent on eIF4E for survival than normal cells (43-44).

The effects of eIF4E knockdown on cellular radiosensitivity are shown in Figure 3. For this study cells were treated as described above, trypsinized and irradiated 6h after seeding. Treatment with siRNA to eIF4E resulted in an increase in the radiosensitivity of each of the 3 tumor cell lines as compared to non-targeted siRNA (Figure 3A-C). The dose enhancement factors at a surviving fraction of 0.1 (DEFs) for MDA-MB-231, DU145, and A549 were 1.34, 1.24, and 1.44, respectively. The same experiment was performed on the two normal cell lines (Figure 3D-E). In contrast to the tumor cell lines, eIF4E knockdown had no effect on the radiosensitivity of the two normal cell lines. These results suggest that eIF4E contributes to survival after irradiation of tumor but not normal cells.

To investigate the mechanism responsible for the tumor cell radiosensitization induced by eIF4E knockdown we focused on MDA-MB-231 cells. Given that eIF4E has been reported to influence translation of a number of proteins involved in cell cycle regulation (45), a reduction in eIF4E levels could result in cell cycle phase redistribution. Because such an effect can be a critical factor in determining radiosensitivity, flow cytometry was used to determine the cell cycle distribution in MDA-MB-231 cells after eIF4E knockdown. As shown in Figure 4A the cell cycle phase distribution pattern was not significantly altered at 72h after exposure to eIF4E siRNA as compared to non-targeted siRNA. These results indicated that redistribution of cells into a radiosensitive phase of the cell cycle does not account for eIF4E knockdown-mediated enhancement in radiation-induced cell killing. eIF4E knockdown has been shown to induce apoptosis in breast cancer cell lines (46). To determine whether the increase in radiosensitivity resulting from eIF4E knockdown was due to an enhancement of radiation-induced

16
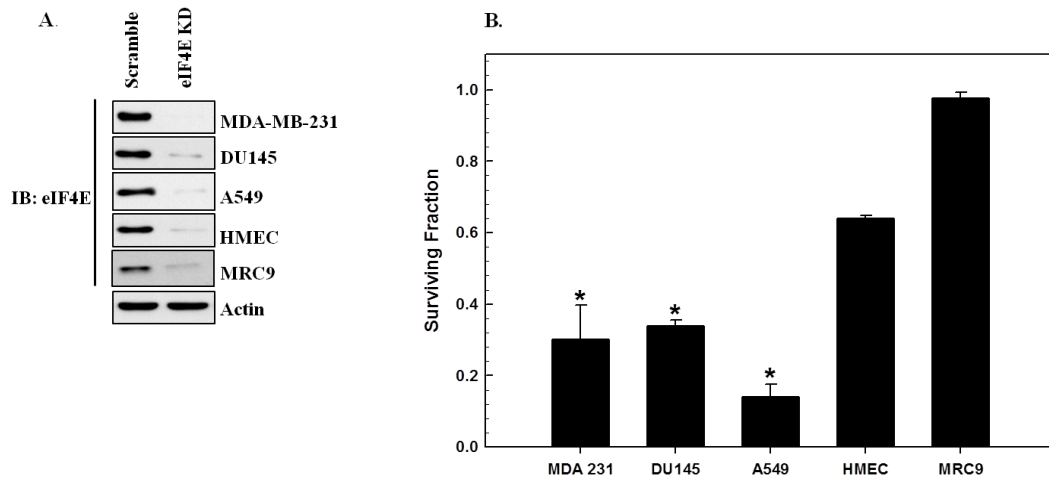
Figure 2:   Effect of eIF4E knockdown on clonogenic cell survival.   Cultures were transfected with siRNA specific to eIF4E (eIF4E KD) or non-targeted siRNA (Scramble). A) Representative immunoblots from each cell line showing extent of eIF4E protein reduction 72h after transfection. B) 72h post-transfection cells were plated at specified densities and colony-forming efficiency was determined 10-14 days later.   Surviving fractions for eIF4E KD cells were calculated after normalizing to the surviving fraction obtained for cells receiving the scrambled siRNA. Values shown represent the means $\pm$ SE for 3-4 independent experiments. *p < 0.04 according to Student's *t* test (all tumor cell lines compared to HMEC).

17
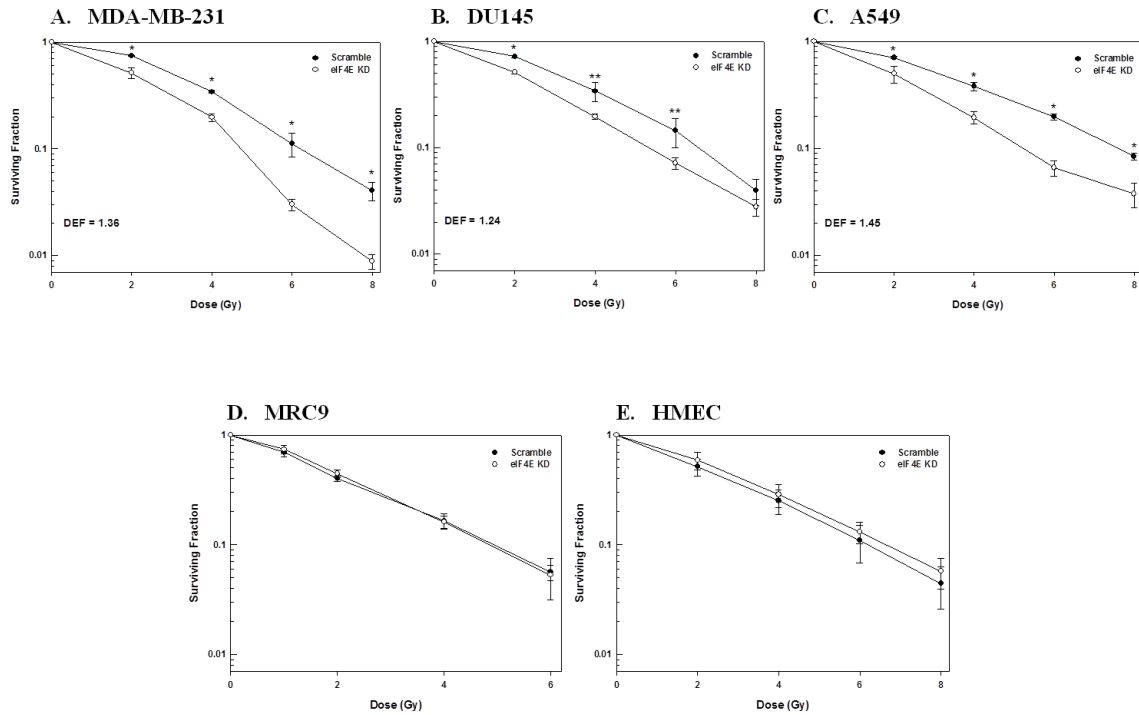
Figure 3: The effects of eIF4E knockdown on cellular radiosensitivity. A) MDA-MB-231, B) A549, C) DU145, D) MRC9, and E) HMEC cells were transfected with non-targeted siRNA (Scramble) or siRNA specific for eIF4E (eIF4E KD). 72h post-transfection cells were plated, allowed to attach for 6h, and irradiated. Colony-forming efficiency was determined 10-14 days later and survival curves were generated after normalizing for cell killing from siRNA alone. DEFs were calculated at a surviving fraction of 0.1. Values shown represent the mean $\pm$ SE for 3-4 independent experiments. * $p < 0.05$; ** $p < 0.1$ according to Student's *t* test.

apoptosis, we determined Annexin V staining at 24 and 48h after exposure to 6 Gy for cells exposed to siRNA to eIF4E and non-target siRNA. As expected for a solid tumor cell line, radiation alone did not induce a significant apoptotic response, and this response was not significantly enhanced with eIF4E knockdown (data not shown). These results indicate that apoptosis is not the mechanism of cell death following radiation in eIF4E deficient cells.

The critical lesion responsible for radiation-induced cell death is the DNA double strand break (DSB). Because γH2AX foci correspond to radiation-induced DSBs and their dispersal correlates with DSB repair (47-48), the effects of eIF4E knockdown on radiation-induced γH2AX were evaluated in MDA-MB-231 cells (Figure 4B). At 1h after exposure to 2 Gy no difference in foci levels was detected between control cells (non-targeted siRNA) and cells in which eIF4E was knocked down, suggesting that eIF4E levels have no effect on the initial level of radiation-induced DSBs. However, at 6 and 24h after irradiation (2 Gy) the number of γH2AX foci remaining in the eIF4E knockdown cells was significantly greater than in control cells. Additionally, a significant level of γH2AX foci retention was observed in eIF4E deficient cells 24 h after 4 Gy when compared to non-targeted siRNA treated cells. These data suggest that eIF4E knockdown results in an inhibition of radiation-induced DNA DSB repair.

Given the apparent inhibition of DSB repair and no increase in radiation-induced apoptosis after eIF4E knockdown, we hypothesized that the mechanism of cell death involved an increase in radiation-induced mitotic catastrophe. Cells with nuclear fragmentation, defined as the presence of two or more distinct nuclear lobes within a single cell, were classified as being in mitotic catastrophe. As shown in Figure 4C, eIF4E

19
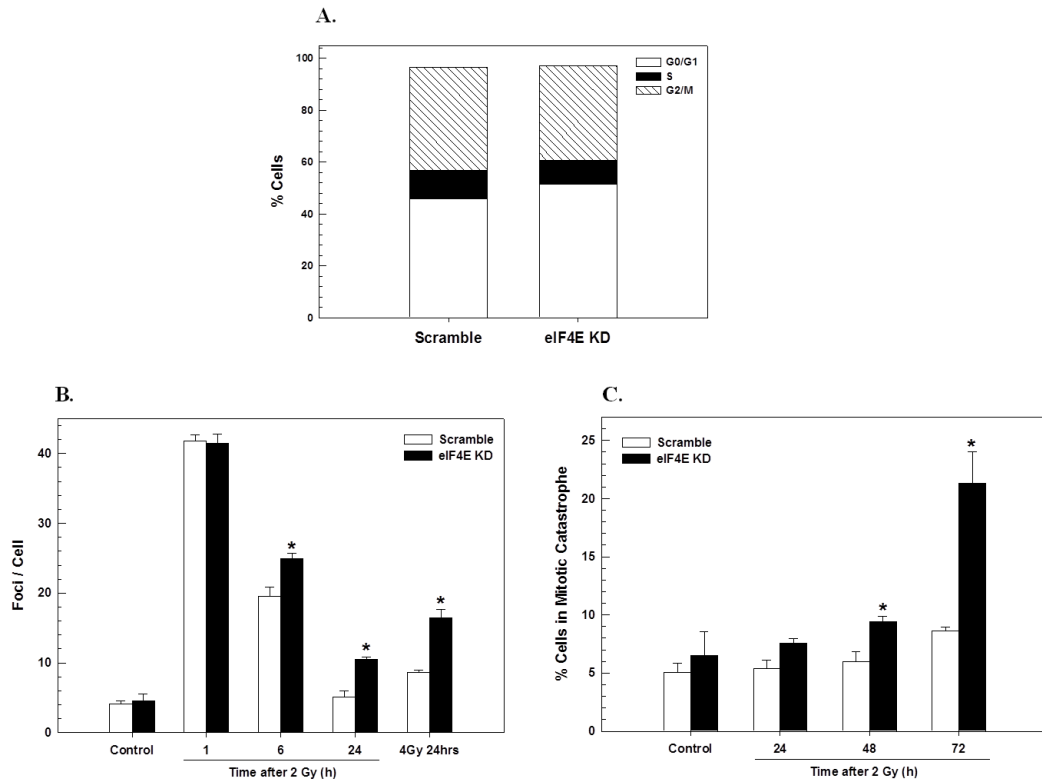
Figure 4: Mechanism of radiosensitization by eIF4E knockdown. In the following experiments MDA-MB-231 cells were transfected with siRNA specific to eIF4E (eIF4E KD) or non-targeted siRNA (Scramble). All experiments were carried out 72 hours post-transfection. A) Cell cycle phase distribution was determined. Values represent the mean of three independent experiments. B) Cells were irradiated with 2 or 4Gy and collected at the specified time; γH2AX foci were counted in at least 50 cells per condition. Values shown represent the means $\pm$ SE for 3 independent experiments, *p < 0.04 according to Student's *t* test (eIF4E KD compared to scramble). C) Cells were irradiated (2 Gy) and collected at the specified time points. Cells were classified as being in mitotic catastrophe by the presence of nuclear fragmentation, which was defined as a single cell containing two or more distinct nuclear lobes. At least 50 cells per condition were scored. Values represent the mean $\pm$ SE for 3 independent experiments. *p< 0.04

20

knockdown resulted in a significant increase in the percentage of cells undergoing mitotic catastrophe at 48 and 72h after exposure to 2 Gy. These results suggest the increase in radiosensitivity following eIF4E knockdown involves the inhibition of DSB repair after radiation, which then contributes to an increase in the number of cells undergoing mitotic catastrophe.

A critical regulator of eIF4E is 4E-BP1, which binds to eIF4E preventing its interaction with eIF4G and subsequently eIF4F complex formation (49). Phosphorylation of 4E-BP1 releases eIF4E resulting in eIF4F formation and cap-dependent translation (28); it has been reported that exposure of normal human cell lines to 8 Gy induces 4E-BP1 phosphorylation (25). However, exposure of MDA-MB-231 cells to 2 Gy under conditions used for clonogenic survival analysis (Figures 1-2) did not increase 4E-BP phosphorylation (Figure 5A), with densitometry shown in Figure 5B. Post-translational activation of eIF4E via phosphorylation at S209 has also been shown to influence eIF4E activity (50); radiation had no effect on eIF4E phosphorylation (Figure 5A). m^7-GTP batch chromatography is a standard approach for assessing eIF4F cap-complex formation (25, 30). Consistent with the lack of effect on 4E-BP1 and eIF4E phosphorylation, radiation had no effect on cap-complex formation, as evidenced by the lack of a change in bound eIF4G levels (Figure 5B). These results suggest that radiation does not increase the overall activity of eIF4E or cap-dependent translation initiation in general.

It is important to emphasize that eIF4E binding to a mRNA exists downstream of a multitude of complex post-transcriptional changes of which many are subject to regulation by radiation (as noted in Introduction). To further investigate the role of

21
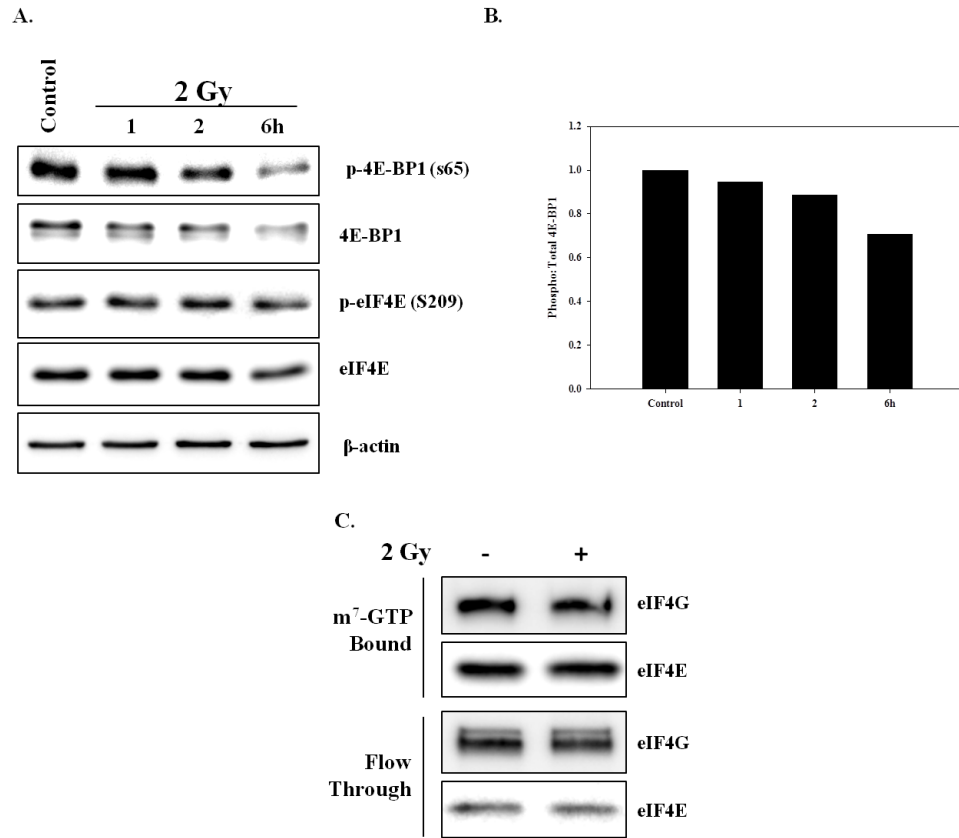
Figure 5: The effect of radiation on eIF4E activation. A) MDA-MB-231 cells were irradiated (2 Gy) and collected at the specified times and subjected to immunoblot analysis. Actin was used as a loading control. B) Densitometric quantitation of phosphor:total 4E-BP1 levels from immunoblot in Panel A. C) m^7-GTP affinity chromatography was performed on MDA-MB-231 cells that were irradiated and collected 1h after 2 Gy, and compared to unirradiated counterparts. m^7-GTP bound and unbound proteins (flow through) were resolved via SDS-PAGE followed by immunoblot analysis. eIF4E was used as a loading control. Blots are representative of two independent experiments.

eIF4E in mediating these post-transcriptional changes induced by radiation, we determined whether radiation influences the mRNAs bound to eIF4E using RIP-Chip analysis (RNA-Binding protein immunoprecipitation followed by microarray analysis of the bound mRNAs). In this experiment, MDA-MB-231 cells were irradiated (2 Gy), 6h later cytoplasmic lysates were collected and eIF4E was immunoprecipitated. RNA was then eluted from the immunoprecipitated eIF4E and subjected to microarray analysis, which was compared to the same process performed on unirradiated cells. In this analysis irradiation was found to increase the eIF4E binding of 1124 unique transcripts (either fold increase $\geq$ 1.5 or not bound to bound as described in Materials in Methods). The full list of genes is shown in Table A1 (Appendices). These transcripts were then subjected to Ingenuity Pathway Analysis (IPA), which distributes genes into networks defined by known interactions and then matches these networks with specific biologically significant pathways. The top ten biological functions associated with the eIF4E bound mRNAs are shown in Figure 6A. The specific functions of the genes contained within the *DNA Replication, Recombination, and Repair* category are further delineated (Figure 6B) and shown to encompass many aspects of the DNA damage response, including DSB repair and checkpoint control. To illustrate the interactions between the mRNA whose binding to eIF4E was affected by radiation, the top ten networks and their associated functions are shown in Table 1. Whereas there are numerous functions associated with these networks, of particular interest with respect to radiosensitivity is Network 4 (Figure 6C), which includes genes associated with *DNA Replication, Recombination and Repair*. Notably, this network contains several hub proteins: Rad17, Rad51, and CHEK1 each of which influences several other proteins. Network 6, which involves genes participating

23
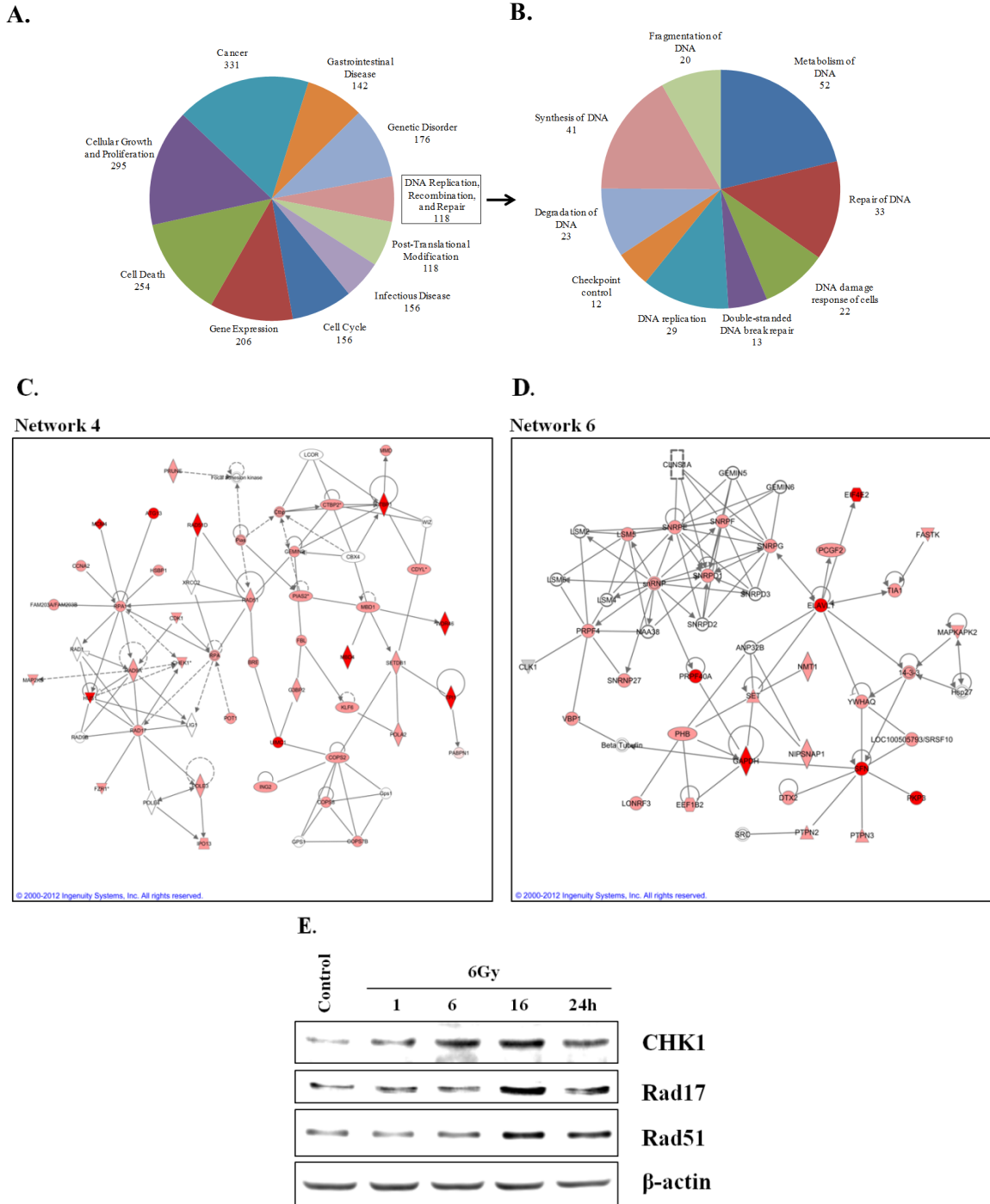
Figure 6: Rip Chip analysis of the effects of radiation on eIF4E mRNA clients. MDA-MB-231 cells were irradiated (2 Gy) and collected 6 hours later. eIF4E was immunoprecipitated, RNA bound to eIF4E was isolated and subjected to microarray analysis and mRNAs whose binding to eIF4E after irradiation were classified using IPA. A) Left panel: top ten biological functions (containing 100 or more genes) of the mRNAs whose binding to eIF4E was increased by radiation; right panel: the biological functions of the mRNAs (with greater than 10 genes) within the DNA Replication, Recombination, and Repair category are further delineated. B) Network 4 is shown with dark red indicating not bound to bound and lighter red indicating fold increase ≥ 1.5. C) Network 6 is shown with dark red indicating not bound to bound and lighter red indicating fold increase ≥ 1.5. D) Immunoblot analysis of DNA Damage Response related proteins predicted by RIP-Chip analysis to be induced by radiation. MDA-MB-231 cells were irradiated (6 Gy) and collected at the specified times. Actin was used as a loading control. Blots are representative of two independent experiments.

24

Table 1: Functions of mRNAs increasingly bound to eIF4E after irradiation

Functions associated with the top ten networks for genes that were increasingly bound to eIF4E after radiation (2Gy 6h) in MDA-MB-231 cells.			
ID	Score	Focus Molecules	Top Functions
1	46	33	Genetic Disorder, Skeletal and Muscular Disorders, Neurological Disease
2	44	33	Cancer, Cellular Movement, Connective Tissue Development and Function
3	44	32	Cancer, Infectious Disease, Respiratory Disease
4	42	31	DNA Replication, Recombination, and Repair, Cell Cycle, Gene Expression
5	39	30	Cellular Function and Maintenance, Cellular Compromise, Tissue Development
6	39	30	RNA Post-Transcriptional Modification, Dermatological Diseases and Conditions, Genetic Disorder
7	37	29	Post-Translational Modification, Cellular Movement, Cell Cycle
8	35	28	Amino Acid Metabolism, Small Molecule Biochemistry, Cellular Assembly and Organization
9	33	27	Post-Translational Modification, Protein Degradation, Protein Synthesis
10	32	27	Endocrine System Development and Function, Lipid Metabolism, Molecular Transport

25

in *RNA post-transcriptional processing* is shown in Figure 6D; it also includes several hub proteins (e.g., ELAVL1, snRNP, and PRPF4). This network illustrates eIF4E's capacity to modulate the post-transcriptional regulation of gene expression both directly,as an RNA Binding Protein (RBP), and indirectly through its influence on other proteins involved in post-transcriptional mRNA processing. The data presented in Figure 6 indicate that genes targeted by eIF4E after irradiation are not a random collection, but instead are functionally related mRNA subsets.

Given eIF4E's role in cap-dependent translation, an increase in the binding of a given mRNA to eIF4E would be expected to result in an increase in its corresponding protein product. Thus, to investigate the functional significance of the RIP-Chip analysis, we determined the effects of radiation on the levels of three of the hub proteins from Network 4 (CHK1, Rad17, and Rad51), proteins with established roles in the DNA damage response (51-53). MDA-MB-231 cells were irradiated (6 Gy) and collected for protein analysis at times out to 24h. As shown in Figure 6E, the levels of CHK1, Rad17, and Rad51 were increased after irradiation, consistent with a correlation between the mRNAs whose binding to eIF4E was increased after irradiation and the increase in their corresponding protein.

Because the data presented above suggest that eIF4E may serve as a target for radiosensitization, we determined the effects of ribavirin on the radiosensitivity of MDA-MD-231 cells. Whereas initially described as an anti-viral therapy, recent laboratory studies have shown that ribavirin inhibits eIF4E activity (44, 54) providing a basis for clinical trials as an anti-neoplastic treatment. To test whether pharmacological inhibition of eIF4E results in similar radiosensitization to eIF4E knockdown, MDA-MB-231 cells

26
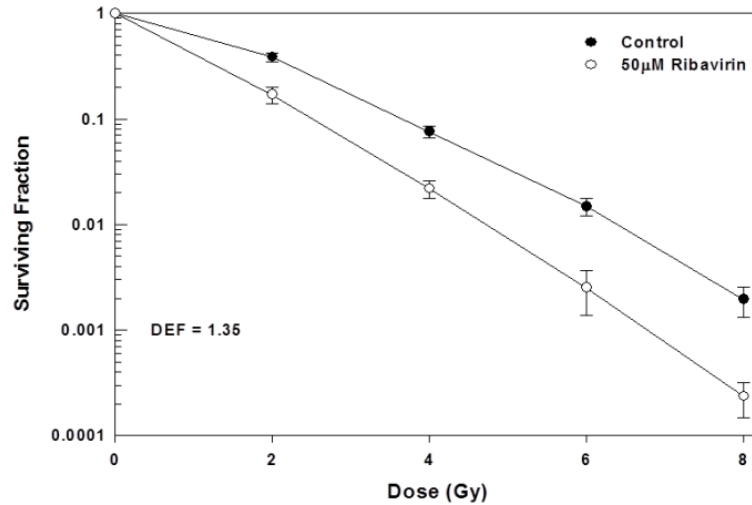
Figure 7: Effects of ribavirin on radiosensitivity. MDA-MB-231 cells were plated for clonogenic survival analysis and treated with 50 μM ribavirin for 1h, followed by radiation. Ribavirin was left on for the duration of the clonogenic assay. Values represent the mean ± SE for 3 independent experiments.

were plated for clonogenic survival analysis, treated with 50 μM ribavirin, a concentration that inhibits eIF4E activity in breast cancer cells (42), for 1h and irradiated. Ribavirin treatment alone reduced the surviving fraction to 0.30 ± 0.07, similar to that induced by eIF4E knockdown. As shown in Figure 7 this ribavirin treatment protocol enhanced the radiosensitivity of MDA-MB-231 cells with a DEF of 1.35. These results suggest that targeting eIF4E may be a valid strategy for radiosensitization.

Discussion

Based on γH2AX data, the mechanism through which eIF4E influences tumor cell radiosensitivity appears to involve DNA DSB repair. It is unlikely that this translation initiation factor directly participates in the DSB repair process suggesting that the mechanism involves an aspect of the post-transcriptional regulation of gene expression. We have previously shown that radiation affects the translation of certain subsets of mRNAs through recruitment of existing mRNAs to and away from polysomes (21-22). The RIP-Chip results presented here showing that radiation enhances the binding of eIF4E to specific mRNA subpopulations is consistent with the radiation-induced translational control of gene expression. Moreover, a major subset of the mRNAs whose eIF4E binding was increased by radiation corresponded to those coding for proteins involved in DNA Replication, Recombination and Repair and Cell Cycle, which could then play a role in determining radiosensitivity. A role for radiation-induced gene translation in the cell survival response is suggested by the recent work by Singh et.al. showing that DNA DSBs are generated not only from the initial radiation deposition, but also from chemical processing occurring for hours after exposure to radiation (55). In this situation a requirement for the rapid increase in DNA repair proteins may contribute

28

to the recovery process. However, based on the experiments using siRNA to knockdown eIF4E (Figure 3), it is not possible to determine whether the tumor cell radiosensitization was the result of eliminating the radiation-induced enhancement in gene translation and/or changes in mRNA translation that are induced before irradiation. Along these lines, the eIF4E inhibitor ribavirin enhanced MDA-MD-231 cells radiosensitivity when given 1h before irradiation (Figure 7). Clearly, the mechanisms through which the reduction of eIF4E levels affect radiation-induced tumor cell killing require additional investigation.

Whereas knockdown of eIF4E levels induced radiosensitization of tumor cells, the same procedure had no effect on the radiosensitivity of normal cell lines. This tumor selectivity may involve the increased dependence of tumor cells on eIF4E activity. For both ribavirin and an antisense oligonucleotide (ASO) to eIF4E, tumor cells are more sensitive in terms of cytoxicity than normal cells. (42-43) Consistent with these previous findings knockdown of eIF4E in the current study reduced survival of the tumor cell lines to a greater degree than on the normal cells. eIF4E serves as a funnel point (56) for a number of oncogenic pathways reflecting the consequences of activation of RTKs along with Ras and PI3K pathways (34, 57-58). The elevated eIF4E availability under these circumstances then putatively enhances the translation selectively and disproportionally of genes mediating cell proliferation and survival and other processes contributing to the neoplastic phenotype (59). It would seem that many of the eIF4E dependent genes whose translation is increased in tumor cells may also contribute to the ability of the cell to survive after a variety of insults including radiation.

Whereas the mechanisms remain to be completely defined, in the study described here knockdown of eIF4E was shown to enhance the radiosensitivty of 3 human tumor lines while having no effect on the radiosensitivity of 2 normal cell lines. These data suggest that eIF4E provides a tumor selective target for radiosensitization. Because laboratory data has already indicated that eIF4E contributes to the neoplastic phenotype, strategies for targeting eIF4E are being investigated at the preclinical and clinical setting. One approach is the use of an ATP-active site inhibitor of mTOR. In contrast to allosteric mTOR inhibitors, i.e. rapalogs, the active site inhibitors completely inhibit mTORC1 function, preventing the phosphorylation of the mTOR substrate 4E-BP1, which prevents release of eIF4E and limits its availability for eIF4F formation (60). An additional approach has been the development of small molecule inhibitors of the eIF4E-eIF4G interaction, which prevent complete formation of the eIF4F cap-complex (61). Inhibiting eIF4E expression with an eIF4E ASO has been shown to reduce eIF4E levels and to inhibit tumor cell growth in preclinical models (43). Finally, there has been considerable pre-clinical data evaluating ribavirin as an eIF4E activity inhibitor (44, 54). The mTOR active site inhibitors, ribavirin, and the eIF4E ASO are currently in clinical trials both as single agents (59, 62-63), as well as in combination with chemotherapy (64). The data presented in the current study showing that reduced eIF4E expression selectively enhances tumor radiosensitivity supports the clinical evaluation of these eIF4E-targeting strategies in combination with radiotherapy.

30

CHAPTER 4:

Ribosomal Protein S6 Kinase 1 as a Determinant of Cellular Radiosensitivity

Abstract

The ribosomal protein S6 kinases (S6Ks) are downstream effectors of the mTOR kinase and regulate a wide variety of cellular processes including translation initiation, ribosome biogenesis, and cell growth. Furthermore, the S6Ks are activated in a variety of malignancies and are associated with an enhancement of the malignant phenotype. To determine the role of S6K1 in regulating intrinsic cellular radiosensitivity, a panel of 3 tumor cell lines initiated tumors of different histologic origin and one normal cell line were treated with siRNA to S6K1. S6K1 knockdown enhanced the radiosensitivity of all 3 tumor lines as determined by clonogenic survival analysis. In contrast, S6K1 knockdown had no effect on the cellular radiosensitivity of the normal lung fibroblast line, MRC9. S6K1 knockdown increased expression of PDCD4, a tumor suppressor implicated in the cellular DNA damage response. Taken together these results suggest S6K1 is a potential tumor specific target for the enhancement of cellular radiosensitivity, and that its effects may be in part mediated by increased expression of PDCD4.

Introduction

As described in Chapter 2 we have shown that eIF4E, a critical and rate-limiting component of the translational machinery determines tumor cell radiosensitivity, and plays an integral role in the translational response to radiation. In addition to eIF4E, the p70 ribosomal protein S6 kinases (S6Ks) have a critical role in the regulation of mRNA

translation (65). There are two distinct genes encoding the p70 S6Ks (S6K1 and S6K2) (49). Most work characterizing these proteins has been done with S6K1, whereas there is less known about the function of S6K2 (49). S6K1 is a downstream effector of mTORC1 and regulate a wide variety of cellular processes including translation initiation, ribosome biogenesis, lipid synthesis, de novo pyrimidine synthesis, and cell growth (66). It exerts control over the translational machinery at multiple levels. The first identified substrate of S6K1 was ribosomal protein S6 (rpS6) a component of the 40S ribosome subunit that positively regulates translation and protein synthesis (66). There is conflicting evidence that S6K1 selectively regulates the translation of mRNAs containing 5' TOP (terminal oligopyrimidine) tracts (67-68). These mRNAs typically encode ribosomal proteins and translation factors (69). S6K1 also controls levels of the tumor suppressor, PDCD4 (programmed cell death 4) (70), a negative regulator of translation that inhibits the translation initiation factor eIF4A (71), a RNA helicase that is a component of the eIF4F cap-complex. eIF4A helicase activity is important for the unwinding of 5' UTRs that are highly structured (65). PDCD4 phosphorylation by S6K is followed by ubiquitylation via the ubiquitin ligase SCF-β-TRCP, and proteosomal degradation (70). Degradation of PDCD4 causes the release of eIF4A from PDCD4 and allows eIF4A to associate with the eIF4F cap-complex (70). Importantly, in the context of our study, PDCD4 has been linked to the cellular DNA damage response (72-73). In particular, PDCD4 knockdown of the human tumor cell line, HeLA, has been shown to decrease sensitivity to UV irradiation (74). Additionally, S6K enhances translation via phosphorylation of the initiation factor eIF4B. eIF4B phosphorylation by S6K1 enhances the helicase activity of eIF4A (65). This activation of eIF4B has been shown to correlate with its ability to

32

promote the translation of mRNAs with long and structured 5' UTRs (29). Lastly, S6K1 phosphorylates and inactivates the repressor of translation elongation eEF2K (eukaryotic elongation factor 2 kinase). eEF2K functions to phosphorylate and inhibit eEF2, a protein that mediates the translocation step of translation elongation (75).

S6K is activated, either through phosphorylation, or overexpression in a wide variety of malignancies and has been associated with poor prognosis in breast cancer (66) and gliomas (76). Activation in breast (77), colon (78), and liver tumors (79) was associated with a more malignant phenotype. S6K has been associated with glial transformation (80). Additionally, in several breast cancer cell lines, S6K has been associated with regulating cell survival (81). Activation of the mTOR/S6K pathway has also been associated with resistance to traditional chemotherapies (e.g. cisplatin) (66). Several factors (EGF, HGF, and SCF) and cytokines signal through S6K to partially exert their oncogenic activity (66). As such there has been considerable interest in the development of agents targeting S6K, with several in clinical trials: LY2584702 and XL418 (66). As radiation influences the translation of specific subsets of mRNAs, and S6K1 regulates translation, we addressed on the role of S6K1 in the cellular radioresponse in both tumor and normal cells.   Reduction of S6K1 levels via siRNA knockdown enhanced the radiosensitivity of 3 tumor lines but not of normal lung fibroblasts. Furthermore, consistent with previous literature, S6K1 knockdown induced the expression of PDCD4 in A549 cells.   These data provide initial insight into the role of S6K1 in regulating the cellular radioresponse as well as provide the basis for further studies investigating the application of S6K inhibitors with radiotherapy.

33

Results

To test the hypothesis that S6 kinase plays a role in determining cellular radiosensitivity we employed a siRNA mediated approach to reduce S6K1 levels. Using 3 tumor lines originated from tumors of distinct histologies (A549 lung adenocarcinoma, MDA-MB-231 breast carcinoma, and Panc1 pancreatic adenocarcinoma) and 1 normal cell line (MRC9 lung fibroblasts) the effects of S6K1 knockdown on cellular radiosensitivity were evaluated with the clonogenic survival assay. Each cell line was treated with siRNA specific to S6K1 (S6K KD) or non-targeted siRNA (scramble); 72h after transfection cultures were trypsinized to generated a single cell suspension and seeded at clonal density for survival analysis. The effects of S6K1 knockdown on cell survival were determined. As shown in Figure 8A, siRNA to S6K1 reduced S6K1 protein levels significantly when compared to non-targeted siRNA. Treatment with S6K1 siRNA reduced the surviving fraction to 0.77 ± 0.03, $0.68 \pm .10$, $0.30 \pm .01$, and 0.11 ± 0.05 in A549, MDA-MB-231, Panc1, and MRC9 cells respectively. These data indicate that in vitro S6K knockdown does not have a consistent cytotoxic effect with respect to tumor versus normal cells.

The effects of S6K1 knockdown on cellular radiosensitivity are shown in Figure 8. For this study cells were treated as described above, and irradiated 6h after seeding. Treatment with siRNA to S6K1 resulted in an increase in the radiosensitivity of each of the 3 tumor cell lines as compared to non-targeted siRNA (Figure 8B-D). The dose enhancement factors at a surviving fraction of 0.1 (DEFs) for A549, MDA-MB-231, and Panc1 were 1.35, 1.42, and 1.44, respectively. The same experiment was performed on the normal lung fibroblast cell line (Figure 8E). In contrast to the tumor cell lines, S6K1 knockdown had no effect on the radiosensitivity of the normal cell line, MRC9. These
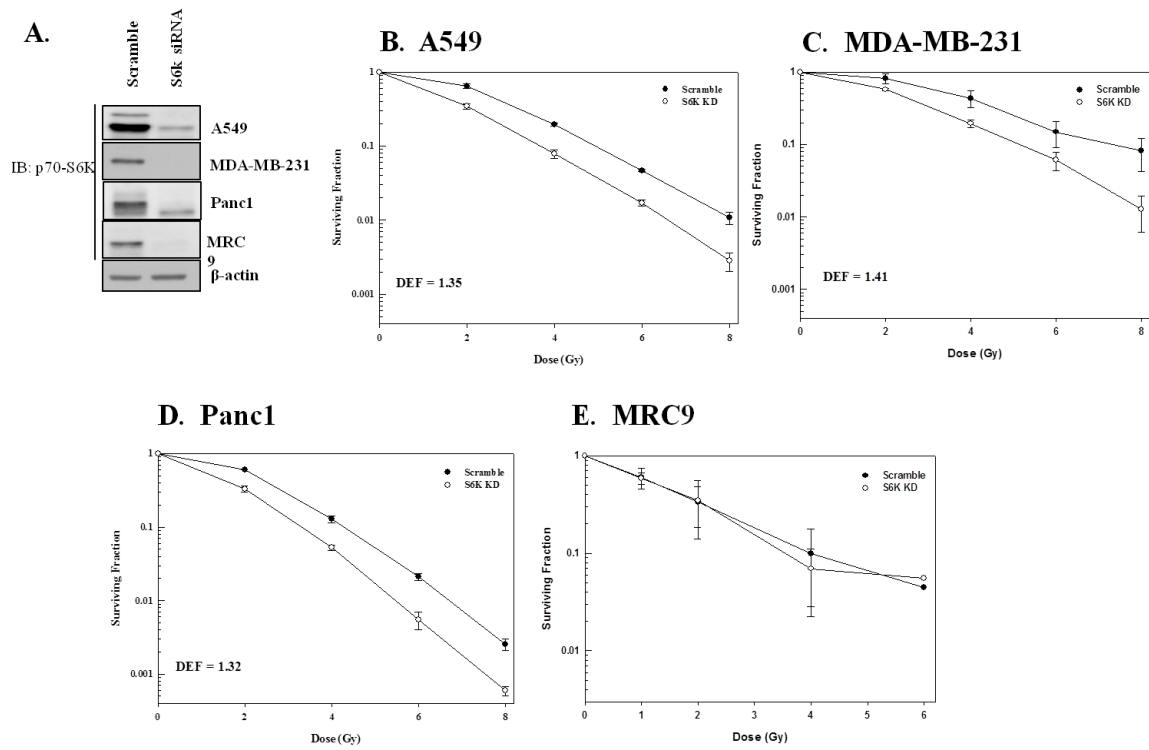
Figure 8: The effects of S6K1 knockdown on cellular radiosensitivity. Cells were transfected with siRNA to S6K1 (S6K KD) or non-targeted siRNA (Scramble). A, immunoblots from each cell line showing extent of S6K protein reduction 72 hours after transfection. A549 (B), MDA-MB-231 (C), Panc1 (D), and MRC9 (E), cells were plated seventy-two hours posttransfection, allowed to attach for 6 hours, and irradiated. Colony-forming efficiency was determined 10 to 14 days later, and survival curves were generated after normalizing for cell killing from siRNA alone. DEFS were calculated at a surviving fraction of 0.1.
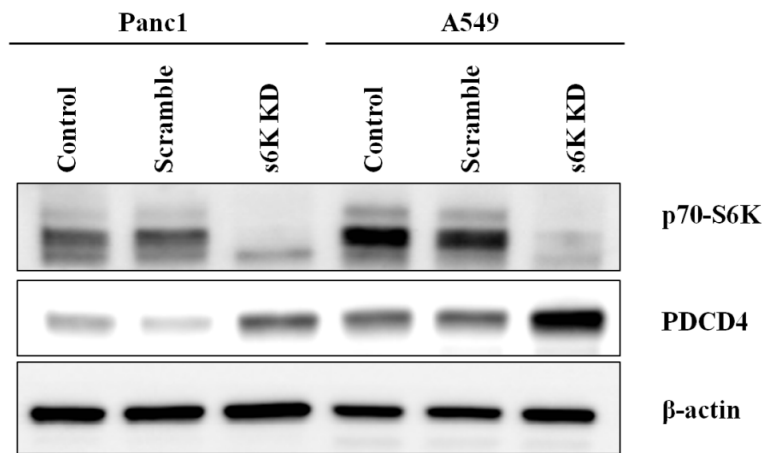
Figure 9: The effects of S6K1 knockdown on PDCD4 expression. A) Immunoblot analysis 6K1 and PDCD4 expression in untreated cells (control) or cells transfected with siRNA to S6K1 (S6K KD) or non-targeted siRNA (Scramble). Actin was used as a loading control.

results suggest that S6K1 contributes to survival after irradiation of tumor but not normal cells.

As described in the Introduction the expression of the tumor suppressor PDCD4 has been shown to be controlled by S6K (70). To determine whether S6K knockdown results in increased expression of PDCD4 in the cell lines studied immunoblot analysis of A549 and Panc1 cells treated with siRNA to S6K or non-targeted siRNA was performed. The results of this analysis are shown in Figure 9. In both cell lines PDCD4 expression was increased upon treatment with siRNA specific to S6K relative to the non-targeted siRNA control, consistent with previous reports.

Discussion

Whereas the mechanism of radiosensitization remains to be defined, in the study presented here knockdown of S6K1 was shown to increase the radiosensitivity of 3 tumor lines initiated from tumors of different histologies. In contrast to the 3 tumor cell lines tested, S6K knockdown had no effect on the cellular radiosensitivity of the normal lung fibroblast line MRC9. In order to make a definitive conclusion about the possible tumor specificity of S6K1 as a target for enhancing radiosensitivity, these results should be extended to other normal cell lines. However, our initial investigations suggest that S6K1 appears to be a potential tumor selective target. Whereas we have not defined the exact mechanisms regarding this potential tumor selectivity, there are numerous studies, both pre-clinically and clinically, showing over-expression and hyperactivation of S6K in tumor versus normal tissue (66, 76-79). Furthermore, as described in the Introduction, S6K is controlled primarily by mTORC1. Numerous genetic alterations and upstream signaling events (e.g. Ras mutations and PI3K/AKT activation) that affect mTORC1

37

signaling have been reported in the context of oncogenesis and tumor progression (82). Additionally, S6K plays an important regulatory role in the control of mRNA translation (49). Data from our laboratory have shown radiation to control gene expression primarily through regulation of gene translation (21-22). These experiments also examined the translational response to radiation in tumor versus normal cells (21). Importantly tumor cells and normal cells had strikingly different translational responses to ionizing radiation exposure (21). It is possible to speculate that this potential tumor selective enhancement in radiosensitization seen with S6K1 knockdown is due to the aforementioned differences in S6K regulation and activity. Determining the differences responsible for this potential tumor selectivity in the context of S6K1 as a target for radiosensitization will be the subject for future investigation.

In the context of DNA damage, PDCD4 has been shown to play a role in determining cell survival after exposure to DNA damage. Specifically, PDCD4 knockdown of HeLa cells has been shown to increase survival to ultraviolet radiation (74). This affect was attributed to PDCD4's ability to suppress the translation of p53 responsive genes, such as p21 and GADD45a (74). While work remains to be done in establishing a causal role of PDCD4 in mediating S6K1 knockdown-induced radiosensitization, our results are in general agreement with this study as we show that S6K knockdown increases PDCD4 expression and decreases cell survival after exposure to ionizing radiation.

In addition, as described in the introduction, S6K1 plays an important role in the regulation of cap-dependent translation through its control of eIF4A. eIF4A has been shown to selectively control the translation of oncogenic transcripts (83). Silvestrol, a

38

naturally occurring compound, has been reported to inhibit the activity of eIF4A and suppress translation of specific subsets of oncogenic mRNAs (84). Furthermore, combination of silvestrol with the DNA damaging agent doxorubicin showed a synergistic effect in extending survival (85). This combination therapy with silvestrol and doxorubicin was only synergistic in mice that harbored activation of the mTOR pathway. Additionally, there is data in inflammatory breast cancer cells showing that eIF4A knockdown or pharmacologic inhibition results in radiosensitization (86). Given these reports as well as our data showing an increase in PDCD4, a repressor of eIF4A activity, it is possible to conclude that S6K1 knockdown's influence on radiosensitivity may be in part due to effects of increased PDCD4 expression on eIF4A activity. Additionally, given the data showing eIF4A inhibition synergizes with DNA damage only in the context of hyperactive PI3K/mTOR signaling (85) and the established activation of PI3K/mTOR signaling observed in tumor cells, it is possible that this is the mechanism for the potential tumor specific radiosensitization observed. In conclusion, these data suggest that targeting S6K is a potential target for tumor selective radiosensitization; however, the mechanisms underlying this effect largely remain undetermined and will be the subject of future investigation.

CHAPTER 5:

Allosteric versus ATP-Competitive mTOR Inhibition and Radiosensitivity

Note to Reader

Abstract

The mechanistic target of rapamycin (mTOR) is a critical kinase in the regulation of gene translation and has been suggested as a potential target for radiosensitization. The goal of this study was to compare the radiosensitizing activities of the allosteric mTOR inhibitor rapamycin with that of the ATP competitive mTOR inhibitor PP242. Based on immunoblot analyses, whereas rapamycin only partially inhibited mTORC1 activity and had no effect on mTORC2, PP242 inhibited the activity of both mTOR containing complexes. Irradiation alone had no effect on mTORC1 or mTORC2 activity. Clonogenic survival was used to define the effects of the mTOR inhibitors on in vitro radiosensitivity. In the two tumor cell lines evaluated, PP242 treatment 1h before

40

irradiation increased radiosensitivity, whereas rapamycin had no effect. Addition of PP242 to culture media immediately, 1, or 6h after irradiation also enhanced the radiosensitivity of both tumor lines. To investigate the mechanism of radiosensitization, the induction and repair of DNA double strand breaks were evaluated according to γH2AX foci. PP242 exposure did not influence the initial level of γH2AX foci after irradiation, but did significantly delay the dispersal of radiation-induced γH2AX foci. In contrast to the tumor cell lines, the radiosensitivity of a normal human fibroblast cell line was not influenced by PP242. Finally, PP242 administration to mice bearing U251 xenografts enhanced radiation-induced tumor growth delay. These results indicate that in a preclinical tumor model PP242 enhances tumor cell radiosensitivity both in vitro and in vivo and suggest this effect involves an inhibition of DNA repair.

Introduction

A primary determinant of eIF4E activity is the mechanistic target of rapamycin (mTOR), which plays a critical role in regulating mRNA translation and protein synthesis in response to a variety of environmental signals (82). mTOR exists in two distinct complexes: mTOR complex 1 (mTORC1), which includes Raptor, Pras40, Deptor, and Mlst8, and mTOR complex 2 (mTORC2), which includes Rictor, mSin1, Protor1/2 and Mlst8 (82). The major substrates for mTORC1 kinase activity are eIF4E-binding protein 1 (4E-BP1), and the ribosomal protein s6 kinase 1 (S6K1). In the hypophosphorylated state, 4E-BP binds to eIF4E preventing its association with eIF4G, the formation of the eIF4F complex, and cap-dependent translation (28). However, when 4E-BP1 is phosphorylated by mTORC1 it is released from eIF4E and the eIF4F cap-complex is assembled. The substrates of mTORC2 are less well defined, but include AGC kinases

41

such as AKT, SGK, and PKC (65). Of note, mTORC2 phosphorylation of AKT at s473 can indirectly lead to enhancement mTORC1 activation (87-88).

mTOR is a major downstream effector of a number of signaling pathways (e.g. PI3K/AKT, RAS/MAPK, and RTKs) (56, 82). Because these pathways are frequently activated or dysregulated in tumors, mTOR has been considered a target for cancer therapy (89). Most studies of mTOR have focused on the use of the allosteric inhibitor rapamycin and its analogs (rapalogs), which incompletely inhibit mTORC1 output and do not inhibit mTORC2 (90). In the context of cancer treatment, these drugs have shown modest activity with respect to patient outcomes (59). The resistance of some tumors to rapalogs as single agents has been attributed to their incomplete inhibition of 4E-BP1 phosphorylation, feedback activation of AKT, and/or the lack of mTORC2 inhibition (90-91). In contrast to the allosteric inhibitors, more recently developed ATP-competitive inhibitors of mTOR inhibit mTORC1 output more completely and inhibit mTORC2, which prevents the feedback activation of AKT following S6K inhibition (87, 92-95). Given mTOR's role in regulating eIF4E activity, we have defined the consequences of an allosteric (rapamycin) and ATP-competitive (PP242) mTOR inhibitor on the radiosensitivity of tumor and normal cells. The data presented here indicate that the mTORC1/2 inhibition achieved using the ATP-competitive inhibitor PP242 enhances tumor cell radiosensitivity in vitro and in vivo and suggest that this effect involves an inhibition of DNA double-strand break (DSB) repair.

Results

To investigate the effects of rapamycin and PP242 on tumor cell radiosensitivity, two human cell lines initiated from solid tumors were used: MDA-MB-231 (breast

carcinoma) and U251 (glioma). Initially, mTORC1 and mTORC2 activity was determined in each cell line after a 1h exposure to PP242 or rapamycin (Figures 10A and B). The goal of this analysis was not only to compare drugs with respect to inhibitory activity but to also define the minimal concentration of each drug necessary to elicit the maximally achievable mTOR kinase inhibition. Towards this end, the levels of p-S6K (t389) and p-4E-BP1 (t37/46 and s65) were used as readouts for mTORC1 activity; p-AKT (s473) was used as a marker for mTORC2 activity. Rapamycin exposure reduced p-S6K and marginally reduced p-4E-BP1 levels in both cell lines with essentially the same reductions induced by 5 and 10nM. No further reductions in these indicators of mTORC1 activity were achieved by increasing rapamycin concentrations out to 500 nM (data not shown), consistent with previous reports (59, 96). PP242 exposure (1 and 2 µmol/L) reduced p-S6k levels to a similar degree as rapamycin. However, PP242 was considerably more effective at reducing the levels of p-4E-BP1 than rapamycin, as previously shown (92-93). In contrast to rapamycin, PP242 inhibited the phosphorylation of AKT at s473 in both tumor cell lines, indicative of an inhibition of mTORC2 activity. Thus, as reported for other cell lines (92-93), in U251 and MDA-MB-231 cells PP242 inhibits the rapamycin resistant functions of mTOR.

To determine whether irradiation influences mTOR activity, U251 and MDA-MB-231 cells were exposed to 2 Gy and collected for immunoblot analysis at times out to 6h (Figures 11A and B). Based on levels of p-AKT, p-S6K, and p-4E-BP1, radiation did not increase mTORC1 or mTORC2 activity in either of these tumor cell lines. These measures were conducted using cells grown under optimal in vitro conditions (i.e. 10% FBS) applicable to clonogenic survival analysis. Whereas previous reports showed that
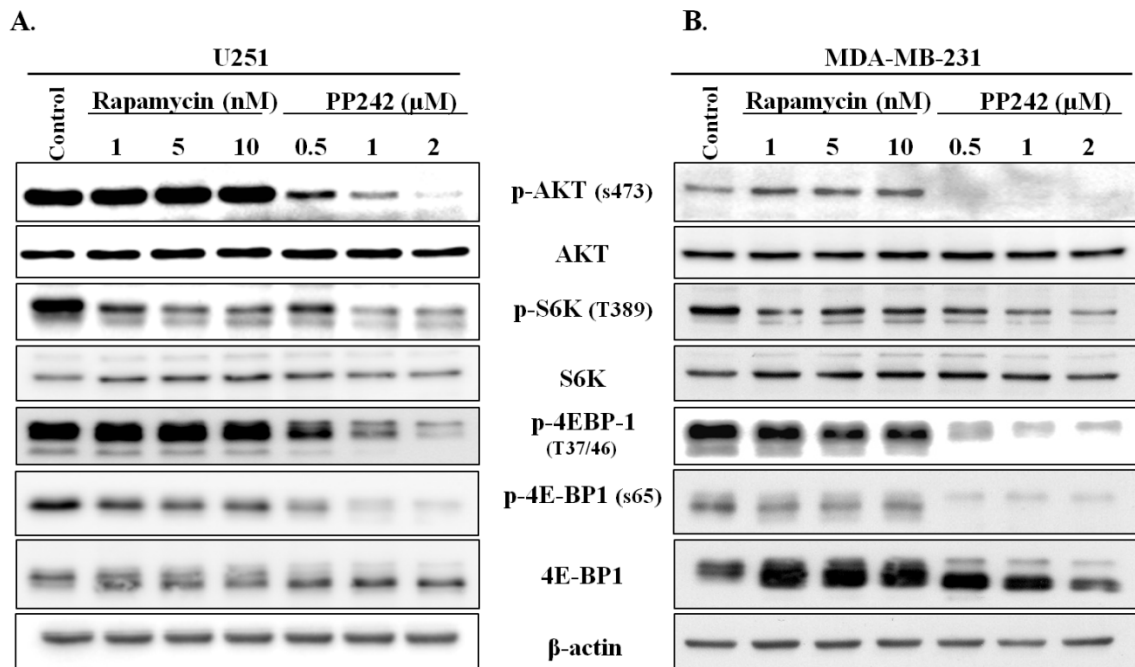
Figure 10: Effects of rapamycin and PP242 on mTORC1/2 activity. A) U251 and B) MDA-MB-231 cells were treated for 1h with the specified dose of inhibitor. Cells were collected and subjected to immunoblot analysis. Actin was used as a loading control.
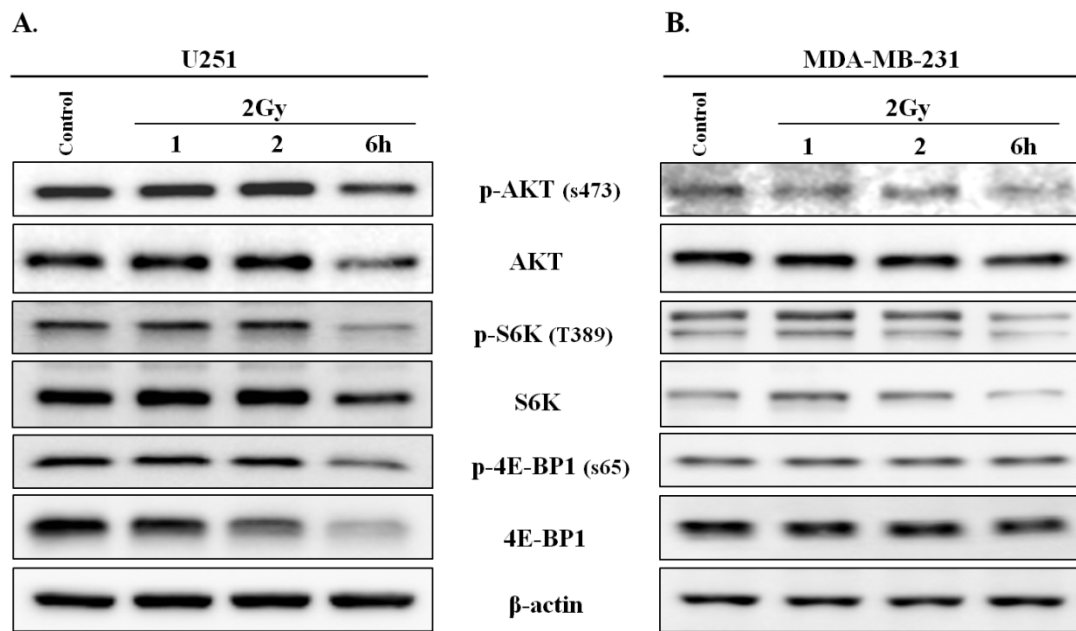
Figure 11: The effect of radiation on mTOR activity. A) U251 and B) MDA-MB-231 cells were irradiated (2 Gy) and collected at the specified times and subjected to immunoblot analysis. Actin was used as a loading control. Immunoblots are representative of two independent experiments.

radiation increased mTORC1 and mTORC2 activity in tumor cells, those studies were performed using serum starved cells (97-98).

The effects of the mTOR inhibitors on tumor cell radiosensitivity as measured by clonogenic survival analysis are shown in Figure 12A and B. For this study, cells were plated at clonogenic density, allowed to attach (5-6 h); the indicated concentration of inhibitor was added 1h before irradiation. Twenty-four hours after irradiation media was removed, fresh drug-free media was added and colonies determined 10-14 days later. Based on the data shown in Figure 10, a concentration of 10 nmol/L rapamycin was used, which induces the maximum achievable level of mTORC1 inhibition. Rapamycin (10 nmol/L, 25h) alone did not reduce the surviving fraction of U251 cells. Moreover, addition of rapamycin 1h before irradiation had no effect on the radiosensitivity of U251 cells (Figure 12A). In U251 cells 1 and 2 μmol/L of PP242 added 1h prior to irradiation increased radiosensitivity in a dose-dependent manner (Figure 12A), consistent with its dose-dependent mTOR inhibition (Figure 10A), resulting in dose enhancement factors at a surviving fraction of 0.1 (DEFs) of 1.27 and 1.52, respectively. PP242 alone at 2 μmol/L slightly reduced the U251 surviving fraction to 0.91 ± 0.04 and had no effect on survival at 1 μmol/L. To determine whether these effects were unique to U251 cells, a similar analysis was used for MDA-MB-231cells (Figure 12B). Rapamycin (10 nmol/L, 25h) alone had no effect on the surviving fraction of MDA-MB-231 cells and had no effect on the radiosensitivity of MDA-MB-231 cells. PP242 (2 μmol/L, 25h) alone reduced surviving fraction of MDA-MB-231 cells to 0.83 ± 0.06; when PP242 was added 1h prior to irradiation enhanced their radiosensitivity with a DEF of 1.34. These data suggest that in contrast to the allosteric mTOR inhibitor rapamycin, the ATP-competitive

46
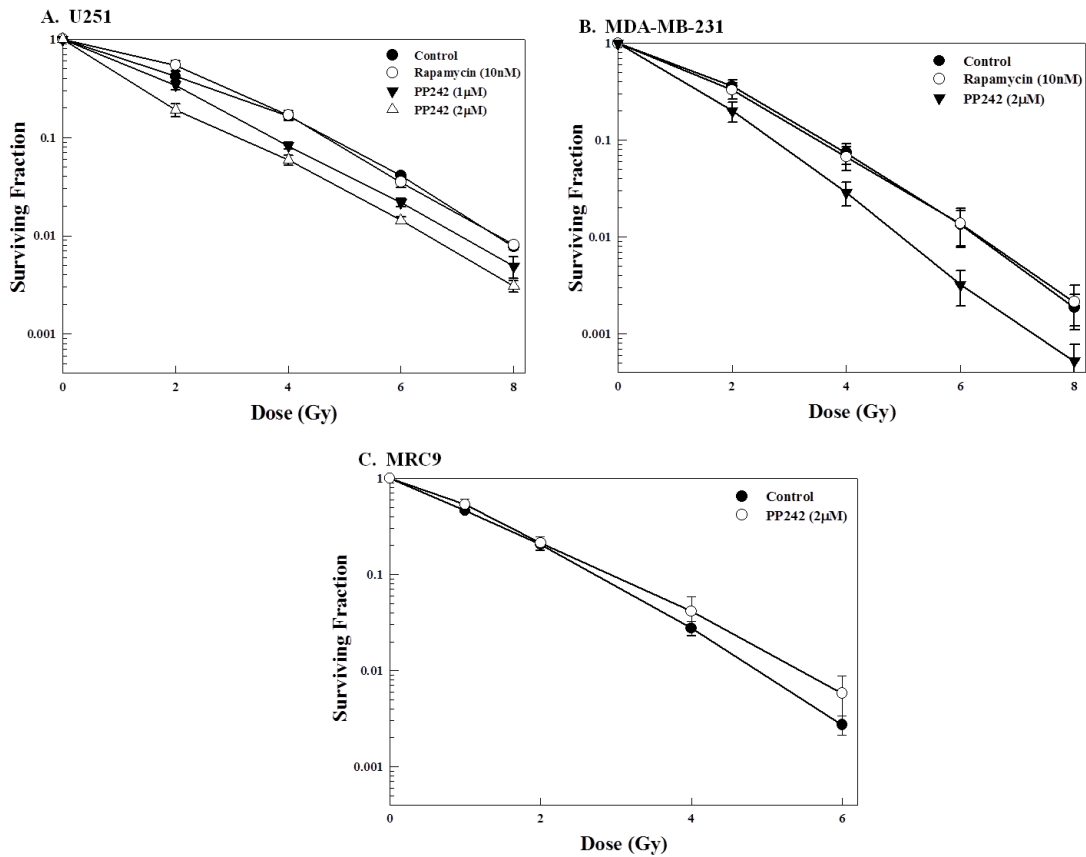
Figure 12: Effects of mTOR inhibitors on cellular radiosensitivity. A) U251, B) MDA-MB-231, and C) MRC9 cells were plated, allowed to attach for 5-6h, and the indicated concentration of inhibitor was added 1h before irradiation. Twenty-four hours after irradiation media was removed and fresh drug-free media was added. Colony-forming efficiency was determined 10-14 days later and survival curves were generated after normalizing for cell killing from drug alone. Values shown represent the mean $\pm$ SEM for 3 independent experiments.
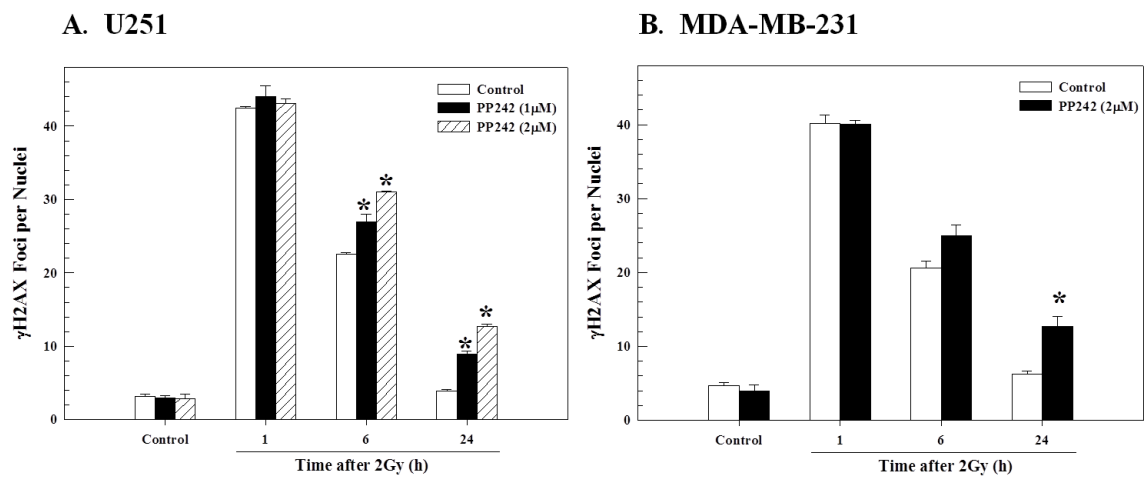
A. U251

B. MDA-MB-231

Figure 13: Influence of PP242 on radiation-induced γH2AX foci. A) U251 and B) MDA-MB-231 cells were exposed to the indicated dose of PP242 1h prior to irradiation (2 Gy). Cells were collected at the specified time; γH2AX foci were counted in at least 50 nuclei per condition. Values shown represent the means $\pm$ SEM for 3 independent experiments, *p < 0.05 according to Student's *t* test (PP242 compared to control).

inhibitor PP242, which more completely inhibits mTORC1 and inhibits mTORC2, enhances radiation-induced cell killing. The same experiment using PP242 was performed using the normal lung fibroblast line, MRC9 (Figure 12C). PP242 alone had no effect on MRC9 survival and, in contrast to the tumor cell lines, had no effect on the radiosensitivity of MRC9 cells. These results suggest that PP242 induces a tumor selective increase in radiosensitivity.

The critical lesion responsible for radiation-induced cell death is the DNA double strand break (DSB). Because γH2AX foci correspond to radiation-induced DSBs and their dispersal correlates with DSB repair (47-48), the effects of PP242 on radiation-induced γH2AX were evaluated in U251 and MDA-MB-231 cells (Figure 13 A and B). In this study PP242 was added 1h before irradiation (2 Gy) with γH2AX nuclear foci determined at times out to 24h. In U251 cells 1 hour after irradiation, no difference in foci levels was detected between control (vehicle) and PP242 treated cells, suggesting that mTOR inhibition had no effect on the initial levels of radiation-induced DSBs. However, at 6 and 24 h after irradiation (2 Gy), the number of γH2AX foci remaining in the PP242 (1 and 2 μmol/L) treated cells was significantly greater than in control cells. This effect was PP242 dose-dependent, consistent with the dose-dependent effect on radiosensitivity in U251 cells. In MDA-MB-231 cells 1 hour after irradiation, no difference in foci levels was detected between vehicle treated and PP242 treated cells. However, at 24h after irradiation, the number of γH2AX foci remaining in the PP242 (2 μmol/L) treated cells was significantly greater than in vehicle treated cells. These data suggest that PP242 induces radiosensitization via an inhibition of the repair of radiation-induced DNA DSBs.

49
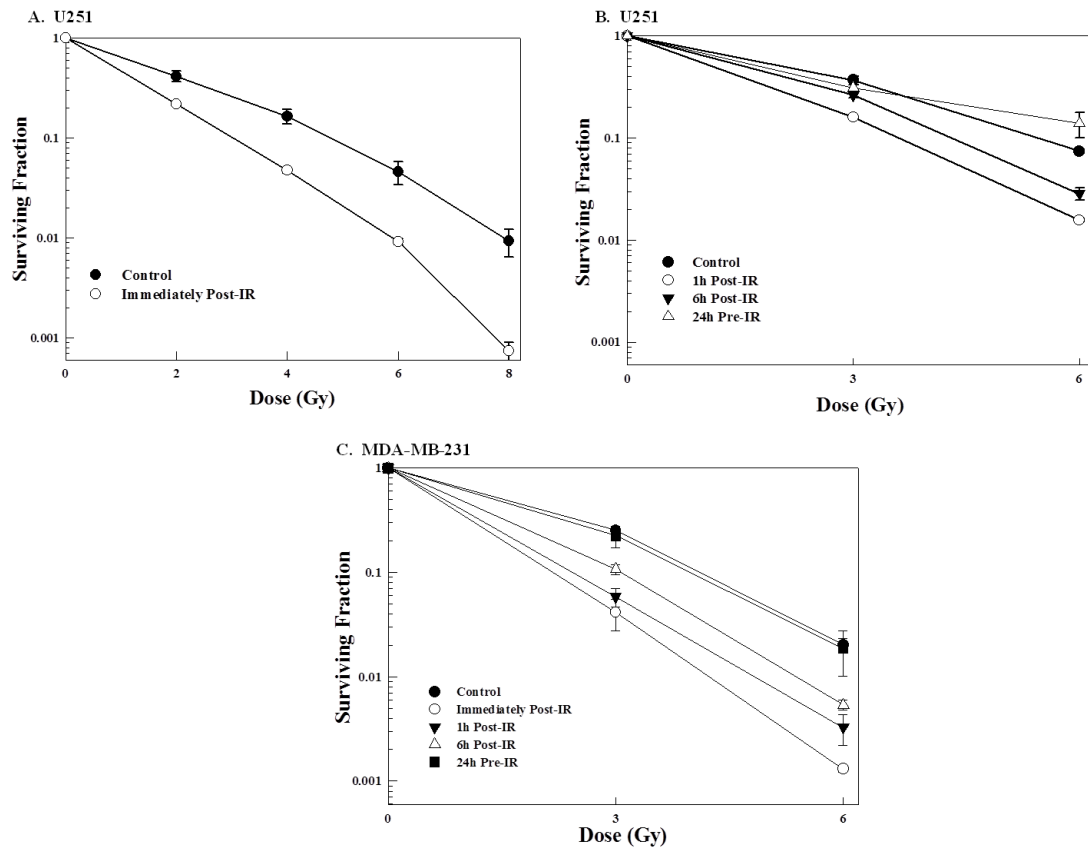
Figure 14: The effects of the timing of PP242 treatment on cellular radiosensitivity. A-B) U251 and C) MDA-MB-231 cells were plated and allowed to attach. Cells were then exposed to PP242 (2 μmol/L) either 24h before irradiation (24h Pre-IR), immediately after (Immediately Post-IR), 1h after (1h Post-IR), or 6h after (6h Post-IR) irradiation. Media was removed and fresh drug-free media was added 24h after irradiation. Colony-forming efficiency was determined 10-14 days later and survival curves were generated after normalizing for cell killing from drug alone. Values shown represent the mean $\pm$ SEM for 3 independent experiments.

50

In the initial treatment protocol evaluating the effects of PP242 on radiosensitivity (Figure 12) the mTOR inhibitor was added to the culture media 1h before irradiation. To determine whether this was the optimal exposure protocol for radiosensitization as well as to generate insight into the mechanisms involved, PP242 (2 µmol/L) was added to culture media at various times before or after irradiation followed by clonogenic survival analysis. In each experiment PP242 was removed 24h after exposure to radiation and all survival curves were generated after normalizing for cell killing caused by PP242 treatment alone. Addition of PP242 immediately after irradiation enhanced the radiosensitivity of U251 cells (Figure 14A) with a DEF of 1.60. Addition of PP242 at 1 and 6h after irradiation also resulted in radiosensitization (DEFs of 1.50 and 1.26, respectively), although the enhancement was substantially less for the 6h time point (Figure 14B). Treatment of U251 cells with PP242 24h prior to irradiation did not enhance their radiosensitivity (Figure 14B). These treatment protocols were also evaluated using MDA-MB-231 cells (Figure 14C). PP242 exposure for 24h before irradiation had no effect on the radiosensitivity of MDA-MB-231 cells, whereas drug addition immediately or 1h after irradiation enhanced radiosensitivity (DEFs of 1.88 and 1.71, respectively) with the sensitization also present, albeit diminished, at the 6h time point (DEF of 1.31). The data presented in Figures 14 indicate that the PP242-induced radiosensitization also occurs when the drug was added to culture media after irradiation.

To determine whether the enhancement of tumor cell radiosensitivity measured *in vitro* extends to an *in vivo* tumor model, U251 cells were grown as xenografts in nude mice. Initially, the ability of PP242 to inhibit mTOR activity in U251 xenografts was defined. PP242 (100 or 200 mg/kg) was delivered by oral gavage to mice bearing U251

51

leg tumors; 6h later tumors were collected and subjected to immunoblot analysis. As shown in Figure 15A, a consistent reduction of p-AKT and p-4EBP1 levels, indicative of mTORC2 and mTORC1 inhibition, respectively, was detected in tumors isolated from mice that received the PP242 at 200 mg/kg. Based on these results, a combination protocol was designed using 200 mg/kg PP242 and 2 Gy and the consequences on U251 tumor growth rate determined. Specifically, mice bearing U251 leg tumors (~210 mm^3) were randomized into four groups: vehicle, PP242, radiation, and PP242 plus radiation. PP242 was delivered once a day (200 mg/kg, oral gavage) for four days with the tumor locally irradiated (2 Gy) 2h after each of the four drug treatments. The growth rates of U251 tumors exposed to each treatment are shown in Figure 15B. For each group, the time to grow from 210 mm^3 (volume at time of treatment initiation) to 1,000 mm^3 was calculated using the tumor volumes from the individual mice in each group (mean ± SEM). These data were then used to determine the absolute growth delays (the time in days for tumors in treated mice to grow from 210 to 1000 mm^3 minus the time in days for tumors to reach the same size in vehicle treated mice).

For U251 tumors (Figure 15B) the absolute growth delays for the PP242 alone and radiation alone groups were 1.0 ± 0.4 and 12.9 ± 2.1 days, respectively. The growth delay in mice treated with the combination of PP242 and radiation was 20.0 ± 1.3 days, which is greater than the sum of the growth delays caused by PP242 alone and radiation alone. To obtain a dose enhancement factor (DEF) comparing the tumor radioresponse in mice with and without PP242 treatment, the normalized tumor growth delays were determined, which accounts for the contribution of PP242 to tumor growth delay induced by the combination treatment. Normalized tumor growth delay was defined as the time

52
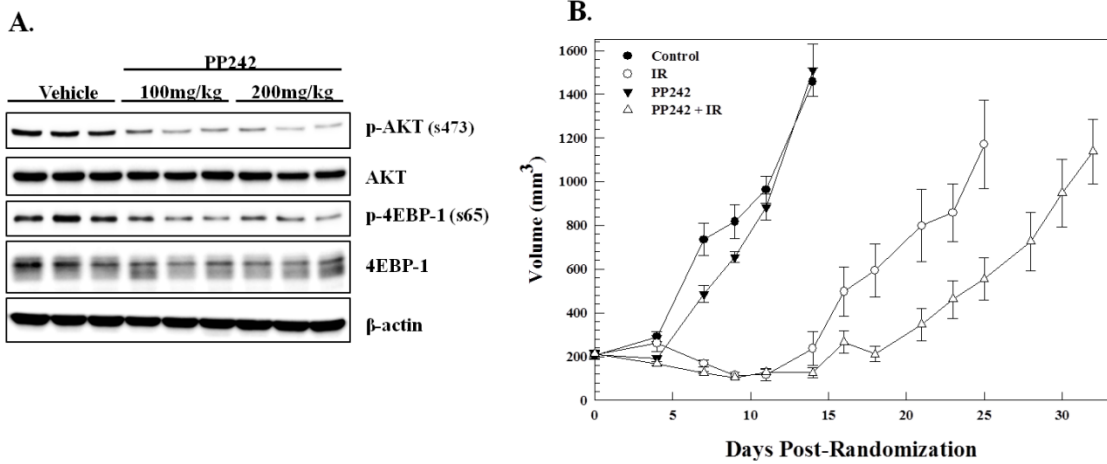
Figure 15: The effects of PP242 on radiation-induced tumor growth delay. A) Mice bearing U251 glioma xenografts were exposed to vehicle or PP242 (oral gavage) at the indicated dose. Six hours later tumors were collected and subjected to immunoblot analysis using actin as a loading control. Each lane represents the tumor from an individual mouse. B) When U251 tumors reached approximately 210 mm^3 in size, mice were randomized into four groups: vehicle, PP242 (200 mg/kg administered once daily by oral gavage), radiation (2 Gy once daily), and PP242 plus radiation. PP242 was delivered once a day (200 mg/kg by oral gavage) for four days with the tumor locally irradiated (2 Gy) 2h after each of the four drug treatments. Each group contained five mice. Values represent the mean tumor volumes $\pm$ SEM.

53

in days for tumors to grow from 210 to 1000 mm^3 in mice exposed to the combined modality minus the time in days for tumors to grow from 210 to 1000 mm^3 in mice treated with PP242 only. The DEF, obtained by dividing the normalized tumor growth delay in mice treated with the radiation/PP242 combination (19.0) by the absolute growth delay in mice treated with radiation only (12.9), was 1.5. Thus, whereas PP242 delivered alone had no significant effect U251 tumor growth, the ATP-competitive mTOR inhibitor enhanced the radiation-induced tumor growth delay.

Discussion

Previous investigations into mTOR as a potential target for tumor cell radiosensitization have focused on rapamycin and various rapalogs. The conclusions of such studies have been somewhat inconsistent with radiosensitization detected for some tumor cell lines (97-99) but not others (100-102). Clearly, such inconsistencies may be attributed to cell type specificity and/or differences in treatment protocols. However, an additional complicating factor is that rapamycin is an incomplete inhibitor of mTOR kinase. That is, although rapamycin inhibits the S6 kinase phosphorylation mediated by mTORC1, it only partially inhibits mTORC1 dependent 4E-BP1 phosphorylation and does not inhibit mTORC2 activity (90). Consequently, attempts to correlate radiosensitization with targeting of mTOR have been limited to the evaluation of S6K phosphorylation (97-101). Along these lines, in a study that evaluated multiple rapamycin concentrations, Murphy et al. showed that exposure of sarcoma cell lines to 300 nmol/L rapamycin resulted in radiosensitization, yet 3 nmol/L was sufficient to eliminate detectable levels of p-S6K, a concentration that had no effect on radiosensitivity (98). Thus, as illustrated by this study, the relationship between

54

rapamycin, mTOR activity and radiosensitization is unclear. To better understand the potential for mTOR to serve as a target for radiosensitization, we defined the radiosensitivity of tumor cells treated with the ATP-competitive mTOR inhibitor PP242, which in addition to inhibiting S6 kinase activation, inhibits 4E-BP phosphorylation as well as the mTORC2 activity (92-93). The data presented here show that for the two human tumor cell lines evaluated PP242 exposure, in contrast to rapamycin, enhanced radiation-induced cell killing.

Given the number of mTORC1 and mTORC2 substrates, whether PP242-induced radiosensitization is initiated via a single downstream event or whether multiple mTOR substrates are involved remains to be determined. However, as previously reported (32, 92, 103) and shown here, although rapamycin and PP242 inhibit S6 kinase phosphorylation to approximately the same degree, PP242 exposure results in a considerably more effective inhibition of 4E-BP1 phosphorylation. Feldman et al (92) reported that the PP242-mediated inhibition of 4E-BP1 phosphorylation prevents its release of eIF4E, thus reducing the level of eIF4E available for cap-dependent translation. Such a scenario would be consistent with our recent data showing that reduced eIF4E levels increase tumor cell radiosensitivity (104) and suggests that inhibiting the mTOR mediated phosphorylation of 4E-BP1 at least plays a role in PP242-induced radiosensitization.

Based on analysis of γH2AX foci induction and dispersion, it appears that PP242-mediated radiosensitization is the result of an inhibition of DNA double strand break repair. Furthermore, the radiosensitization obtained when PP242 was added at times out to 6h after irradiation suggests that mTOR inhibition affects a later stage in the DNA

repair process. Although the direct interaction of mTOR or one of its substrates with a component of the DNA repair machinery cannot be eliminated, the role of mTOR as a critical regulator of gene translation in response to a variety of stress and environmental signals may also provide a mechanistic basis for the inhibition of DSB repair in PP242 treated cells. A recent study using microarray analysis of polysome-bound RNA showed that after PP242 exposure, among the genes whose translation was significantly suppressed included a number corresponding to DNA repair proteins (103). Ribosome profiling also indicated that among the genes whose translation was reduced after PP242 exposure were a number involved in DNA repair (105). With respect to the effects PP242 on radiosensitivity, microarray analysis of polysome-bound RNA has shown that radiation-induced changes in gene expression can be primarily attributed to translational control processes (21-22). Moreover, in our recent study using RIP-Chip analysis (104), irradiation of MDA-MB-231 cells was found to increase eIF4E binding to over 1000 unique transcripts, a significant number of which were associated with the functional category of DNA Replication, Recombination and Repair. Thus, the PP242-mediated inhibition of gene translation may also play a role in its radiosensitizing actions, which will be the subject of future studies.

It has previously been reported that mTOR activity is increased at 15 minutes after irradiation with a return to control levels by 1h (106). Whereas we did not evaluate mTOR activity at times less than 1h after irradiation, addition of PP242 at times up to 6h after irradiation was shown to result in radiosensitization. This would suggest that if there was a transient increase in mTOR activity after irradiation returning to control levels by 1h, it was not critical to the mechanism of PP242-induced radiosensitization.

56

Furthermore, the study by Contessa et al. used serum-starved cells, which results in a reduction in basal mTOR activity as compared to standard growth conditions (106). In contrast, we determined the effects of radiation on mTOR activity using the same conditions of clonogenic survival analysis (media supplemented with 10% serum).

Whereas PP242 exposure enhanced the radiosensitivity of human tumor cell lines, the same procedure had no effect on the radiosensitivity of the normal fibroblast line MRC9. Because mTOR activity in MRC9 cells was reduced by PP242 treatment to the same extent as in the tumor cells (data not shown), the lack of radiosensitization may reflect the previously established fundamental differences in mTOR activity and/or function in tumor versus normal cells (88). To further evaluate the clinical potential of PP242 delivered in combination with radiotherapy, its effects on mTOR activity and radiation-induced tumor growth delay were defined in a preclinical model system. Although PP242 inhibited mTOR activity in U251 xenografts, drug delivery for 4 days had no significant effect on tumor growth rate, which is in contrast to previous studies showing substantial tumor growth inhibition with prolonged daily PP242 treatment (93, 107). However, this drug treatment protocol did result in a significant increase in radiation-induced tumor growth delay. A number of ATP-competitive mTOR inhibitors are being evaluated in clinical trials (64). The data presented here showing that PP242 enhances tumor cell radiosensitivity both in vitro and in vivo suggests that these inhibitors delivered in combination with radiotherapy may be of value as a cancer treatment strategy.

ATP-Competitive mTOR Inhibition by the Clinically Available mTOR Inhibitor

INK128 Enhances In Vitro and In Vivo Radiosensitivity of Pancreatic

Adenocarcinoma

Abstract

As shown in Chapter 5, ATP-competitive inhibition of mTOR is required for tumor radiosensitization. Radiotherapy is a primary treatment modality for the treatment of locally advanced pancreatic ductal adenocarcinoma, where its use improves local control and survival. Additionally, constitutive mTOR activation has been shown in pancreatic adenocarcinoma. The purpose of this study was to define the effects of the clinically available ATP-competitive mTOR inhibitor, INK128, on pancreatic cancer radiosensitivity. Clonogenic survival was used to define the effects of INK128 on cellular radiosensitivity. In 3 pancreatic cancer cell lines addition of INK128 immediately after radiation resulted in radiosensitization. Removal of drug from culture media either 12 or 24 but not 6h resulted in radiosensitization. To investigate the mechanism of radiosensitization, the induction and repair of DNA double strand breaks were evaluated according to γH2AX foci. INK128 exposure did not influence the initial level of γH2AX foci after irradiation, but did significantly delay the dispersal of radiation-induced γH2AX foci. INK128 inhibits mTOR activity in vivo in a time and dose-dependent manner. Inhibition of mTOR by INK128 inhibits cap-complex formation in PSN1 tumor

xenografts. Finally, the effects of INK128 on in vivo tumor radiosensitivity were defined and optimized using both in vitro and in vivo pharmacodynamic data.

Introduction

As described in Chapter 5 our laboratory recently compared the effects of the two classes of mTOR inhibitors on tumor cell radiosensitivity. ATP-competitive mTOR inhibition by PP242 enhanced tumor cell radiosensitivity both in vitro and in vivo (108). However, PP242 has been shown to have poor pharmacokinetic and pharmacodynamics properties in vivo (105). This led to the development of an analogue of PP242, INK128 (105), which possesses much-improved in vivo pharmacodynamics and pharmacokinetic properties. INK128 is currently undergoing analysis in the clinical trial setting now (64).

The overall survival rate for patients with pancreatic ductal adenocarcinoma (PDAC) remains dismal with an overall survival rate of approximately 5% despite advances in systemic therapy (109-110). Gemcitabine is the standard systemic therapy (111), however local control is an important component of therapy as it has been reported that approximately one-third of pancreatic cancer mortality is due to local disease (112). The importance of local control is highlighted by clinical data showing the combination of radiation with gemcitabine significantly prolongs survival when compared to gemcitabine alone (113). However, whereas there have been improvements in therapy, the prognosis for patients with pancreatic adenocarcinoma still remains poor. This emphasizes the need for the development of agents aimed at improving the efficacy of radiotherapy. High incidences of activating mutations in K-RAS have been reported in PDAC (114). These activating mutations in K-RAS increase MAPK as well as PI3K/AKT/mTOR signaling (114). Consistent with the role of activating mutations in K-

59

RAS it has been reported that approximately 70% of PDAC have constitutive mTOR activation (115). Given the proposed role of eIF4E and mTOR as determinants of tumor radiosensitivity, as well as the reported activation of mTOR in PDAC, the effects of the clinically available mTOR ATP-competitive inhibitor INK128 on pancreatic cancer cell radiosensitivity were defined. The data presented here indicate that mTORC1/2 inhibition by INK128 enhances PDAC radiosensitivity in vitro and in vivo and that this effect involves inhibition of DNA double strand break repair. Furthermore, these data provide preclinical insight into the design of protocols combining radiation and mTOR ATP-competitive inhibitors.

Results

To investigate the effects of mTOR inhibition by the mTOR ATP-competitive inhibitor INK128 on pancreatic cancer cell radiosensitivity, 3 human pancreatic cancer cell lines were used: Miapaca-2, Panc1, and PSN1. Initially mTORC1 and mTORC2 activity was determined in each cell line after various length of exposure to INK128 (Figure 16). Towards this end, the levels p-4E-BP1 (t37/46) were used as readouts for mTORC1 activity; p-AKT (s473) was used as a marker for mTORC2 activity. INK128 exposure in all three cell lines reduced activity of mTORC1 and mTORC2 in a time-dependent manner, consistent with reports in the literature (105).

The effects of INK128 on pancreatic cancer cell radiosensitivity as measured by clonogenic survival analysis are shown in Figure 17A-C. For this study cells were plated at clonogenic density, allowed to attach overnight, irradiated, followed immediately by adding the specified concentration of INK128. This protocol was chosen based upon our recently published work showing maximal radiosensitization by the ATP-competitive

60
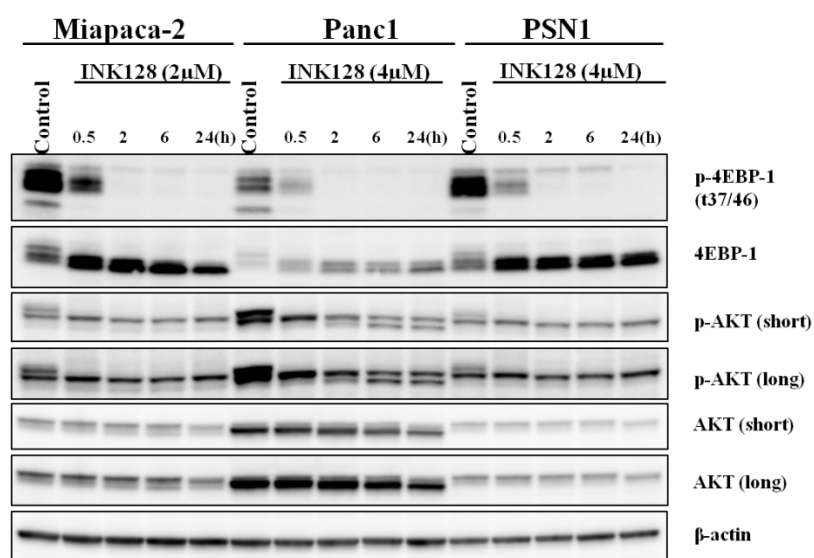
Figure 16: Effects of INK128 on mTORC1/2 activity. A) The indicated cells were treated with the specified dose of inhibitor. Cells were collected at the specified time points and subjected to immunoblot analysis. Actin was used as a loading control.
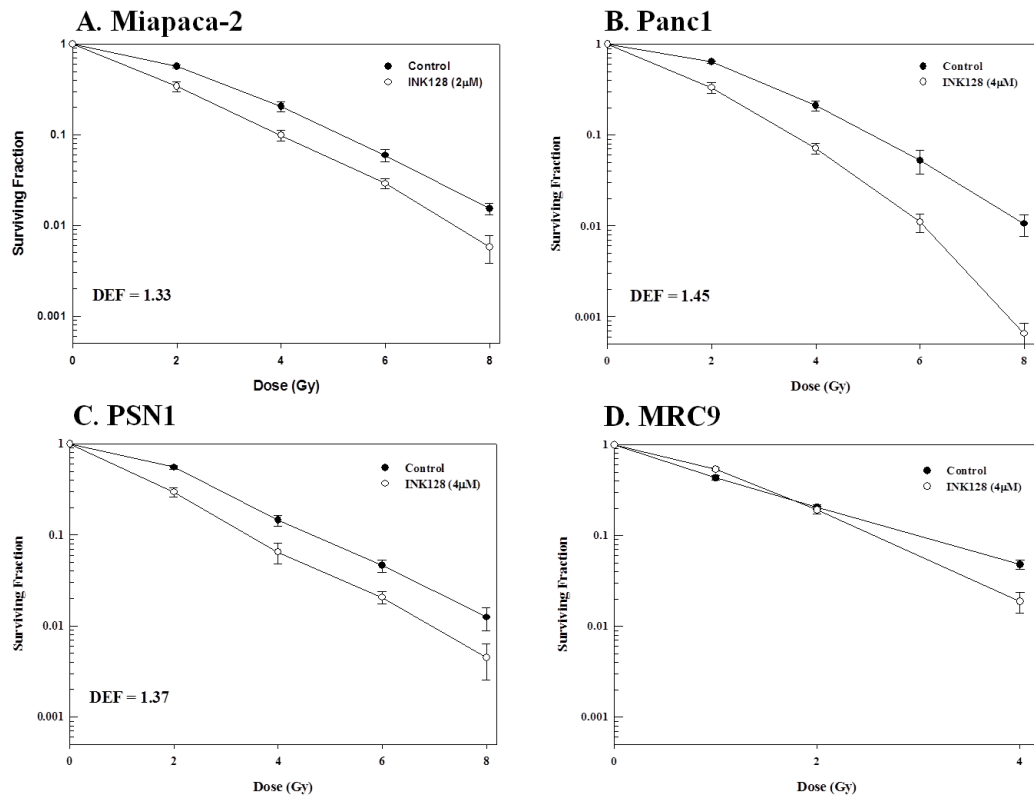
Figure 17: Effects of INK128 on cellular radiosensitivity. A) Miapaca-2, B) Panc1, C) PSN1, and D) MRC9 cells were plated, allowed to attach overnight, irradiated and the indicated concentration of inhibitor was added immediately after radiation. Twenty-four hours after irradiation media was removed and fresh drug-free media was added. Colony-forming efficiency was determined 10-14 days later and survival curves were generated after normalizing for cell killing from drug alone. Values shown represent the mean $\pm$ SEM for 3 independent experiments.

mTOR inhibitor PP242 when added immediately after radiation (108). Twenty-four hours after irradiation media was removed, fresh drug-free media was added and colonies determined 10-14 days later. INK128 treatment alone reduced the surviving fraction to 0.85 ± 0.02 in Miapaca-2 cells. In contrast, INK128 treatment had no effect on the surviving fraction of Panc1 or PSN1 cells. In all 3 pancreatic cancer cell lines treatment with INK128 immediately after irradiation resulted in an increase in cellular radiosensitivity. The dose-enhancement factors at a surviving fraction of 0.1 (DEF) were 1.33, 1.45, and 1.37 for Miapaca-2, Panc1, and PSN1 cells respectively. The same experiment using INK128 was performed using the normal lung fibroblast line, MRC9 (Figure 17D). INK128 treatment alone reduced the MRC9 surviving fraction to 0.73 ± 0.05, and in contrast to the 3 pancreatic cancer cell lines had no significant effect on the radiosensitivity of MRC9 cells. These results are consistent with our previous results where PP242 enhanced tumor but not normal cell radiosensitivity (108). These results suggest that INK128 treatment causes an increase in the radiosensitivity of pancreatic cancer cells.

The critical lesion responsible for radiation-induced cell death is the DNA double strand break (DSB). Because γH2AX foci correspond to radiation-induced DSBs and their dispersal correlates with DSB repair (47-48), the effects of INK128 on radiation-induced γH2AX were evaluated in PSN1 cells (Figure 18). In this study the same treatment protocol used for the clonogenic survival assays above was used, which consisted of adding INK128 immediately after irradiation (2 Gy) with γH2AX nuclear foci determined at times out to 24h. No difference in foci levels was detected between control (vehicle) and INK128 treated cells 1 hour after irradiation, suggesting that mTOR
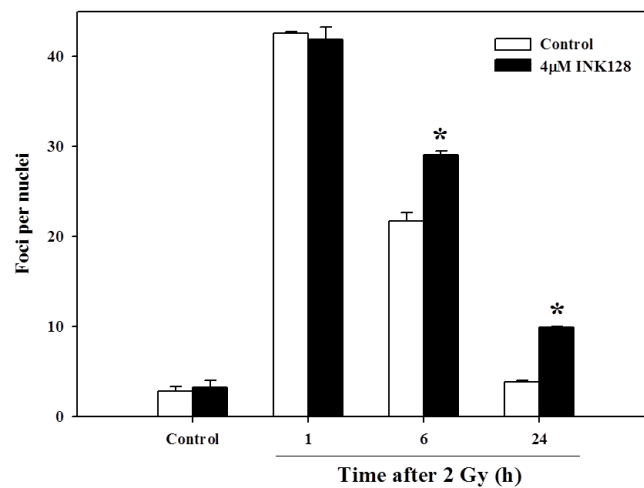
Figure 18: Influence of INK128 on radiation-induced γH2AX foci. A) PSN1 cells were exposed to the indicated dose of INK128 immediately after irradiation (2 Gy). Cells were collected at the specified time; γH2AX foci were counted in at least 50 nuclei per condition. Values shown represent the means $\pm$ SEM for 3 independent experiments, *p < 0.05 according to Student's *t* test (INK128 compared to control).

inhibition has no effect on the initial levels of radiation-induced DSBs. However at 6 and 24h after irradiation, the number of γH2AX foci reaming was significantly greater in the

INK128 treated cells relative to control cells. These data are consistent with our recently published data showing eIF4E knockdown and pharmacologic inhibition of eIF4E by the mTOR ATP-competitive inhibitor PP242 delay the dispersal of radiation-induced γH2AX foci. These results suggest that INK128-mediated radiosensitization is caused by an inhibition of radiation-induced DNA DSB repair.

Understanding the pharmacodynamic and pharmacokinetic properties of a drug is critical for the rational design of protocols combining radiation and chemotherapies. To begin to evaluate these effects in a preclinical setting Miapaca-2 and PSN1 cells were grown as xenografts in nude mice. The ability of INK128 to inhibit mTOR activity in both Miapaca-2 and PSN1 xenografts (Figure 19 A and B respectively) was determined via immunohistochemical analysis of p-4E-BP1 (t37/46) an established marker for mTOR activity. INK128 (1 or 3 mg/kg) was delivered by oral gavage to mice bearing Miapaca-2 or PSN1 tumor xenografts; tumors were collected either 2 or 6h after drugging, and processed for immunohistochemical analysis. In Miapaca-2 tumor xenografts treatment with INK128 (both 1 and 3 mg/kg) inhibited mTOR activity 2 hours after the initial dose as judged by a decrease in p-4E-BP1 staining, with a more pronounced inhibition with the 3 mg/kg dose. 6 hours after INK128 treatment mTOR activity is beginning to increase, albeit not to control levels, with a greater return to

65
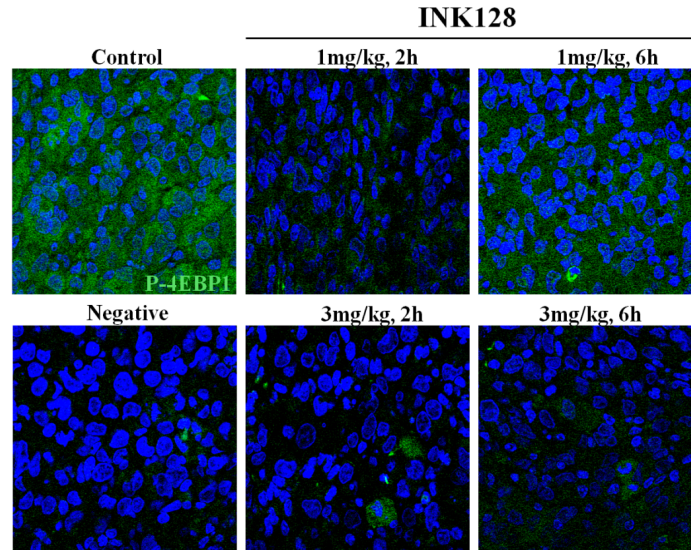
A. Miapaca-2

B. PSN1
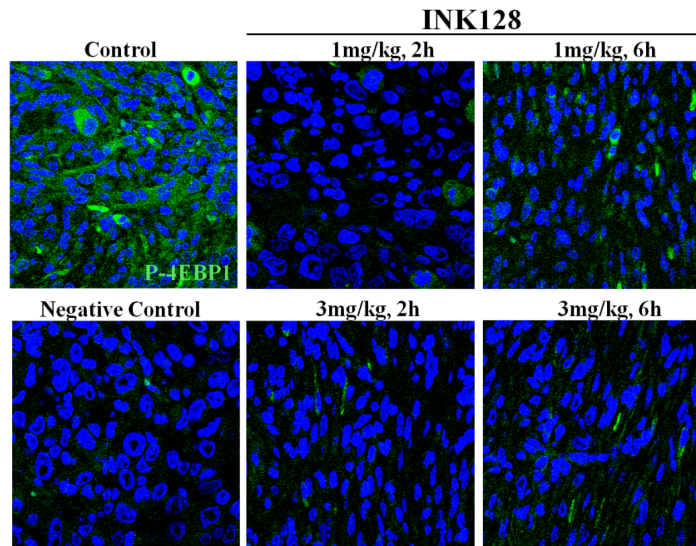
Figure 19: The effects of INK128 treatment on mTOR activity in pancreatic tumor xenografts. Mice bearing Miapaca-2 (A) or PSN1 (B) xenografts were exposed to vehicle or the indicated dose of INK128 (oral gavage). Tumors were collected 2 or 6 hours later and prepared for immunohistochemical staining. Sections were probed with an antibody specific to p-4E-BP1 T37/46 followed by staining with a FITC coupled secondary antibody (green). Nuceli were visualized with DAPI (blue). Each image is of representative of at least two mice per treatment group.

66

baseline in the 1 mg/kg treated tumors. In PSN1 tumor xenografts treatment with both 1 and 3 mg/kg inhibited mTOR activity to a similar degree 2 hours after the initial drug dose. Consistent with the results obtained for Miapaca-2 tumor xenografts, 6 hours after drug dosing mTOR activity is beginning to return. These results suggest that INK128 inhibits mTOR activity in a dose and time-dependent manner in pancreatic tumor xenografts.

As described in the Introduction, mTOR controls eIF4F cap-complex formation primarily by phosphorylation of the translation inhibitor 4E-BP1. Upon phosphorylation, 4E-BP1 is released from the 5' mRNA cap followed by binding of eIF4G and subsequently the initiation of translation (32). To extend the immunohistochemical analysis of INK128-mediated mTOR inhibition to its effects on *in vivo* cap-complex formation, m^7-GTP batch chromatography was employed on tumor PSN1 tumor xenografts treated with INK128 (3 mg/kg) and collected 2 or 6 hours later (Figure 20). m^7-GTP batch chromatography is a standard approach for assessing eIF4F cap-complex formation (25, 30). Consistent with the constitutive phosphorylation of 4E-BP1 seen by immunohistochemical staining (Figure 19) vehicle treated mice have substantial eIF4F cap-complex formation as judged by bound eIF4G. Treatment with INK128 decreased eIF4F cap-complex as evidenced by an increase in bound 4E-BP1 and decrease in bound eIF4G. Furthermore, consistent with the time-dependent effect on mTOR activity seen by immunohistochemical staining, the effects of INK128 treatment on eIF4F cap-complex formation were time dependent with bound eIF4G beginning to increase 6 hours after drugging. These results suggest that *in vivo* mTOR inhibition by the mTOR ATP-competitive inhibitor, INK128, results in a decrease in eIF4F cap-complex formation.
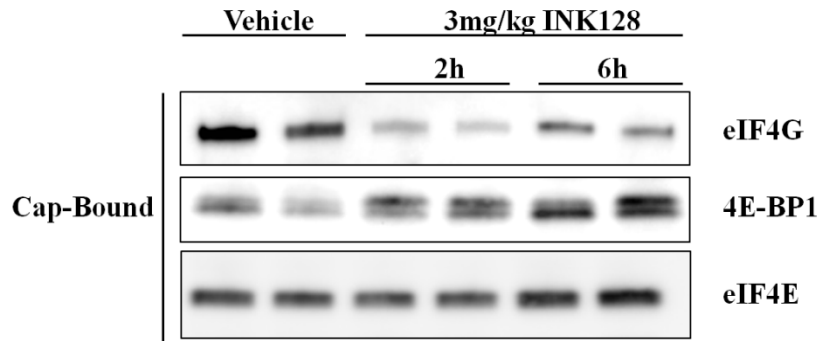
Figure 20: The effects of INK128 on PSN1 tumor xenograft eIF4F complex formation. A) m^7-GTP affinity chromatography was performed on PSN1 tumor xenografts that were exposed to 3 mg/kg INK128 (oral gavge) or vehicle and collected at the specified timepoints. m^7-GTP bound proteins were resolved via SDS-PAGE followed by immunoblot analysis. eIF4E was used as a loading control. Each lane represents the tumor from an individual mouse.

To determine whether the observed radiosensitization *in vitro* could be translated to an *in vivo* setting a tumor regrowth delay experiment was performed using PSN1 tumor xenografts in nude mice. Based upon the immunohistochemical analysis of INK128 treatment in PSN1 xenografts, a combination protocol was designed using INK128 and a single fraction of 6 Gy. Specifically, mice bearing PSN1 leg tumors ($\sim 180mm^3$) were randomized into four groups: vehicle, INK128 (3 mg/kg, delivered by oral gavage), radiation (6 Gy), and the combination of INK128 and radiation. INK128 was delivered once immediately after the locally delivered radiation dose. The growth rates of PSN1 tumors exposed to each treatment are shown in Figure 21A. As shown there was no difference in the growth rates of mice receiving radiation or mice that received the combination of radiation and a single dose of INK128. As such, this treatment protocol did not result in an enhancement of *in vivo* tumor radiosensitivity. The initial treatment protocol evaluating the effects of INK128 on pancreatic cancer cell radiosensitivity *in vitro* consisted of adding INK128 to culture media and removing drug 24h after radiation. In light of the lack of sensitization seen in the single dose *in vivo* tumor growth delay experiments as well as the immunohistochemical analysis showing mTOR activity beginning to return as early as 6h post a single drug dose we postulated that duration of mTOR inhibition post-radiation could be an important factor in the determining the radiosensitization seen with INK128 treatment. To begin to address this question *in vitro* we performed clonogenic survival analysis with PSN1 cells using a modified treatment protocol. This protocol consisted of addition of INK128 to culture media immediately after radiation and removing the drug 6, 12, or 24h post-radiation. The results of this analysis are shown in Figure 21B. In all 3 treatment protocols INK128 alone had no

69
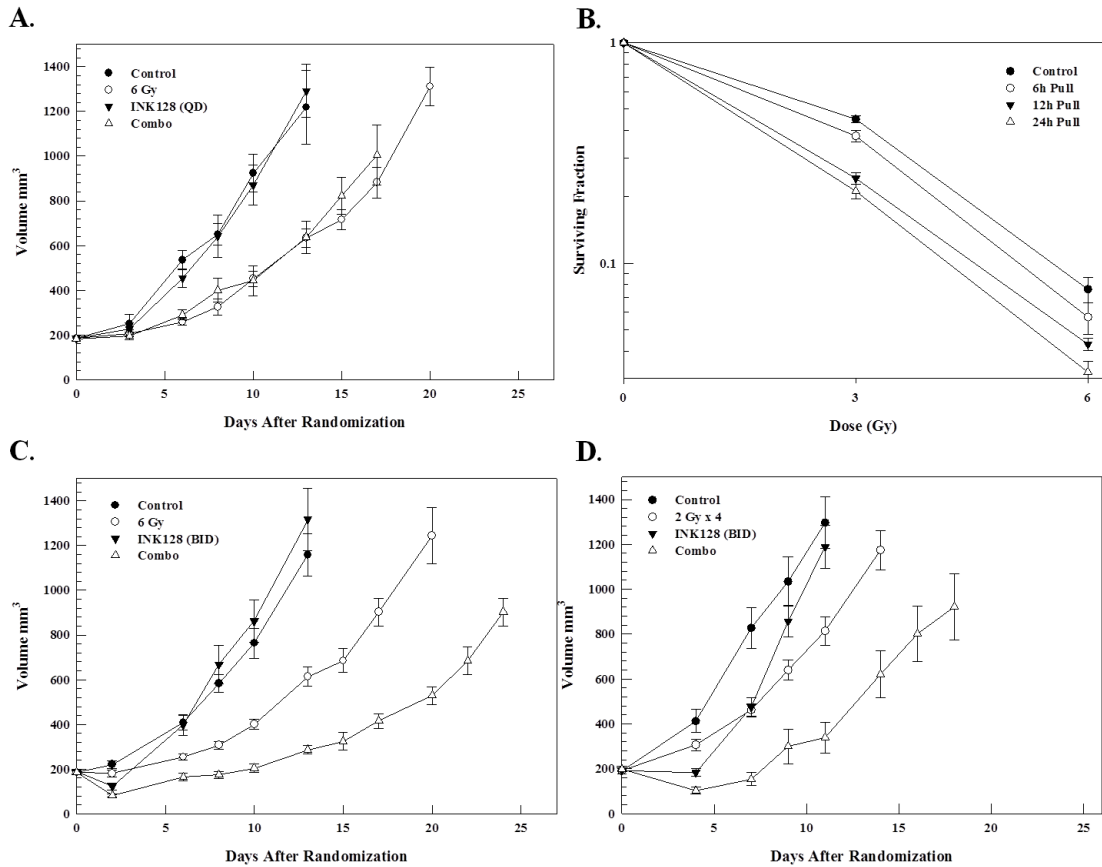
Figure 21: The effects of duration of mTOR inhibition on in vitro and in vivo radiosensitivity. . When PSN1 tumor xenografts reached approximately 180 mm^3 in size, mice were randomized into four groups: vehicle, INK128 (oral gavage), radiation, and INK128 plus radiation. A) The tumors were locally irradiated (6 Gy) followed by a single dose of INK128 (3 mg/kg.) Each group contained six mice. Values represent the mean tumor volumes $\pm$ SEM. B.) PSN1 cells were plated at clonal density and allowed to attach overnight irradiated and INK128 (4μM) was added immediately after irradiation. At the specified times after irradiation media was removed and fresh drug-free media was added. Colony-forming efficiency was determined 10-14 days later and survival curves were generated after normalizing for cell killing from drug alone. DEFs were calculated at a surviving fraction of 0.1. Values shown represent the mean $\pm$ SEM for 3 independent experiments. C) INK128 was delivered twice daily (1.5 mg/kg) for two days with the tumor locally irradiated (6Gy) 1h after the first drugging followed by a second drug dose delivered 6h later. INK128 alone contained 5 mice and all other group contained 6 mice. Values represent the mean tumor volumes $\pm$ SEM. D) INK128 was delivered twice daily (1.5 mg/kg) for 4 days with the tumor locally irradiated (2 Gy) 1h after the first drugging followed by a second drug dose delivered 6h later. On the fifth day INK128 was delivered twice with each dose separated by 7h. The INK128/radiation combination group contained 6 mice and all other group contained 7 mice. Values represent the mean tumor volumes $\pm$ SEM.

70

effect on the surviving fraction. The treatment protocol where INK128 was removed 6h post-irradiation had no significant effect on the radiosensitivty of PSN1 cells, whereas removing INK128 12 or 24h after irradiation enhanced PSN1 tumor cell radiosensitivity with DEFs of 1.23 and 1.33 respectively. These data suggest that duration of mTOR inhibition after radiation is an important determinant of the radiosensitizing effects seen with INK128 treatment.

In light of the *in vitro* data suggesting that sustained mTOR inhibition beyond 6h is critical for radiosensitization with INK128 as well as immunohistochemical analysis and eIF4F cap-complex formation data in PSN1 tumors suggesting mTOR activity begins to return as early as 6h after a single drug exposure, a modified tumor growth delay experiment combining radiation and INK128 was designed. Specifically, mice bearing PSN1 tumor xenografts were randomized into four treatment groups: vehicle, INK128 (1.5 mg/kg), radiation, or combination treatment. This experiment was performed with a single dose of locally delivered radiation (6 Gy) given 1h after INK128 treatment. INK128 was given again 6h after irradiation, followed the next day by two additional INK128 doses separated by 7h. The effects of the different treatment protocols on tumor growth are shown in Figure 21C. For each group the time to grow from 180mm^3 (volume of tumors at initiation of treatment) to 1000mm^3 was calculated using the tumor volumes from the individual mice in each group (mean ± SEM). These data were then used to determine the absolute growth delays. For PSN1 tumors the absolute growth delay for radiation alone was 6.3± 0.7 days. INK128 treatment alone had no significant effect on tumor growth delay. For tumors treated with the combination of INK128 and radiation the absolute growth delay was 12.3 ± 0.4 days. Importantly, this growth delay

71

is greater than the sum of the growth delays from the individual treatments indicative of an enhancement of tumor radiosensitivity. To obtain a dose enhancement factor (DEF) comparing the tumor radioresponse in mice with and without INK128 treatment, the normalized tumor growth delays were determined, which accounts for the contribution of INK128 to tumor growth delay induced by the combination treatment. Normalized tumor growth delay was defined as the time in days for tumors to grow from 180 to 1000 mm^3 in mice exposed to the combined modality minus the time in days for tumors to grow from 180 to 1000 mm^3 in mice treated with INK128 only. The DEF, obtained by dividing the normalized tumor growth delay in mice treated with the radiation/INK128 combination (12.3) by the absolute growth delay in mice treated with radiation only (6.3), was 2.0. Consistent with *in vitro* data, these *in vivo* data suggest extended mTOR inhibition for periods longer than 6h are required for INK128-induced radiosensitization.

To extend the single dose *in vivo* tumor growth delay study to a clinically relevant radiation protocol, a tumor growth delay experiment was performed with fractionated radiation. Specifically, mice bearing PSN1 tumor xenografts were randomized into four treatment groups: vehicle, INK128 (1.5 mg/kg), radiation (2Gy x 4), or combination treatment. This experiment was performed with locally delivered radiation (2 Gy) given 1h after INK128 treatment. INK128 was given again 6h after irradiation. This was performed for four consecutive days. On the fifth day two additional INK128 doses separated by 7h were given. The effects of the different treatment protocols on tumor growth are shown in Figure 21D. For each group the time to grow from 180mm^3 (volume of tumors at initiation of treatment) to 1000mm^3 was calculated using the tumor volumes from the individual mice in each group (mean ± SEM). These data were then

used to determine the absolute growth delays (the time in days for tumors in treated mice to grow from 180mm^3 to 1000 mm^3 minus the time in days for tumors to reach the same size in vehicle treated mice). For PSN1 tumors the absolute growth delays for INK128 alone and radiation alone were 1.0 ± 0.6 and 3.7 ± 0.6 days respectively. For tumors treated with the combination of INK128 and radiation the absolute growth delay was 10.1 ± 1.8 days. Importantly, this growth delay is greater than the sum of the growth delays from the individual treatments, indicative of an enhancement of tumor radiosensitivity. Normalized tumor growth delay was defined as the time in days for tumors to grow from 180 to 1000 mm^3 in mice exposed to the combined modality minus the time in days for tumors to grow from 180 to 1000 mm^3 in mice treated with INK128 only. The DEF, obtained by dividing the normalized tumor growth delay in mice treated with the radiation/INK128 combination (9.1) by the absolute growth delay in mice treated with radiation only (3.7), was 2.5. Consistent with the single radiation dose experiment the combination of INK128 with a clinically relevant fractionated radiation protocol enhanced *in vivo* tumor radiosensitivity.

Discussion

Based upon the analysis of radiation-induced γH2AX foci after radiation in PSN1 cells treated with INK128 it appears that the mechanism of radiosensitization involves an inhibition of DNA DSB repair. These results are consistent with our recently published results showing mTOR ATP-competitive inhibition of tumor cell lines resulted in an inhibition of DNA DSB repair. Furthermore in vitro clonogenic survival analysis showing maintenance of mTOR inhibition for greater than 6h was required for effective radiosensitization, suggests that INK128 inhibits a later stage of DNA DSB repair.

73

Although the direct interaction of mTOR or one of its substrates with a component of the DNA repair machinery cannot be eliminated, the role of mTOR as a critical regulator of gene translation in response to a variety of environmental and stress signals may provide a mechanistic basis for the inhibition of DSB repair in INK128 treated cells. A recent study using microarray analysis of polysome-bound RNA showed that after PP242 exposure, the translation of genes suppressed included many corresponding to DNA repair proteins (103). Furthermore, another recent report using ribosome profiling to identify actively translated mRNAs showed INK128 treatment inhibited the translation of many mRNAs encoding proteins related to DNA DSB repair (105). As microarray analysis of polysome-bound RNA has shown that radiation-induced changes in gene expression can be primarily attributed to translational control processes (21-22) it is possible to conclude that INK128's effects on radiosensitivity are due in part to inhibition of cap-dependent translation. Moreover, in our recent study using RIP-Chip analysis (104), irradiation of MDA-MB-231 cells was found to increase eIF4E binding to over 1000 unique transcripts, a significant number of which were associated with the functional category of DNA Replication, Recombination and Repair. Thus, the INK128-mediated inhibition of gene translation may also play a role in its radiosensitizing actions, which will be the subject of future studies.

mTOR is the primary kinase involved in the regulation of cap-dependent translation initiation due in part to it control of 4E-BP1 phosphoryaltion (49). Using immunohistochemical staining we showed a time and dose-dependent inhibition of mTOR activity in both Miapaca-2 and PSN1 tumor xenografts. It has been shown that inhibition of mTOR by an ATP-competitive inhibitor results in the decrease of 4E-BP1

74

phosphorylation (92, 103). This effect has been translated to an increase in binding of 4E-BP1 and a concomitant decrease in the amount of eIF4G binding to the 5' mRNA cap *in vitro* (93). However, to the best of our knowledge, the effects of mTOR ATP-competitive inhibition on eIF4F cap-complex formation have not been evaluated in vivo. Using m^7-GTP batch chromatography in PSN1 tumor xenografts we showed inhibition of mTOR activity by INK128 does indeed translate to an inhibition of cap-complex formation in human tumor xenografts. This inhibition of cap-dependent translation in vivo is consistent with the hypothesis that an inhibition of radiation-induced translation is involved in the mechanism of radiosensitization by the mTOR ATP-competitive inhibitor INK128.

The study of in vivo pharmacodynamics and pharmacokinetic properties of a drug is important for the potential clinical translation of a drug, particularly when designing protocols combining multiple treatment modalities. These effects are evidenced by our in vivo tumor growth delay experiments as well as in vitro clonogenic survival data. The initial in vivo tumor growth delay experiment showing a lack of radiosensitization with a single dose of INK128 given immediately after radiation, emphasize the understanding of target engagement in vivo. Both immunohistochemical analysis as well as analysis of cap-complex formation in vivo suggest mTOR activity in PSN1 tumor xenografts is beginning to return to baseline as early as 6h after the initial drug treatment. When combined with the in vitro clonogenic survival data suggesting that mTOR inhibition for greater than 6h is required for effective radiosensitization, a redesign of the protocol to include additional drug dosing was performed. In this protocol, INK128, when given twice daily with radiation, significantly enhanced radiation-induced tumor growth delay,

once again emphasizing the need for a thorough understanding of the pharmacodynamics and pharmacokinetics of drugs both in vitro and in vivo. There are several ATP-competitive inhibitors currently in clinical trials (including INK128) (64). The data presented here showing that INK128 enhances pancreatic cancer radiosensitivity both in vitro and in vivo suggests that these inhibitors delivered in combination with radiotherapy may be of value as a treatment strategy for pancreatic cancer.

CHAPTER 7

Overall Conclusions

As described in the Chapter 1, radiation-induced control of gene expression appears to be controlled primarily at the level of mRNA translation (21-22). The data presented in this thesis begin to elucidate the specific role of critical components of the translational machinery in determining the cellular response to ionizing radiation. While there are numerous regulatory proteins in involved in translational control, eIF4E, S6K, and the mTOR kinase, which regulates both eIF4E and S6K, affect the rate-limiting step of mRNA translation; translation initiation (82). As such the work presented in this thesis focused on determining the role of each protein in the radiation response. In the case of both eIF4E and S6K, the initial studies aimed at determining the role of each protein in controlling cellular radiosensitivity focused on the use of siRNAs targeting these components. In each case, siRNA specific to eIF4E and S6K enhanced the cellular radiosensitivity of tumor lines of various histologies.

For a radiosensitizing compound to be clinically useful it must enhance the response of the tumor to radiation while sparing the normal tissue, as normal tissue toxicity is the dose-limiting factor in radiotherapy. As described previously, inhibition of eIF4E, S6K, and mTOR expression or activity enhanced the radiosensitivity of various tumors, while having no effect on the *in vitro* radiosensitivity of normal tissues. While these were studies were performed only *in vitro* they begin to address whether these regulatory components of the translational machinery could potentially serve as tumor

77

specific targets. While the exact reason for this tumor specificity remains to be determined it is possible to speculate that the established differences in translational regulation between tumor and normal cells may be explanatory. In the context of cellular signaling, tumors have been shown to have aberrant activation of numerous signaling pathways that transduce their signals through mTOR/eIF4E/S6K and hence activate mRNA translation (e.g. RTK, RAS/MAPK, and PI3K) (34, 57-58). In fact 4E-BP1, the major regulator of eIF4E activity, has been referred to as a funnel factor (56), in so much as it exists as a downstream effector of many of the aforementioned hyper-activated oncogenic signaling pathways. Specifically, the translational response to radiation has been shown to differ greatly in tumor and normal cells (21). Lastly, in the context of combination therapy with standard DNA damaging chemotherapies and translation inhibitors, the combination was only synergistic when tumors had deregulated translation (85). As such it is possible to conclude that the tumor specific radiosensitization seen with inhibition of these components of the translational machinery may be due to activation of oncogenic signaling pathways leading to an aberrant translational program. Future studies comparing the translational response of tumor versus normal cells in the context of mTOR inhibition may be used to begin to understand the tumor selectivity of targeting the above-mentioned components of the translational machinery.

mRNA translation and components of the translational machinery have been implicated in cellular transformation and oncogenesis (28). All three critical components of the translational machinery studied in this thesis have individually been shown to be critical for various aspects of cancer initiation and progression (e.g. cell growth, invasion, and cellular transformation) (34, 39, 66, 88). Overexpression and hyperactivity of both

eIF4E (41-42) and the mTOR kinase (60) have been shown to impart a poor prognosis on patients with various tumors . As such, agents aimed at targeting these components have been developed and are currently available for clinical use (64). Some of the agents such as the ISIS eIF4E antisense, mTOR ATP-competitive inhibitors (e.g. INK128), and S6K inhibitors (e.g. LY2584702) have been mentioned previously in this dissertation. The work presented here begins to highlight the importance of the translational machinery in determining tumor survival after radiation. Given the clinical availability of agents targeting the translational machinery as well as the data presented showing that inhibition of these components enhances tumor cell radiosensitivity, it is logical to suggest evaluation of these agents in combination with radiation in the clinical trial setting.

On the basis of analysis γH2AX induction and dispersal, both eIF4E as well as competitive mTOR inhibition appear to inhibit the repair of radiation-induced DNA DSBs. Although direct interaction of eIF4E, mTOR, or an mTOR substrate with a component of the DNA repair machinery cannot be eliminated, the critical role of both proteins in the translational response to a wide variety of environmental and stress signals may provide a mechanistic basis for the observed inhibition of DNA DSB repair. Several studies have shown that inhibition of mTOR activity results in inhibition of translation of mRNA corresponding to DNA repair genes (103, 105). As detailed in Chapter 2, using microarray analysis of eIF4E-bound mRNAs, radiation was shown to induce eIF4E binding to more than 1000 unique transcripts. A significant proportion of these mRNAs encode proteins related to DNA replication, recombination, and repair. In agreement with our results a recent study using microarray analysis of polyribosome-bound mRNA found that radiation-induced translation of mRNAs that were involved in DNA damage

repair, several of which overlapped with proteins our study showed to be increasingly bound to eIF4G after irradiation. Importantly, Singh and colleagues (55) have shown that DNA DSBs are generated not only from the initial radiation exposure, but also from chemical processing occurring for hours after exposure to radiation. In this situation, a rapid induction in DNA damage response proteins may contribute to cell survival after radiation. While our initial studies with eIF4E knockdown were unable to determine whether the tumor cell radiosensitization was due to an inhibition of radiation-induced gene expression, or changes in mRNA translation prior to irradiation, subsequent studies, with post-radiation addition of PP242 and INK128, suggest that the mechanism of radiosensitization involves an inhibition of a radiation-induced process (e.g. gene translation). Thus, mTOR inhibition in the context of altering the radiation-induced translational response is currently the focus of additional studies in our laboratory.

In summary, the data provided in this thesis have begun to characterize the role of the translational machinery in determining the cellular response to radiation. While there is work that remains to be completed in understanding the exact mechanisms involved in the radiosensitization seen by targeting components of the translational machinery, we believe the work presented in this thesis argue that targeting components of the translational machinery is a strategy that deserves consideration for evaluation in the clinical trial setting.

REFERENCES

1.   Amundson SA, Bittner M, Chen Y, Trent J, Meltzer P, Fornace AJ, Jr. Fluorescent cDNA microarray hybridization reveals complexity and heterogeneity of cellular genotoxic stress responses. Oncogene. 1999;18:3666-72.

2.   Azzam EI, de Toledo SM, Little JB. Expression of CONNEXIN43 is highly sensitive to ionizing radiation and other environmental stresses. Cancer Research. 2003;63:7128-35.

3.   Khodarev NN, Park JO, Yu J, Gupta N, Nodzenski E, Roizman B, et al. Dose-dependent and independent temporal patterns of gene responses to ionizing radiation in normal and tumor cells and tumor xenografts. Proceedings of the National Academy of Sciences of the United States of America. 2001;98:12665-70.

4.   Kruse JJ, te Poele JA, Russell NS, Boersma LJ, Stewart FA. Microarray analysis to identify molecular mechanisms of radiation-induced microvascular damage in normal tissues. International Journal of Radiation Oncology, Biology, Physics. 2004;58:420-6.

5.   Otomo T, Hishii M, Arai H, Sato K, Sasai K. Microarray analysis of temporal gene responses to ionizing radiation in two glioblastoma cell lines: up-regulation of DNA repair genes. J Radiat Res. 2004;45:53-60.

6.   Yin E, Nelson DO, Coleman MA, Peterson LE, Wyrobek AJ. Gene expression changes in mouse brain after exposure to low-dose ionizing radiation. International Journal of Radiation Biology. 2003;79:759-75.

7.   Szkanderova S, Port M, Stulik J, Hernychova L, Kasalova I, Van Beuningen D, et al. Comparison of the abundance of 10 radiation-induced proteins with their differential gene expression in L929 cells. International Journal of Radiation Biology. 2003;79:623-33.

8.   Birrell GW, Brown JA, Wu HI, Giaever G, Chu AM, Davis RW, et al. Transcriptional response of Saccharomyces cerevisiae to DNA-damaging agents does not identify the genes that protect against these agents. Proc Natl Acad Sci U S A. 2002;99:8778-83.

9.   Gygi SP, Rochon Y, Franza BR, Aebersold R. Correlation between protein and mRNA abundance in yeast. Mol Cell Biol. 1999;19:1720-30.

10.   Ideker T, Thorsson V, Ranish JA, Christmas R, Buhler J, Eng JK, et al. Integrated genomic and proteomic analyses of a systematically perturbed metabolic network. Science. 2001;292:929-34.

11.   Shenton D, Smirnova JB, Selley JN, Carroll K, Hubbard SJ, Pavitt GD, et al. Global translational responses to oxidative stress impact upon multiple levels of protein synthesis. J Biol Chem. 2006;281:29011-21.

12.   Smirnova JB, Selley JN, Sanchez-Cabo F, Carroll K, Eddy AA, McCarthy JE, et al. Global gene expression profiling reveals widespread yet distinctive translational responses to different eukaryotic translation initiation factor 2B-targeting stress pathways. Mol Cell Biol. 2005;25:9340-9.

13.   Shankavaram UT, Reinhold WC, Nishizuka S, Major S, Morita D, Chary KK, et al. Transcript and protein expression profiles of the NCI-60 cancer cell panel: an integromic microarray study. Mol Cancer Ther. 2007;6:820-32.

14.   Harding HP, Novoa I, Zhang Y, Zeng H, Wek R, Schapira M, et al. Regulated translation initiation controls stress-induced gene expression in mammalian cells. Mol Cell. 2000;6:1099-108.

15.   Pradet-Balade B, Boulme F, Beug H, Mullner EW, Garcia-Sanz JA. Translation control: bridging the gap between genomics and proteomics? Trends in biochemical sciences. 2001;26:225-9.

16.   Wilkie GS, Dickson KS, Gray NK. Regulation of mRNA translation by 5'- and 3'-UTR-binding factors. Trends in biochemical sciences. 2003;28:182-8.

17.   Kuersten S, Goodwin EB. The power of the 3' UTR: translational control and development. Nature reviews Genetics. 2003;4:626-37.

18.   Mikulits W, Pradet-Balade B, Habermann B, Beug H, Garcia-Sanz JA, Mullner EW. Isolation of translationally controlled mRNAs by differential screening. FASEB journal : official publication of the Federation of American Societies for Experimental Biology. 2000;14:1641-52.

19.   Petroulakis E, Wang E. Nerve growth factor specifically stimulates translation of eukaryotic elongation factor 1A-1 (eEF1A-1) mRNA by recruitment to polyribosomes in PC12 cells. J Biol Chem. 2002;277:18718-27.

20.   Rajasekhar VK, Viale A, Socci ND, Wiedmann M, Hu X, Holland EC. Oncogenic Ras and Akt signaling contribute to glioblastoma formation by differential recruitment of existing mRNAs to polysomes. Mol Cell. 2003;12:889-901.

21.   Kumaraswamy S, Chinnaiyan P, Shankavaram UT, Lu X, Camphausen K, Tofilon PJ. Radiation-induced gene translation profiles reveal tumor type and cancer-specific components. Cancer Res. 2008;68:3819-26.

22.   Lu X, de la Pena L, Barker C, Camphausen K, Tofilon PJ. Radiation-induced changes in gene expression involve recruitment of existing messenger RNAs to and away from polysomes. Cancer Res. 2006;66:1052-61.

82

23.   Badura M, Braunstein S, Zavadil J, Schneider RJ. DNA damage and eIF4G1 in breast cancer cells reprogram translation for survival and DNA repair mRNAs. Proc Natl Acad Sci U S A. 2012;109:18767-72.

24.   Keene JD. RNA regulons: coordination of post-transcriptional events. Nature reviews Genetics. 2007;8:533-43.

25.   Braunstein S, Badura ML, Xi Q, Formenti SC, Schneider RJ. Regulation of protein synthesis by ionizing radiation. Mol Cell Biol. 2009;29:5645-56.

26.   Masuda K, Abdelmohsen K, Kim MM, Srikantan S, Lee EK, Tominaga K, et al. Global dissociation of HuR-mRNA complexes promotes cell survival after ionizing radiation. The EMBO journal. 2011;30:1040-53.

27.   Mazan-Mamczarz K, Hagner PR, Zhang Y, Dai B, Lehrmann E, Becker KG, et al. ATM regulates a DNA damage response posttranscriptional RNA operon in lymphocytes. Blood. 2011;117:2441-50.

28.   Sonenberg N, Hinnebusch AG. Regulation of translation initiation in eukaryotes: mechanisms and biological targets. Cell. 2009;136:731-45.

29.   Ma XM, Blenis J. Molecular mechanisms of mTOR-mediated translational control. Nat Rev Mol Cell Biol. 2009;10:307-18.

30.   Li Y, Yue P, Deng X, Ueda T, Fukunaga R, Khuri FR, et al. Protein phosphatase 2A negatively regulates eukaryotic initiation factor 4E phosphorylation and eIF4F assembly through direct dephosphorylation of Mnk and eIF4E. Neoplasia. 2010;12:848-55.

31.   Edgar R, Domrachev M, Lash AE. Gene Expression Omnibus: NCBI gene expression and hybridization array data repository. Nucleic Acids Res. 2002;30:207-10.

32.   Hsieh AC, Truitt ML, Ruggero D. Oncogenic AKTivation of translation as a therapeutic target. Br J Cancer. 2011;105:329-36.

33.   Culjkovic B, Borden KL. Understanding and Targeting the Eukaryotic Translation Initiation Factor eIF4E in Head and Neck Cancer. J Oncol. 2009;2009:981679.

34.   Graff JR, Konicek BW, Carter JH, Marcusson EG. Targeting the eukaryotic translation initiation factor 4E for cancer therapy. Cancer Res. 2008;68:631-4.

35.   Mamane Y, Petroulakis E, Rong L, Yoshida K, Ler LW, Sonenberg N. eIF4E-- from translation to transformation. Oncogene. 2004;23:3172-9.

36.   Larsson O, Li S, Issaenko OA, Avdulov S, Peterson M, Smith K, et al. Eukaryotic translation initiation factor 4E induced progression of primary human mammary epithelial cells along the cancer pathway is associated with targeted translational deregulation of oncogenic drivers and inhibitors. Cancer Res. 2007;67:6814-24.

37.   Lazaris-Karatzas A, Montine KS, Sonenberg N. Malignant transformation by a eukaryotic initiation factor subunit that binds to mRNA 5' cap. Nature. 1990;345:544-7.

38.   Ruggero D, Montanaro L, Ma L, Xu W, Londei P, Cordon-Cardo C, et al. The translation factor eIF-4E promotes tumor formation and cooperates with c-Myc in lymphomagenesis. Nat Med. 2004;10:484-6.

39.   Graff JR, Konicek BW, Lynch RL, Dumstorf CA, Dowless MS, McNulty AM, et al. eIF4E activation is commonly elevated in advanced human prostate cancers and significantly related to reduced patient survival. Cancer Res. 2009;69:3866-73.

40.   De Benedetti A, Harris AL. eIF4E expression in tumors: its possible role in progression of malignancies. Int J Biochem Cell Biol. 1999;31:59-72.

41.   Chen CN, Hsieh FJ, Cheng YM, Lee PH, Chang KJ. Expression of eukaryotic initiation factor 4E in gastric adenocarcinoma and its association with clinical outcome. J Surg Oncol. 2004;86:22-7.

42.   Pettersson F, Yau C, Dobocan MC, Culjkovic-Kraljacic B, Retrouvey H, Puckett R, et al. Ribavirin treatment effects on breast cancers overexpressing eIF4E, a biomarker with prognostic specificity for luminal B-type breast cancer. Clin Cancer Res. 2011;17:2874-84.

43.   Graff JR, Konicek BW, Vincent TM, Lynch RL, Monteith D, Weir SN, et al. Therapeutic suppression of translation initiation factor eIF4E expression reduces tumor growth without toxicity. J Clin Invest. 2007;117:2638-48.

44.   Kentsis A, Topisirovic I, Culjkovic B, Shao L, Borden KL. Ribavirin suppresses eIF4E-mediated oncogenic transformation by physical mimicry of the 7-methyl guanosine mRNA cap. Proc Natl Acad Sci U S A. 2004;101:18105-10.

45.   Culjkovic B, Topisirovic I, Skrabanek L, Ruiz-Gutierrez M, Borden KL. eIF4E is a central node of an RNA regulon that governs cellular proliferation. J Cell Biol. 2006;175:415-26.

46.   Dong K, Wang R, Wang X, Lin F, Shen JJ, Gao P, et al. Tumor-specific RNAi targeting eIF4E suppresses tumor growth, induces apoptosis and enhances cisplatin cytotoxicity in human breast carcinoma cells. Breast Cancer Res Treat. 2009;113:443-56.

47.   Bonner WM, Redon CE, Dickey JS, Nakamura AJ, Sedelnikova OA, Solier S, et al. GammaH2AX and cancer. Nat Rev Cancer. 2008;8:957-67.

48.   Lobrich M, Shibata A, Beucher A, Fisher A, Ensminger M, Goodarzi AA, et al. gammaH2AX foci analysis for monitoring DNA double-strand break repair: strengths, limitations and optimization. Cell Cycle. 2010;9:662-9.

49.   Hay N, Sonenberg N. Upstream and downstream of mTOR. Genes Dev. 2004;18:1926-45.

50.   Furic L, Rong L, Larsson O, Koumakpayi IH, Yoshida K, Brueschke A, et al. eIF4E phosphorylation promotes tumorigenesis and is associated with prostate cancer progression. Proc Natl Acad Sci U S A. 2010;107:14134-9.

51.   Morgan MA, Parsels LA, Zhao L, Parsels JD, Davis MA, Hassan MC, et al. Mechanism of radiosensitization by the Chk1/2 inhibitor AZD7762 involves abrogation of the G2 checkpoint and inhibition of homologous recombinational DNA repair. Cancer Res. 2010;70:4972-81.

52.   Post S, Weng YC, Cimprich K, Chen LB, Xu Y, Lee EY. Phosphorylation of serines 635 and 645 of human Rad17 is cell cycle regulated and is required for G(1)/S checkpoint activation in response to DNA damage. Proc Natl Acad Sci U S A. 2001;98:13102-7.

53.   Zhao H, Luoto KR, Meng AX, Bristow RG. The receptor tyrosine kinase inhibitor amuvatinib (MP470) sensitizes tumor cells to radio- and chemo-therapies in part by inhibiting homologous recombination. Radiother Oncol. 2011;101:59-65.

54.   Tan K, Culjkovic B, Amri A, Borden KL. Ribavirin targets eIF4E dependent Akt survival signaling. Biochem Biophys Res Commun. 2008;375:341-5.

55.   Singh SK, Wang M, Staudt C, Iliakis G. Post-irradiation chemical processing of DNA damage generates double-strand breaks in cells already engaged in repair. Nucleic Acids Res. 2011;39:8416-29.

56.   Armengol G, Rojo F, Castellvi J, Iglesias C, Cuatrecasas M, Pons B, et al. 4E-binding protein 1: a key molecular "funnel factor" in human cancer with clinical implications. Cancer Res. 2007;67:7551-5.

57.   She QB, Halilovic E, Ye Q, Zhen W, Shirasawa S, Sasazuki T, et al. 4E-BP1 is a key effector of the oncogenic activation of the AKT and ERK signaling pathways that integrates their function in tumors. Cancer Cell. 2010;18:39-51.

58.   Zindy P, Berge Y, Allal B, Filleron T, Pierredon S, Cammas A, et al. Formation of the eIF4F translation-initiation complex determines sensitivity to anticancer drugs targeting the EGFR and HER2 receptors. Cancer Res. 2011;71:4068-73.

59.   Hsieh AC, Ruggero D. Targeting eukaryotic translation initiation factor 4E (eIF4E) in cancer. Clin Cancer Res. 2010;16:4914-20.

85

60.   Dowling RJ, Topisirovic I, Fonseca BD, Sonenberg N. Dissecting the role of mTOR: lessons from mTOR inhibitors. Biochim Biophys Acta. 2010;1804:433-9.

61.   Moerke NJ, Aktas H, Chen H, Cantel S, Reibarkh MY, Fahmy A, et al. Small-molecule inhibition of the interaction between the translation initiation factors eIF4E and eIF4G. Cell. 2007;128:257-67.

62.   Assouline S, Culjkovic B, Cocolakis E, Rousseau C, Beslu N, Amri A, et al. Molecular targeting of the oncogene eIF4E in acute myeloid leukemia (AML): a proof-of-principle clinical trial with ribavirin. Blood. 2009;114:257-60.

63.   Hong DS, Kurzrock R, Oh Y, Wheler J, Naing A, Brail L, et al. A phase 1 dose escalation, pharmacokinetic, and pharmacodynamic evaluation of eIF-4E antisense oligonucleotide LY2275796 in patients with advanced cancer. Clin Cancer Res. 2011;17:6582-91.

64.   ClinicalTrials.gov [database on the Internet]. Bethesda (MD): National Library of Medicine (US); 2000 - [cited 2012 August 1]; Available from: http://clinicaltrials.gov/

65.   Zoncu R, Efeyan A, Sabatini DM. mTOR: from growth signal integration to cancer, diabetes and ageing. Nat Rev Mol Cell Biol. 2011;12:21-35.

66.   Ip CK, Wong AS. Exploiting p70 S6 kinase as a target for ovarian cancer. Expert Opin Ther Targets. 2012;16:619-30.

67.   Hagner PR, Mazan-Mamczarz K, Dai B, Balzer EM, Corl S, Martin SS, et al. Ribosomal protein S6 is highly expressed in non-Hodgkin lymphoma and associates with mRNA containing a 5' terminal oligopyrimidine tract. Oncogene. 2011;30:1531-41.

68.   Tang H, Hornstein E, Stolovich M, Levy G, Livingstone M, Templeton D, et al. Amino acid-induced translation of TOP mRNAs is fully dependent on phosphatidylinositol 3-kinase-mediated signaling, is partially inhibited by rapamycin, and is independent of S6K1 and rpS6 phosphorylation. Mol Cell Biol. 2001;21:8671-83.

69.   Damgaard CK, Lykke-Andersen J. Translational coregulation of 5'TOP mRNAs by TIA-1 and TIAR. Genes and Development. 2011;25:2057-68.

70.   Dorrello NV, Peschiaroli A, Guardavaccaro D, Colburn NH, Sherman NE, Pagano M. S6K1- and betaTRCP-mediated degradation of PDCD4 promotes protein translation and cell growth. Science. 2006;314:467-71.

71.   Chang JH, Cho YH, Sohn SY, Choi JM, Kim A, Kim YC, et al. Crystal structure of the eIF4A-PDCD4 complex. Proceedings of the National Academy of Sciences of the United States of America. 2009;106:3148-53.

72.   Singh P, Marikkannu R, Bitomsky N, Klempnauer KH. Disruption of the Pdcd4 tumor suppressor gene in chicken DT40 cells reveals its role in the DNA-damage response. Oncogene. 2009;28:3758-64.

73.   Wedeken L, Singh P, Klempnauer KH. Tumor suppressor protein Pdcd4 inhibits translation of p53 mRNA. J Biol Chem. 2011;286:42855-62.

74.   Bitomsky N, Wethkamp N, Marikkannu R, Klempnauer KH. siRNA-mediated knockdown of Pdcd4 expression causes upregulation of p21(Waf1/Cip1) expression. Oncogene. 2008;27:4820-9.

75.   Averous J, Proud CG. When translation meets transformation: the mTOR story. Oncogene. 2006;25:6423-35.

76.   Chakravarti A, Zhai G, Suzuki Y, Sarkesh S, Black PM, Muzikansky A, et al. The prognostic significance of phosphatidylinositol 3-kinase pathway activation in human gliomas. J Clin Oncol. 2004;22:1926-33.

77.   Filonenko VV, Tytarenko R, Azatjan SK, Savinska LO, Gaydar YA, Gout IT, et al. Immunohistochemical analysis of S6K1 and S6K2 localization in human breast tumors. Exp Oncol. 2004;26:294-9.

78.   Nozawa H, Watanabe T, Nagawa H. Phosphorylation of ribosomal p70 S6 kinase and rapamycin sensitivity in human colorectal cancer. Cancer Lett. 2007;251:105-13.

79.   Sahin F, Kannangai R, Adegbola O, Wang J, Su G, Torbenson M. mTOR and P70 S6 kinase expression in primary liver neoplasms. Clin Cancer Res. 2004;10:8421-5.

80.   Nakamura JL, Garcia E, Pieper RO. S6K1 plays a key role in glial transformation. Cancer Res. 2008;68:6516-23.

81.   Sridharan S, Basu A. S6 kinase 2 promotes breast cancer cell survival via Akt. Cancer Res. 2011;71:2590-9.

82.   Laplante M, Sabatini DM. mTOR signaling in growth control and disease. Cell. 2012;149:274-93.

83.   Jin C, Rajabi H, Rodrigo CM, Porco JA, Jr., Kufe D. Targeting the eIF4A RNA helicase blocks translation of the MUC1-C oncoprotein. Oncogene. 2012.

84.   Schatz JH, Oricchio E, Wolfe AL, Jiang M, Linkov I, Maragulia J, et al. Targeting cap-dependent translation blocks converging survival signals by AKT and PIM kinases in lymphoma. J Exp Med. 2011;208:1799-807.

85.   Bordeleau ME, Robert F, Gerard B, Lindqvist L, Chen SM, Wendel HG, et al. Therapeutic suppression of translation initiation modulates chemosensitivity in a mouse lymphoma model. J Clin Invest. 2008;118:2651-60.

86.   Silvera D, Connolly E, Arju R, Venetu T, Schneider R. Targeting mRNA Translation to Enhance the Radiosensitivity of Inflammatory Breast Cancer Stem Cells Cancer Res. 2012;73(24 Suppl):P5-03-2.

87.   Chresta CM, Davies BR, Hickson I, Harding T, Cosulich S, Critchlow SE, et al. AZD8055 is a potent, selective, and orally bioavailable ATP-competitive mammalian target of rapamycin kinase inhibitor with in vitro and in vivo antitumor activity. Cancer Res. 2010;70:288-98.

88.   Guertin DA, Sabatini DM. Defining the role of mTOR in cancer. Cancer Cell. 2007;12:9-22.

89.   Willems L, Tamburini J, Chapuis N, Lacombe C, Mayeux P, Bouscary D. PI3K and mTOR signaling pathways in cancer: new data on targeted therapies. Curr Oncol Rep. 2012;14:129-38.

90.   Benjamin D, Colombi M, Moroni C, Hall MN. Rapamycin passes the torch: a new generation of mTOR inhibitors. Nat Rev Drug Discov. 2011;10:868-80.

91.   Choo AY, Blenis J. Not all substrates are treated equally: implications for mTOR, rapamycin-resistance and cancer therapy. Cell Cycle. 2009;8:567-72.

92.   Feldman ME, Apsel B, Uotila A, Loewith R, Knight ZA, Ruggero D, et al. Active-site inhibitors of mTOR target rapamycin-resistant outputs of mTORC1 and mTORC2. PLoS Biol. 2009;7:e38.

93.   Hsieh AC, Costa M, Zollo O, Davis C, Feldman ME, Testa JR, et al. Genetic dissection of the oncogenic mTOR pathway reveals druggable addiction to translational control via 4EBP-eIF4E. Cancer Cell. 2010;17:249-61.

94.   Thoreen CC, Kang SA, Chang JW, Liu Q, Zhang J, Gao Y, et al. An ATP-competitive mammalian target of rapamycin inhibitor reveals rapamycin-resistant functions of mTORC1. J Biol Chem. 2009;284:8023-32.

95.   Yu K, Shi C, Toral-Barza L, Lucas J, Shor B, Kim JE, et al. Beyond rapalog therapy: preclinical pharmacology and antitumor activity of WYE-125132, an ATP-competitive and specific inhibitor of mTORC1 and mTORC2. Cancer Res. 2010;70:621-31.

96.   Choo AY, Yoon SO, Kim SG, Roux PP, Blenis J. Rapamycin differentially inhibits S6Ks and 4E-BP1 to mediate cell-type-specific repression of mRNA translation. Proc Natl Acad Sci U S A. 2008;105:17414-9.

97.   Albert JM, Kim KW, Cao C, Lu B. Targeting the Akt/mammalian target of rapamycin pathway for radiosensitization of breast cancer. Mol Cancer Ther. 2006;5:1183-9.

98.   Murphy JD, Spalding AC, Somnay YR, Markwart S, Ray ME, Hamstra DA. Inhibition of mTOR radiosensitizes soft tissue sarcoma and tumor vasculature. Clin Cancer Res. 2009;15:589-96.

99.   Cao C, Subhawong T, Albert JM, Kim KW, Geng L, Sekhar KR, et al. Inhibition of mammalian target of rapamycin or apoptotic pathway induces autophagy and radiosensitizes PTEN null prostate cancer cells. Cancer Res. 2006;66:10040-7.

100.   Ekshyyan O, Rong Y, Rong X, Pattani KM, Abreo F, Caldito G, et al. Comparison of radiosensitizing effects of the mammalian target of rapamycin inhibitor CCI-779 to cisplatin in experimental models of head and neck squamous cell carcinoma. Mol Cancer Ther. 2009;8:2255-65.

101.   Eshleman JS, Carlson BL, Mladek AC, Kastner BD, Shide KL, Sarkaria JN. Inhibition of the mammalian target of rapamycin sensitizes U87 xenografts to fractionated radiation therapy. Cancer Res. 2002;62:7291-7.

102.   Rosenzweig KE, Youmell MB, Palayoor ST, Price BD. Radiosensitization of human tumor cells by the phosphatidylinositol3-kinase inhibitors wortmannin and LY294002 correlates with inhibition of DNA-dependent protein kinase and prolonged G2-M delay. Clin Cancer Res. 1997;3:1149-56.

103.   Larsson O, Morita M, Topisirovic I, Alain T, Blouin MJ, Pollak M, et al. Distinct perturbation of the translatome by the antidiabetic drug metformin. Proc Natl Acad Sci U S A. 2012;109:8977-82.

104.   Hayman TJ, Williams ES, Jamal M, Shankavaram UT, Camphausen K, Tofilon PJ. Translation initiation factor eIF4E is a target for tumor cell radiosensitization. Cancer Res. 2012;72:2362-72.

105.   Hsieh AC, Liu Y, Edlind MP, Ingolia NT, Janes MR, Sher A, et al. The translational landscape of mTOR signalling steers cancer initiation and metastasis. Nature. 2012;485:55-61.

106.   Contessa JN, Hampton J, Lammering G, Mikkelsen RB, Dent P, Valerie K, et al. Ionizing radiation activates Erb-B receptor dependent Akt and p70 S6 kinase signaling in carcinoma cells. Oncogene. 2002;21:4032-41.

107.   Li H, Lin J, Wang X, Yao G, Wang L, Zheng H, et al. Targeting of mTORC2 prevents cell migration and promotes apoptosis in breast cancer. Breast Cancer Res Treat. 2012;134:1057-66.

108.   Hayman TJ, Kramp T, Kahn J, Jamal M, Camphausen K, Tofilon PJ. Competitive but not allosteric mTOR kinase inhibition enhances tumor cell radiosensitivity. Translational Oncology. 2013;6:In Press.

109.   Hidalgo M. Pancreatic cancer. N Engl J Med. 2010;362:1605-17.

110.   Raimondi S, Maisonneuve P, Lowenfels AB. Epidemiology of pancreatic cancer: an overview. Nat Rev Gastroenterol Hepatol. 2009;6:699-708.

111.   Sharma C, Eltawil KM, Renfrew PD, Walsh MJ, Molinari M. Advances in diagnosis, treatment and palliation of pancreatic carcinoma: 1990-2010. World J Gastroenterol. 2011;17:867-97.

112.   Iacobuzio-Donahue CA, Fu B, Yachida S, Luo M, Abe H, Henderson CM, et al. DPC4 gene status of the primary carcinoma correlates with patterns of failure in patients with pancreatic cancer. J Clin Oncol. 2009;27:1806-13.

113.   Wei D, Li H, Yu J, Sebolt JT, Zhao L, Lawrence TS, et al. Radiosensitization of human pancreatic cancer cells by MLN4924, an investigational NEDD8-activating enzyme inhibitor. Cancer Res. 2012;72:282-93.

114.   Hezel AF, Kimmelman AC, Stanger BZ, Bardeesy N, Depinho RA. Genetics and biology of pancreatic ductal adenocarcinoma. Genes Dev. 2006;20:1218-49.

115.   Bellizzi AM, Bloomston M, Zhou XP, Iwenofu OH, Frankel WL. The mTOR pathway is frequently activated in pancreatic ductal adenocarcinoma and chronic pancreatitis. Appl Immunohistochem Mol Morphol. 2010;18:442-7.

APPENDIX

Table A1: List of 1124 genes increasingly bound to eIF4E after irradiation

Fold Increase	Gene Symbol	Gene Description		Fold Increase	Gene Symbol	Gene Description
						dehydrogenase, type III)
2.2	ABCA11	ATP-binding cassette, sub-family A (ABC1), member 11 (pseudogene)		1.8	AKR7A2	aldo-keto reductase family 7, member A2 (aflatoxin aldehyde reductase)
3.1	ABHD4	abhydrolase domain containing 4		4.1	ALKBH	alkB, alkylation repair homolog (E. coli)
1.9	ABHD6	abhydrolase domain containing 6		1.9	AMFR	autocrine motility factor receptor
1.5	ABT1	activator of basal transcription 1		1.7	ANAPC5	anaphase promoting complex subunit 5
1.8	ACAD8	acyl-Coenzyme A dehydrogenase family, member 8		1.8	ANKRD40	ankyrin repeat domain 40
1.8	ACAT1	acetyl-Coenzyme A acetyltransferase 1 (acetoacetyl Coenzyme A thiolase)		4.5	ANXA11	annexin A11
				1.5	AP4M1	adaptor-related protein complex 4, mu 1 subunit
1.7	ACOT7	acyl-CoA thioesterase 7		1.7	APBB1	amyloid beta (A4) precursor protein-binding, family B, member 1 (Fe65)
1.5	ACOT9	acyl-CoA thioesterase 9				
1.6	ACTR5	ARP5 actin-related protein 5 homolog (yeast)		2	APLP2	amyloid beta (A4) precursor-like protein 2
3	ADCK2	aarF domain containing kinase 2		1.5	APOL3	apolipoprotein L, 3
1.8	ADPGK	ADP-dependent glucokinase		1.5	APTX	aprataxin
2.4	ADSL	adenylosuccinate lyase		2.9	ARF3	ADP-ribosylation factor 3
2.2	AGPAT2	1-acylglycerol-3-phosphate O-acyltransferase 2 (lysophosphatidic acid acyltransferase, beta)		1.5	ARL6IP5	ADP-ribosylation-like factor 6 interacting protein 5
				10.8	ARPC2	actin related protein 2/3 complex, subunit 2, 34kDa
1.5	AIM1L	absent in melanoma 1-like		1.5	ARRB2	arrestin, beta 2
1.5	AKR1C2	aldo-keto reductase family 1, member C2 (dihydrodiol dehydrogenase 2; bile acid binding protein; 3-alpha hydroxysteroid		1.8	ASB13	ankyrin repeat and SOCS box-containing 13
				11.2	ASCIZ	ATM/ATR-Substrate Chk2-Interacting Zn2+-finger protein
				2.3	ATP1B3	ATPase, Na+/K+ transporting, beta 3

92

		polypeptide
1.7	ATP5B	ATP synthase, H+ transporting, mitochondrial F1 complex, beta polypeptide
1.6	ATP5C1	ATP synthase, H+ transporting, mitochondrial F1 complex, gamma polypeptide 1
1.5	ATP5L	ATP synthase, H+ transporting, mitochondrial F0 complex, subunit g
2	ATP6V0E	ATPase, H+ transporting, lysosomal 9kDa, V0 subunit e
1.6	ATP6V1D	ATPase, H+ transporting, lysosomal 34kDa, V1 subunit D
1.8	ATP8A2	ATPase, aminophospholipid transporter-like, Class I, type 8A, member 2
1.8	ATPAF2	ATP synthase mitochondrial F1 complex assembly factor 2
2.2	B4GALT4	UDP-Gal:betaGlcNAc beta 1,4-galactosyltransferase, polypeptide 4
8.6	BBP	Beta-amyloid binding protein precursor
2.1	BBS4	Bardet-Biedl syndrome 4
1.7	BCAT1	branched chain aminotransferase 1, cytosolic
2.6	BCL10	B-cell CLL/lymphoma 10
4.7	BCL2L11	BCL2-like 11 (apoptosis facilitator)
3.5	BIRC5	baculoviral IAP repeat-containing 5 (survivin)
2.1	BMPR1A	bone morphogenetic protein receptor, type IA
1.7	BNIP2	BCL2/adenovirus E1B 19kDa interacting protein 2
1.9	BNIP3	BCL2/adenovirus E1B 19kDa interacting protein 3
1.7	BRE	brain and reproductive organ-expressed (TNFRSF1A modulator)
2.3	BTG1	B-cell translocation gene 1, anti-proliferative
1.6	C10orf57	chromosome 10 open reading frame 57
2.7	C10orf61	chromosome 10 open reading frame 61
2	C10orf97	chromosome 10 open reading frame 97
1.7	C11orf24	chromosome 11 open reading frame 24
4.8	C12orf41	chromosome 12 open reading frame 41
1.6	C12orf49	chromosome 12 open reading frame 49
1.6	C12orf52	chromosome 12 open reading frame 52
1.7	C14orf138	chromosome 14 open reading frame 138
1.5	C14orf172	chromosome 14 open reading frame 172
1.5	C16orf45	chromosome 16 open reading frame 45
1.7	C16orf58	chromosome 16 open reading frame 58
1.6	C17orf39	chromosome 17 open reading frame 39
1.8	C19orf2	chromosome 19 open reading frame

93

		2
1.5	C19orf50	chromosome 19 open reading frame 50
8.2	C1orf144	chromosome 1 open reading frame 144
7.4	C1orf163	chromosome 1 open reading frame 163
1.7	C1orf174	chromosome 1 open reading frame 174
1.8	C1orf33	chromosome 1 open reading frame 33
4.8	C20orf111	chromosome 20 open reading frame 111
1.7	C20orf24	chromosome 20 open reading frame 24
3	C20orf29	chromosome 20 open reading frame 29
5.3	C20orf44	chromosome 20 open reading frame 44
3.8	C20orf45	chromosome 20 open reading frame 45
3	C21orf91	chromosome 21 open reading frame 91
4.8	C2orf43	chromosome 2 open reading frame 43
1.5	C3orf18	chromosome 3 open reading frame 18
1.7	C3orf37	chromosome 3 open reading frame 37
1.8	C5orf30	chromosome 5 open reading frame 30
3.7	C6orf106	chromosome 6 open reading frame 106
4	C6orf49	chromosome 6 open reading frame 49
1.8	C6orf82	chromosome 6 open reading frame 82
1.6	C7orf26	chromosome 7 open reading frame 26
10	C8orf30A	chromosome 8 open reading frame 30A
3	C9orf78	chromosome 9 open reading frame 78
5.4	C9orf82	chromosome 9 open reading frame 82
4.1	CABIN1	calcineurin binding protein 1
6.1	CALM1	calmodulin 1 (phosphorylase kinase, delta)
4.3	CAMLG	calcium modulating ligand
2.3	CAMTA2	calmodulin binding transcription activator 2
4.7	CASP3	caspase 3, apoptosis-related cysteine peptidase
1.8	CASP9	caspase 9, apoptosis-related cysteine peptidase
1.5	CAV2	caveolin 2
2.2	CCDC132	coiled-coil domain containing 132
3.9	CCNA1	cyclin A1
1.7	CCNA2	cyclin A2
1.6	CCNB1IP1	cyclin B1 interacting protein 1
2.5	CCNE2	cyclin E2
1.9	CCS	copper chaperone for superoxide dismutase
3	CD164	CD164 antigen, sialomucin
1.7	CD59	CD59 antigen p18-20 (antigen identified by monoclonal antibodies 16.3A5, EJ16, EJ30, EL32 and G344)
4.3	CD63	CD63 antigen (melanoma 1 antigen)
1.6	CDC2	cell division cycle 2, G1 to S and G2 to M

94

4.9	CDC25C	cell division cycle 25C
2.2	CDC42EP2	CDC42 effector protein (Rho GTPase binding) 2
1.6	CDCA4	cell division cycle associated 4
1.7	CDKL3	cyclin-dependent kinase-like 3
1.9	CDKN1A	cyclin-dependent kinase inhibitor 1A (p21, Cip1)
1.7	CDKN2C	cyclin-dependent kinase inhibitor 2C (p18, inhibits CDK4)
1.5	CDKN3	cyclin-dependent kinase inhibitor 3 (CDK2-associated dual specificity phosphatase)
2.3	CDYL	chromodomain protein, Y-like
2	CENPB	centromere protein B, 80kDa
3.2	CENPO	centromere protein O
6.1	CEP57	centrosomal protein 57kDa
1.5	CEPT1	choline/ethanolamine phosphotransferase 1
2.3	CHCHD7	coiled-coil-helix-coiled-coil-helix domain containing 7
7.6	CHEK1	CHK1 checkpoint homolog (S. pombe)
3.1	CHST10	carbohydrate sulfotransferase 10
1.8	CIDEC	cell death-inducing DFFA-like effector c
1.6	CINP	cyclin-dependent kinase 2-interacting protein
2.2	CIR	CBF1 interacting corepressor
3.1	CLIC1	chloride intracellular channel 1
5.5	CLIC4	chloride intracellular channel 4

2	CLINT1	clathrin interactor 1
1.5	CLN5	ceroid-lipofuscinosis, neuronal 5
1.7	CLTA	clathrin, light polypeptide (Lca)
7.5	CNGA1	cyclic nucleotide gated channel alpha 1
2.3	CNIH3	cornichon homolog 3 (Drosophila)
1.9	CNKSR1	connector enhancer of kinase suppressor of Ras 1
5.5	CNP	2',3'-cyclic nucleotide 3' phosphodiesterase
9.9	COG2	component of oligomeric golgi complex 2
1.7	COPS2	COP9 constitutive photomorphogenic homolog subunit 2 (Arabidopsis)
6.1	COPS7B	COP9 constitutive photomorphogenic homolog subunit 7B (Arabidopsis)
1.5	COPS8	COP9 constitutive photomorphogenic homolog subunit 8 (Arabidopsis)
1.9	COQ2	coenzyme Q2 homolog, prenyltransferase (yeast)
1.8	COTL1	coactosin-like 1 (Dictyostelium)
3.5	COX11	COX11 homolog, cytochrome c oxidase assembly protein (yeast)
1.5	COX7A2	cytochrome c oxidase subunit VIIa polypeptide 2 (liver)
1.8	COX7B	cytochrome c oxidase subunit VIIb
1.5	CREB1	cAMP responsive element binding protein 1
2.3	CREG1	cellular repressor of E1A-stimulated

95

		genes 1
2.1	CRELD1	cysteine-rich with EGF-like domains 1
15.7	CRI1	CREBBP/EP300 inhibitor 1
1.5	CSNK1A1	casein kinase 1, alpha 1
6.2	CTBP2	C-terminal binding protein 2
4.4	CTDSP1	CTD (carboxy-terminal domain, RNA polymerase II, polypeptide A) small phosphatase 1
2.5	CTDSP2	CTD (carboxy-terminal domain, RNA polymerase II, polypeptide A) small phosphatase 2
1.7	CTDSPL	CTD (carboxy-terminal domain, RNA polymerase II, polypeptide A) small phosphatase-like
2.4	CTGLF1	centaurin, gamma-like family, member 1
6.5	CTH	cystathionase (cystathionine gamma-lyase)
1.7	CTSB	cathepsin B
1.8	CTSS	cathepsin S
1.9	CXorf12	chromosome X open reading frame 12
3.9	CXorf15	chromosome X open reading frame 15
5.5	CYB5B	cytochrome b5 type B (outer mitochondrial membrane)
2.5	CYB5R3	cytochrome b5 reductase 3
4.3	DBT	dihydrolipoamide branched chain transacylase E2
24.9	DCLRE1B	DNA cross-link repair 1B (PSO2 homolog, S. cerevisiae)

1.6	DCTD	dCMP deaminase
2.2	DCTN4	dynactin 4 (p62)
2.9	DCTN5	dynactin 5 (p25)
1.6	DDX19A	DEAD (Asp-Glu-Ala-As) box polypeptide 19A
1.6	DDX28	DEAD (Asp-Glu-Ala-Asp) box polypeptide 28
3.1	DDX50	DEAD (Asp-Glu-Ala-Asp) box polypeptide 50
1.7	DENND2D	DENN/MADD domain containing 2D
3.1	DFFB	DNA fragmentation factor, 40kDa, beta polypeptide (caspase-activated DNase)
1.8	DHRS12	dehydrogenase/reductase (SDR family) member 12
2.4	DHRS3	dehydrogenase/reductase (SDR family) member 3
9.3	DIP	death-inducing-protein
1.6	DKFZP564K0822	hypothetical protein DKFZp564K0822
2.9	DMWD	dystrophia myotonica-containing WD repeat motif
2.1	DNAJB12	DnaJ (Hsp40) homolog, subfamily B, member 12
1.7	DNAJB9	DnaJ (Hsp40) homolog, subfamily B, member 9
2.1	DNAJC17	DnaJ (Hsp40) homolog, subfamily C, member 17
2	DNAJC8	DnaJ (Hsp40) homolog, subfamily C, member 8
1.9	DNAJC9	DnaJ (Hsp40) homolog, subfamily C,

		member 9
4.7	DR1	down-regulator of transcription 1, TBP-binding (negative cofactor 2)
2.5	DSTN	destrin (actin depolymerizing factor)
4.4	DTX2	deltex homolog 2 (Drosophila)
1.8	DUSP1	dual specificity phosphatase 1
1.5	DYNLL1	dynein, light chain, LC8-type 1
1.8	DYNLT1	dynein, light chain, Tctex-type 1
1.7	DYNLT3	dynein, light chain, Tctex-type 3
7.1	E2F6	E2F transcription factor 6
1.6	EBAG9	estrogen receptor binding site associated, antigen, 9
3.9	EEF1B2	eukaryotic translation elongation factor 1 beta 2
1.5	EFCAB2	EF-hand calcium binding domain 2
165.8	EFEMP2	EGF-containing fibulin-like extracellular matrix protein 2
3.2	EFNA4	ephrin-A4
1.8	EGFL9	EGF-like-domain, multiple 9
3.7	EI24	etoposide induced 2.4 mRNA
1.7	EIF3S4	eukaryotic translation initiation factor 3, subunit 4 delta, 44kDa
4	EIF5	eukaryotic translation initiation factor 5
1.7	EML2	echinoderm microtubule associated protein like 2
2.3	EMP1	epithelial membrane protein 1
4.3	EMP2	epithelial membrane protein 2
1.6	ENDOGL1	endonuclease G-like 1
5.3	ENOSF1	enolase superfamily member 1
1.7	ENOX1	ecto-NOX disulfide-thiol exchanger 1
3.3	ENSA	endosulfine alpha
2.3	EPOR	erythropoietin receptor
1.9	ERCC8	excision repair cross-complementing rodent repair deficiency, complementation group 8
12.5	ETF1	eukaryotic translation termination factor 1
1.6	ETNK2	ethanolamine kinase 2
2.8	ETS2	v-ets erythroblastosis virus E26 oncogene homolog 2 (avian)
3.2	ETV7	ets variant gene 7 (TEL2 oncogene)
7	EXOC5	exocyst complex component 5
2.5	EXOSC2	exosome component 2
3.1	F2RL1	coagulation factor II (thrombin) receptor-like 1
1.5	FAF1	Fas (TNFRSF6) associated factor 1
2.6	FAHD2A	fumarylacetoacetate hydrolase domain containing 2A
1.7	FAM105A	family with sequence similarity 105, member A
2.4	FAM131A	family with sequence similarity 131, member A
4.7	FAM48A	family with sequence similarity 48, member A

7.3	FAM57A	family with sequence similarity 57, member A
2.2	FAS	Fas (TNF receptor superfamily, member 6)
1.9	FASTK	Fas-activated serine/threonine kinase
2.1	FASTKD5	FAST kinase domains 5
1.8	FAU	Finkel-Biskis-Reilly murine sarcoma virus (FBR-MuSV) ubiquitously expressed (fox derived); ribosomal protein S30
1.6	FBL	fibrillarin
5	FBXL4	F-box and leucine-rich repeat protein 4
1.7	FBXO28	F-box protein 28
1.7	FBXO9	F-box protein 9
2.2	FBXW11	F-box and WD-40 domain protein 11
1.6	FDFT1	farnesyl-diphosphate farnesyltransferase 1
1.5	FKBP2	FK506 binding protein 2, 13kDa
1.7	FLJ22222	hypothetical protein FLJ22222
1.8	FN3KRP	fructosamine-3-kinase-related protein
1.5	FOXF2	forkhead box F2
2.3	FRAG1	FGF receptor activating protein 1
1.5	FTH1	ferritin, heavy polypeptide 1
3.1	FTHP1	ferritin, heavy polypeptide pseudogene 1
2.5	FTL	ferritin, light polypeptide
7.6	FUSIP1	FUS interacting protein (serine/arginine-rich) 1
2.1	FZR1	fizzy/cell division cycle 20 related 1 (Drosophila)
2	G3BP2	GTPase activating protein (SH3 domain) binding protein 2
12.8	GABARAPL1	GABA(A) receptor-associated protein like 1
2.7	GAD1	glutamate decarboxylase 1 (brain, 67kDa)
1.9	GAS2L1	growth arrest-specific 2 like 1
2.7	GAS6	growth arrest-specific 6
3.2	GCDH	glutaryl-Coenzyme A dehydrogenase
6.9	GDF11	growth differentiation factor 11
1.5	GENX-3414	genethonin 1
1.5	GGA2	golgi associated, gamma adaptin ear containing, ARF binding protein 2
1.5	GGH	gamma-glutamyl hydrolase (conjugase, folylpolygammaglutamyl hydrolase)
1.6	GGPS1	geranylgeranyl diphosphate synthase 1
8.4	GGTL4	gamma-glutamyltransferase-like 4
1.8	GHITM	growth hormone inducible transmembrane protein
1.8	GINS4	GINS complex subunit 4 (Sld5 homolog)
2.2	GLUD1	glutamate dehydrogenase 1
4	GM2A	GM2 ganglioside activator
1.6	GNAS	GNAS complex locus
2.2	GNB1L	guanine nucleotide binding protein (G protein), beta polypeptide 1-like

98

1.9	GPR110	G protein-coupled receptor 110
2.3	GPR172A	G protein-coupled receptor 172A
2.4	GPR30	G protein-coupled receptor 30
3	GPX7	glutathione peroxidase 7
2.7	GRB10	growth factor receptor-bound protein 10
1.7	GRK6	G protein-coupled receptor kinase 6
2	GRPEL1	GrpE-like 1, mitochondrial (E. coli)
3	GSK3A	glycogen synthase kinase 3 alpha
4	GTDC1	glycosyltransferase-like domain containing 1
1.6	GTF2H2	general transcription factor IIH, polypeptide 2, 44kDa
1.9	GTF3C2	general transcription factor IIIC, polypeptide 2, beta 110kDa
1.9	GYG1	glycogenin 1
11.8	HCP5	HLA complex P5
1.7	HEMK1	HemK methyltransferase family member 1
5.3	HEXB	hexosaminidase B (beta polypeptide)
1.9	HIGD1A	HIG1 domain family, member 1A
1.6	HINT1	histidine triad nucleotide binding protein 1
2.6	HIST1H1E	histone 1, H1e
1.7	HIST1H2BD	histone 1, H2bd
2.1	HIST1H2BK	histone 1, H2bk
1.8	HIST1H2BM	histone 1, H2bm
39.4	HLA-F	major histocompatibility complex, class I, F
1.5	HMOX1	heme oxygenase (decycling) 1

2	HSBP1	heat shock factor binding protein 1
1.5	HSD17B7P2	hydroxysteroid (17-beta) dehydrogenase 7 pseudogene 2
2.4	HSF2BP	heat shock transcription factor 2 binding protein
1.6	HSPA4	heat shock 70kDa protein 4
1.8	HSPBAP1	HSPB (heat shock 27kDa) associated protein 1
1.9	HSPC111	hypothetical protein HSPC111
3.4	HTATIP	HIV-1 Tat interacting protein, 60kDa
1.9	IDH2	isocitrate dehydrogenase 2 (NADP+), mitochondrial
2.1	IDH3B	isocitrate dehydrogenase 3 (NAD+) beta
1.7	IDI1	isopentenyl-diphosphate delta isomerase 1
1.6	IER3	immediate early response 3
1.6	IGFBP7	insulin-like growth factor binding protein 7
2.7	IIP45	invasion inhibitory protein 45
2	IL11	interleukin 11
2.1	IL11RA	interleukin 11 receptor, alpha
4.1	IL13RA1	interleukin 13 receptor, alpha 1
1.8	IL15	interleukin 15
1.6	ING1	inhibitor of growth family, member 1
5.1	ING2	inhibitor of growth family, member 2
1.9	ING4	inhibitor of growth family, member 4
1.6	INSIG1	insulin induced gene 1
5.4	IPO13	importin 13
1.7	IQCC	IQ motif containing C
6.4	IRX5	iroquois homeobox protein 5

99

2	ISG20L2	interferon stimulated exonuclease gene 20kDa-like 2	2.8	LASS2	LAG1 longevity assurance homolog 2 (S. cerevisiae)
3.9	IVD	isovaleryl Coenzyme A dehydrogenase	63.1	LGALS1	lectin, galactoside-binding, soluble, 1 (galectin 1)
4.6	JOSD1	Josephin domain containing 1	1.6	LGALS8	lectin, galactoside-binding, soluble, 8 (galectin 8)
2.2	KATNA1	katanin p60 (ATPase-containing) subunit A 1	1.6	LHFP	lipoma HMGIC fusion partner
2.8	KCTD13	potassium channel tetramerisation domain containing 13	2.8	LITAF	lipopolysaccharide-induced TNF factor
1.5	KCTD14	potassium channel tetramerisation domain containing 14	2	LOC26010	viral DNA polymerase-transactivated protein 6
1.6	KDELR2	KDEL (Lys-Asp-Glu-Leu) endoplasmic reticulum protein retention receptor 2	2.1	LOC441294	similar to CTAGE6
			1.9	LOC54103	hypothetical protein LOC54103
20.5	KDELR3	KDEL (Lys-Asp-Glu-Leu) endoplasmic reticulum protein retention receptor 3	1.9	LONRF3	LON peptidase N-terminal domain and ring finger 3
1.5	KIAA0409	KIAA0409	3	LRRFIP2	leucine rich repeat (in FLII) interacting protein 2
1.9	KIF22	kinesin family member 22	2.1	LSM5	LSM5 homolog, U6 small nuclear RNA associated (S. cerevisiae)
1.5	KLF2	Kruppel-like factor 2 (lung)			
2	KLF4	Kruppel-like factor 4 (gut)	2.7	LYPLA1	lysophospholipase I
29.4	KLF6	Kruppel-like factor 6	1.7	LYRM1	LYR motif containing 1
1.6	KPNA2	karyopherin alpha 2 (RAG cohort 1, importin alpha 1)	2.3	MAFF	v-maf musculoaponeurotic fibrosarcoma oncogene homolog F (avian)
1.5	KPNA6	karyopherin alpha 6 (importin alpha 7)	1.7	MANEA	mannosidase, endo-alpha
2.2	LANCL1	LanC lantibiotic synthetase component C-like 1 (bacterial)	1.8	MAP2K4	mitogen-activated protein kinase kinase 4
			1.5	MAP2K5	mitogen-activated protein kinase kinase 5
2.1	LARP6	La ribonucleoprotein domain family, member 6	2.3	MAP2K7	mitogen-activated protein kinase kinase 7
			1.7	MAP3K7IP2	mitogen-activated protein kinase kinase kinase 7

100

		interacting protein 2
2.1	MAPK12	mitogen-activated protein kinase 12
1.5	MAPKAPK2	mitogen-activated protein kinase-activated protein kinase 2
1.5	MBD1	methyl-CpG binding domain protein 1
1.5	MBIP	MAP3K12 binding inhibitory protein 1
1.7	MCFP	mitochondrial carrier family protein
1.5	MCOLN1	mucolipin 1
2.1	MCP	membrane cofactor protein (CD46, trophoblast-lymphocyte cross-reactive antigen)
1.5	MDH1	malate dehydrogenase 1, NAD (soluble)
10.4	ME2	malic enzyme 2, NAD(+)-dependent, mitochondrial
2	ME3	malic enzyme 3, NADP(+)-dependent, mitochondrial
3.3	MECP2	methyl CpG binding protein 2 (Rett syndrome)
2.8	MED18	mediator of RNA polymerase II transcription, subunit 18 homolog (yeast)
5.3	MED9	mediator of RNA polymerase II transcription, subunit 9 homolog (yeast)
2.4	MEST	mesoderm specific transcript homolog (mouse)
1.7	METTL2	methyltransferase like 2
1.5	MFN2	mitofusin 2
1.7	MFSD5	major facilitator superfamily

		domain containing 5
1.6	MGC14376	hypothetical protein MGC14376
1.9	MGC2752	hypothetical protein MGC2752
1.5	MGST2	microsomal glutathione S-transferase 2
1.5	MICA	MHC class I polypeptide-related sequence A
2.2	MID1IP1	MID1 interacting protein 1 (gastrulation specific G12-like (zebrafish))
2.3	MIS12	MIS12 homolog (yeast)
1.6	MKNK2	MAP kinase interacting serine/threonine kinase 2
1.5	MLL4	myeloid/lymphoid or mixed-lineage leukemia 4
1.9	MLX	MAX-like protein X
1.9	MLYCD	malonyl-CoA decarboxylase
1.7	MMD	monocyte to macrophage differentiation-associated
1.5	MMP14	matrix metallopeptidase 14 (membrane-inserted)
23	MMP9	matrix metallopeptidase 9 (gelatinase B, 92kDa gelatinase, 92kDa type IV collagenase)
2.7	MPZL1	myelin protein zero-like 1
11.4	MR1	major histocompatibility complex, class I-related
1.5	MRPL3	mitochondrial ribosomal protein L3
2.1	MRPL9	mitochondrial ribosomal protein

101

		L9
1.5	MRPS10	mitochondrial ribosomal protein S10
1.7	MRPS12	mitochondrial ribosomal protein S12
2.5	MRS2L	MRS2-like, magnesium homeostasis factor (S. cerevisiae)
2.8	MT1H	metallothionein 1H
40.7	MT1X	metallothionein 1X
1.7	MTA1	metastasis associated 1
3.7	MTHFD2L	methylenetetrahydrofolate dehydrogenase (NADP+ dependent) 2-like
2.8	MTO1	mitochondrial translation optimization 1 homolog (S. cerevisiae)
1.9	MTRR	5-methyltetrahydrofolate-homocysteine methyltransferase reductase
1.5	MVK	mevalonate kinase (mevalonic aciduria)
4.4	MXRA7	matrix-remodelling associated 7
1.6	MYCBP	c-myc binding protein
1.9	MYD88	myeloid differentiation primary response gene (88)
2.3	MYL4	myosin, light polypeptide 4, alkali; atrial, embryonic
3.6	MYNN	myoneurin
2.3	MYO9B	myosin IXB
1.8	MYOHD1	myosin head domain containing 1
2.4	MYST1	MYST histone acetyltransferase 1
8.9	na	similar to 60S ribosomal protein

		L13 (A52)
2.2	NAB1	NGFI-A binding protein 1 (EGR1 binding protein 1)
1.7	NADK	NAD kinase
1.8	NAPG	N-ethylmaleimide-sensitive factor attachment protein, gamma
1.5	NDUFA5	NADH dehydrogenase (ubiquinone) 1 alpha subcomplex, 5, 13kDa
3.6	NEK11	NIMA (never in mitosis gene a)-related kinase 11
1.5	NEK2	NIMA (never in mitosis gene a)-related kinase 2
1.5	NFYC	nuclear transcription factor Y, gamma
2.1	NGFRAP1	nerve growth factor receptor (TNFRSF16) associated protein 1
1.9	NGRN	neugrin, neurite outgrowth associated
1.8	NIPSNAP1	nipsnap homolog 1 (C. elegans)
2.5	NMD3	NMD3 homolog (S. cerevisiae)
1.8	NMT1	N-myristoyltransferase 1
3.4	NMT2	N-myristoyltransferase 2
2.1	NOSIP	nitric oxide synthase interacting protein
1.5	NPAS2	neuronal PAS domain protein 2
6.8	NSDHL	NAD(P) dependent steroid dehydrogenase-like
2.1	NSMAF	neutral sphingomyelinase (N-SMase) activation associated factor
4	OAZ1	ornithine

		decarboxylase antizyme 1
1.5	OR7E47P	olfactory receptor, family 7, subfamily E, member 47 pseudogene
1.8	ORC4L	origin recognition complex, subunit 4-like (yeast)
1.6	OTUB1	OTU domain, ubiquitin aldehyde binding 1
1.8	P2RX5	purinergic receptor P2X, ligand-gated ion channel, 5
12.7	P2RY2	purinergic receptor P2Y, G-protein coupled, 2
1.6	PABPN1	poly(A) binding protein, nuclear 1
1.5	PAIP1	poly(A) binding protein interacting protein 1
1.8	PAOX	polyamine oxidase (exo-N4-amino)
2.2	PAX8	paired box gene 8
1.5	PBX2	pre-B-cell leukemia transcription factor 2
4	PCGF2	polycomb group ring finger 2
1.8	PCLO	piccolo (presynaptic cytomatrix protein)
2.9	PCOLCE2	procollagen C-endopeptidase enhancer 2
2.1	PCTP	phosphatidylcholine transfer protein
9	PCYT1A	phosphate cytidylyltransferase 1, choline, alpha
2.9	PDCD2	programmed cell death 2
1.6	PDE10A	phosphodiesterase 10A
1.9	PDS5A	PDS5, regulator of cohesion maintenance, homolog A (S. cerevisiae)
2.1	PEX16	peroxisomal biogenesis factor 16
1.7	PEX3	peroxisomal biogenesis factor 3
2.4	PFKL	phosphofructokinase, liver
1.7	PGF	placental growth factor, vascular endothelial growth factor-related protein
6.7	PGGT1B	protein geranylgeranyltransferase type I, beta subunit
1.5	PHB	prohibitin
1.5	PHF1	PHD finger protein 1
1.9	PHF2	PHD finger protein 2
1.6	PHTF1	putative homeodomain transcription factor 1
15.2	PHTF2	putative homeodomain transcription factor 2
3.3	PIAS2	protein inhibitor of activated STAT, 2
7.7	PIGB	phosphatidylinositol glycan, class B
2.5	PIK4CB	phosphatidylinositol 4-kinase, catalytic, beta polypeptide
1.8	PIM2	pim-2 oncogene
2.3	PIP5K1A	phosphatidylinositol-4-phosphate 5-kinase, type I, alpha
2	PKNOX1	PBX/knotted 1 homeobox 1
2.9	PLA2G4B	phospholipase A2, group IVB (cytosolic)
3.3	PLAC1	placenta-specific 1
1.5	PLAUR	plasminogen activator, urokinase receptor
1.5	PLEKHM2	pleckstrin homology domain containing, family M (with RUN domain) member 2
1.6	PLSCR3	phospholipid scramblase 3

103

2.1	PMAIP1	phorbol-12-myristate-13-acetate-induced protein 1
18.4	PMP22	peripheral myelin protein 22
1.9	PMS2L3	postmeiotic segregation increased 2-like 3
1.6	PMS2L5	postmeiotic segregation increased 2-like 5
4.8	POLA2	polymerase (DNA directed), alpha 2 (70kD subunit)
2	POLDIP2	polymerase (DNA-directed), delta interacting protein 2
6.2	POLDIP3	polymerase (DNA-directed), delta interacting protein 3
9.4	POLE3	polymerase (DNA directed), epsilon 3 (p17 subunit)
1.6	PON3	paraoxonase 3
2.7	POT1	POT1 protection of telomeres 1 homolog (S. pombe)
1.6	PPA1	pyrophosphatase (inorganic) 1
2.3	PPFIA1	protein tyrosine phosphatase, receptor type, f polypeptide (PTPRF), interacting protein (liprin), alpha 1
2.8	PPIA	peptidylprolyl isomerase A (cyclophilin A)
1.6	PPID	peptidylprolyl isomerase D (cyclophilin D)
2.5	PPP1R7	protein phosphatase 1, regulatory subunit 7
4.8	PPP2R1B	protein phosphatase 2 (formerly 2A), regulatory subunit A (PR 65), beta isoform
10	PPP3R1	protein phosphatase 3 (formerly 2B), regulatory subunit B, 19kDa, alpha isoform (calcineurin B, type I)
2.2	PPT2	palmitoyl-protein thioesterase 2
1.8	PRG1	proteoglycan 1, secretory granule
1.5	PRKAB1	protein kinase, AMP-activated, beta 1 non-catalytic subunit
2.4	PRKD3	protein kinase D3
4.3	PRKRIP1	PRKR interacting protein 1 (IL11 inducible)
2.2	PRPF4	PRP4 pre-mRNA processing factor 4 homolog (yeast)
5.6	PRSS23	protease, serine, 23
1.5	PRUNE	prune homolog (Drosophila)
12.4	PSKH1	protein serine kinase H1
1.8	PSMA1	proteasome (prosome, macropain) subunit, alpha type, 1
1.5	PSMA7	proteasome (prosome, macropain) subunit, alpha type, 7
5.5	PSMB4	proteasome (prosome, macropain) subunit, beta type, 4
1.6	PSMC5	proteasome (prosome, macropain) 26S subunit, ATPase, 5
2	PSMD4	proteasome (prosome, macropain) 26S subunit, non-ATPase, 4
1.7	PSME1	proteasome (prosome, macropain)

104

		activator subunit 1 (PA28 alpha)
2	PTP4A1	protein tyrosine phosphatase type IVA, member 1
1.6	PTPLAD1	protein tyrosine phosphatase-like A domain containing 1
7.1	PTPN11	protein tyrosine phosphatase, non-receptor type 11 (Noonan syndrome 1)
11.7	PTPN2	protein tyrosine phosphatase, non-receptor type 2
1.6	PTPN3	protein tyrosine phosphatase, non-receptor type 3
1.6	PTPN9	protein tyrosine phosphatase, non-receptor type 9
3.9	PTPRA	protein tyrosine phosphatase, receptor type, A
1.7	PTTG1	pituitary tumor-transforming 1
7.8	QKI	quaking homolog, KH domain RNA binding (mouse)
1.9	RAB2	RAB2, member RAS oncogene family
2.9	RAB23	RAB23, member RAS oncogene family
8.8	RABEP1	rabaptin, RAB GTPase binding effector protein 1
2	RABL2B	RAB, member of RAS oncogene family-like 2B
1.8	RAC3	ras-related C3 botulinum toxin substrate 3 (rho family, small GTP binding protein Rac3)
1.5	RAD17	RAD17 homolog (S. pombe)
1.8	RAD51	RAD51 homolog (RecA homolog, E. coli) (S. cerevisiae)
1.7	RAD51AP1	RAD51 associated protein 1

1.9	RAD9A	RAD9 homolog A (S. pombe)
1.7	RALA	v-ral simian leukemia viral oncogene homolog A (ras related)
6.5	RANBP3	RAN binding protein 3
1.7	RANGAP1	Ran GTPase activating protein 1
2.2	RBMS2	RNA binding motif, single stranded interacting protein 2
1.7	RBMX2	RNA binding motif protein, X-linked 2
1.5	RCL1	RNA terminal phosphate cyclase-like 1
3.7	RCP9	Calcitonin gene-related peptide-receptor component protein
2.3	RGS19	regulator of G-protein signalling 19
1.5	RHEB	Ras homolog enriched in brain
2.4	RHOA	ras homolog gene family, member A
7	RHOBTB3	Rho-related BTB domain containing 3
1.8	RHOT1	ras homolog gene family, member T1
1.6	RHOT2	ras homolog gene family, member T2
1.6	RIPK2	receptor-interacting serine-threonine kinase 2
2	RNF146	ring finger protein 146
1.5	RNF41	ring finger protein 41
1.9	RNPEPL1	arginyl aminopeptidase (aminopeptidase B)-like 1
3.2	RPA1	replication protein A1, 70kDa
2.4	RPL13	ribosomal protein L13
2.4	RPL18	ribosomal protein L18
2.6	RPL35	ribosomal protein

105

		L35
18.5	RPL35A	ribosomal protein L35a
1.7	RPS10	ribosomal protein S10
2	RPS14	ribosomal protein S14
1.9	RPS20	ribosomal protein S20
3	RPS6KA4	ribosomal protein S6 kinase, 90kDa, polypeptide 4
1.5	RPS6KB1	ribosomal protein S6 kinase, 70kDa, polypeptide 1
4.5	RRAGD	Ras-related GTP binding D
1.5	RRM2	ribonucleotide reductase M2 polypeptide
1.9	RRP15	ribosomal RNA processing 15 homolog (S. cerevisiae)
2	RRS1	RRS1 ribosome biogenesis regulator homolog (S. cerevisiae)
1.7	RSU1	Ras suppressor protein 1
1.5	RY1	putative nucleic acid binding protein RY-1
1.9	S100A10	S100 calcium binding protein A10 (annexin II ligand, calpactin I, light polypeptide (p11))
2	S100A4	S100 calcium binding protein A4 (calcium protein, calvasculin, metastasin, murine placental homolog)
3.1	SAP30	sin3-associated polypeptide, 30kDa
170.9	SAPS2	SAPS domain family, member 2
2.3	SCARB2	scavenger receptor class B, member 2
2	SCMH1	sex comb on midleg homolog 1 (Drosophila)
2.5	SCPEP1	serine carboxypeptidase 1
1.5	SDAD1	SDA1 domain containing 1
2.1	SDCCAG3	serologically defined colon cancer antigen 3
4.8	SEC22L1	SEC22 vesicle trafficking protein-like 1 (S. cerevisiae)
15.1	SEC23A	Sec23 homolog A (S. cerevisiae)
1.6	SECISBP2	SECIS binding protein 2
1.8	SECTM1	secreted and transmembrane 1
1.5	SENP2	SUMO1/sentrin/SMT3 specific peptidase 2
6.7	SEPHS1	selenophosphate synthetase 1
2.2	SERGEF	secretion regulating guanine nucleotide exchange factor
1.5	SET	SET translocation (myeloid leukemia-associated)
1.6	SETDB1	SET domain, bifurcated 1
2.5	SF4	splicing factor 4
1.9	SH2D3A	SH2 domain containing 3A
15.6	SIAH1	seven in absentia homolog 1 (Drosophila)
1.6	SIP1	survival of motor neuron protein interacting protein 1
19.4	SIRT3	sirtuin (silent mating type information regulation 2 homolog) 3 (S. cerevisiae)
2.2	SIX2	sine oculis homeobox homolog 2 (Drosophila)
1.8	SLC12A9	solute carrier family 12 (potassium/chloride transporters),

106

member 9

2.9	SLC22A14	solute carrier family 22 (organic cation transporter), member 14
1.6	SLC25A14	solute carrier family 25 (mitochondrial carrier, brain), member 14
7.2	SLC25A5	solute carrier family 25 (mitochondrial carrier; adenine nucleotide translocator), member 5
2	SLC31A1	solute carrier family 31 (copper transporters), member 1
2	SLC31A2	solute carrier family 31 (copper transporters), member 2
1.6	SLC35A2	solute carrier family 35 (UDP-galactose transporter), member A2
1.5	SLC35C2	solute carrier family 35, member C2
3.5	SLC35F2	solute carrier family 35, member F2
1.5	SLC38A6	solute carrier family 38, member 6
1.5	SLC39A6	solute carrier family 39 (zinc transporter), member 6
3.9	SLC39A8	solute carrier family 39 (zinc transporter), member 8
2	SLC41A3	solute carrier family 41, member 3
1.8	SLC43A1	solute carrier family 43, member 1
28.4	SLCO1B3	solute carrier organic anion transporter family, member 1B3
1.5	SMAD2	SMAD, mothers against DPP homolog 2 (Drosophila)
3.5	SMARCD2	SWI/SNF related, matrix associated, actin dependent regulator of chromatin, subfamily d, member 2
1.5	SMN1	survival of motor neuron 1, telomeric
1.5	SNAI2	snail homolog 2 (Drosophila)
2.2	SNRPD1	small nuclear ribonucleoprotein D1 polypeptide 16kDa
2.8	SNRPE	small nuclear ribonucleoprotein polypeptide E
1.5	SNRPF	small nuclear ribonucleoprotein polypeptide F
1.6	SNRPG	small nuclear ribonucleoprotein polypeptide G
2.4	SOCS2	suppressor of cytokine signaling 2
2.1	SOD1	superoxide dismutase 1, soluble (amyotrophic lateral sclerosis 1 (adult))
2.3	SORBS3	sorbin and SH3 domain containing 3
59.9	SORT1	sortilin 1
1.8	SPCS3	signal peptidase complex subunit 3 homolog (S. cerevisiae)
2.6	SPHK1	sphingosine kinase 1
26.2	SPOP	speckle-type POZ protein
32.5	SPRY4	sprouty homolog 4 (Drosophila)

107

Value	Gene	Description
4.2	SRD5A1	steroid-5-alpha-reductase, alpha polypeptide 1 (3-oxo-5 alpha-steroid delta 4-dehydrogenase alpha 1)
9	SREBF2	sterol regulatory element binding transcription factor 2
2.1	SRI	sorcin
1.5	SRP72	signal recognition particle 72kDa
1.7	SRPK1	SFRS protein kinase 1
58.5	SRPRB	signal recognition particle receptor, B subunit
2.4	SS18	synovial sarcoma translocation, chromosome 18
14.9	SSBP3	single stranded DNA binding protein 3
1.9	STAT1	signal transducer and activator of transcription 1, 91kDa
1.7	STK11	serine/threonine kinase 11 (Peutz-Jeghers syndrome)
9.1	STK6	serine/threonine kinase 6
12.5	STOM	stomatin
10.7	STX18	syntaxin 18
1.5	SULT1A1	sulfotransferase family, cytosolic, 1A, phenol-preferring, member 1
7.9	SULT1A3	sulfotransferase family, cytosolic, 1A, phenol-preferring, member 3
1.8	SUMO3	SMT3 suppressor of mif two 3 homolog 3 (yeast)
3.7	SYPL1	synaptophysin-like 1
1.9	TAF6	TAF6 RNA polymerase II, TATA box binding protein (TBP)-associated factor, 80kDa
1.6	TANK	TRAF family member-associated NFKB activator
2.5	TAX1BP3	Tax1 (human T-cell leukemia virus type I) binding protein 3
2.2	TBC1D22A	TBC1 domain family, member 22A
3.1	TBC1D8	TBC1 domain family, member 8 (with GRAM domain)
1.5	TCEAL1	transcription elongation factor A (SII)-like 1
2.3	TCFL5	transcription factor-like 5 (basic helix-loop-helix)
2.6	TCP11L1	t-complex 11 (mouse) like 1
1.5	TEGT	testis enhanced gene transcript (BAX inhibitor 1)
3.2	TENC1	tensin like C1 domain containing phosphatase (tensin 2)
2.9	TFAM	transcription factor A, mitochondrial
9.5	TFCP2	transcription factor CP2
1.5	TFDP1	transcription factor Dp-1
7.9	TFDP2	transcription factor Dp-2 (E2F dimerization partner 2)
5.1	TFPI	tissue factor pathway inhibitor (lipoprotein-associated coagulation inhibitor)
1.7	TGDS	TDP-glucose 4,6-dehydratase
8.3	THAP10	THAP domain containing 10
1.6	THG1L	tRNA-histidine guanylyltransferase 1-like (S. cerevisiae)

108

2.5	TIA1	TIA1 cytotoxic granule-associated RNA binding protein
3.4	TIMM17A	translocase of inner mitochondrial membrane 17 homolog A (yeast)
1.5	TINF2	TERF1 (TRF1)-interacting nuclear factor 2
4.2	TK2	thymidine kinase 2, mitochondrial
1.9	TMBIM4	transmembrane BAX inhibitor motif containing 4
1.5	TMCO1	transmembrane and coiled-coil domains 1
1.5	TMED9	transmembrane emp24 protein transport domain containing 9
1.9	TMPO	thymopoietin
9	TMSB10	thymosin, beta 10
13218.9	TNFRSF11B	tumor necrosis factor receptor superfamily, member 11b (osteoprotegerin)
1.8	TNFRSF14	tumor necrosis factor receptor superfamily, member 14 (herpesvirus entry mediator)
2.6	TNFSF10	tumor necrosis factor (ligand) superfamily, member 10
2	TNFSF13	tumor necrosis factor (ligand) superfamily, member 13
2.3	TNFSF9	tumor necrosis factor (ligand) superfamily, member 9
3.7	TOR1A	torsin family 1, member A (torsin A)
2.6	TOR1AIP1	torsin A interacting protein 1
3.5	TP53AP1	TP53 activated protein 1
2	TPD52	tumor protein D52
3.2	TPM4	tropomyosin 4
1.5	TRAM1	translocation associated membrane protein 1
2.2	TRAPPC2	trafficking protein particle complex 2
1.9	TRAPPC4	trafficking protein particle complex 4
2.7	TRBC1	T cell receptor beta constant 1
2.5	TRIM68	tripartite motif-containing 68
2.7	TSPAN3	tetraspanin 3
5.2	TSPAN9	tetraspanin 9
3.8	TTC19	tetratricopeptide repeat domain 19
1.8	TXNL2	thioredoxin-like 2
10.6	UBA52	ubiquitin A-52 residue ribosomal protein fusion product 1
1.8	UBAP1	ubiquitin associated protein 1
1.5	UBE2D3	ubiquitin-conjugating enzyme E2D 3 (UBC4/5 homolog, yeast)
4.5	UBE2G1	ubiquitin-conjugating enzyme E2G 1 (UBC7 homolog, yeast)
2.8	UBE2J1	ubiquitin-conjugating enzyme E2, J1 (UBC6 homolog, yeast)
4.4	UBE2L3	ubiquitin-conjugating enzyme E2L 3
1.5	UBE2L6	ubiquitin-conjugating enzyme E2L 6
1.5	UBE2N	ubiquitin-conjugating enzyme E2N (UBC13 homolog, yeast)
2.5	UBE2V1	ubiquitin-conjugating

2.3	UBE2V2	enzyme E2 variant 1 / ubiquitin-conjugating enzyme E2 variant 2	7.9	YWHAQ	tyrosine 3-monooxygenase/tryptophan 5-monooxygenase activation protein, theta polypeptide
1.5	UBE3B	ubiquitin protein ligase E3B	3.4	ZC3H14	zinc finger CCCH-type containing 14
3.5	UBL3	ubiquitin-like 3	1.5	ZDHHC6	zinc finger, DHHC-type containing 6
1.9	UBXD6	UBX domain containing 6	1.7	ZFP36	zinc finger protein 36, C3H type, homolog (mouse)
1.7	UCHL5IP	UCHL5 interacting protein	6.3	ZNF133	zinc finger protein 133 (clone pHZ-13)
1.7	UFC1	ubiquitin-fold modifier conjugating enzyme 1	1.7	ZNF143	zinc finger protein 143 (clone pHZ-1)
3.5	UNG2	uracil-DNA glycosylase 2	1.5	ZNF22	zinc finger protein 22 (KOX 15)
2.4	USP3	ubiquitin specific peptidase 3	3.6	ZNF232	zinc finger protein 232
1.7	VBP1	von Hippel-Lindau binding protein 1	1.7	ZNF239	zinc finger protein 239
8.5	VEGF	vascular endothelial growth factor	1.5	ZNF277	zinc finger protein 277
1.6	VGF	VGF nerve growth factor inducible	2.7	ZNF278	zinc finger protein 278
6.4	VPS37C	vacuolar protein sorting 37C (yeast)	27	ZNF34	zinc finger protein 34 (KOX 32)
1.6	VRK3	vaccinia related kinase 3	4.5	ZNF410	zinc finger protein 410
3.2	WASPIP	Wiskott-Aldrich syndrome protein interacting protein	13	ZNF435	zinc finger protein 435
13.8	WBP5	WW domain binding protein 5	57.8	ZNF45	zinc finger protein 45
1.7	WDR23	WD repeat domain 23	4.2	ZNF473	zinc finger protein 473
5.8	WDR62	WD repeat domain 62	8.3	ZNF673	zinc finger protein 673
1.9	WHSC1	Wolf-Hirschhorn syndrome candidate 1	25	ZNF768	zinc finger protein 768
6.1	WIPI2	WD repeat domain, phosphoinositide interacting 2	2	ZNF9	zinc finger protein 9 (a cellular retroviral nucleic acid binding protein)
2.1	WSB2	WD repeat and SOCS box-containing 2	1.6	ZSCAN5	zinc finger and SCAN domain containing 5
3.6	XAB1	XPA binding protein 1, GTPase			
2.1	XAF1	XIAP associated factor-1	**Not Bound to Bound**		

110

Symbol	Description
AASDHPPT	aminoadipate-semialdehyde dehydrogenase-phosphopantetheinyl transferase
ABCA2	ATP-binding cassette, sub-family A (ABC1), member 2
ACVR1	activin A receptor, type I
ADAM10	ADAM metallopeptidase domain 10
ADH5	alcohol dehydrogenase 5 (class III), chi polypeptide
AGA	aspartylglucosaminidase
AK2	adenylate kinase 2
ALDH1B1	aldehyde dehydrogenase 1 family, member B1
ALDH3A2	aldehyde dehydrogenase 3 family, member A2
ALMS1	Alstrom syndrome 1
AMD1	adenosylmethionine decarboxylase 1
ANGPT1	angiopoietin 1
ANKRD49	ankyrin repeat domain 49
APOL2	apolipoprotein L, 2
APS	adaptor protein with pleckstrin homology and src homology 2 domains
ARIH2	ariadne homolog 2 (Drosophila)
ARL8B	ADP-ribosylation factor-like 8B
ARNTL2	aryl hydrocarbon receptor nuclear translocator-like 2
ARSB	arylsulfatase B
ASF1A	ASF1 anti-silencing function 1 homolog A (S. cerevisiae)
ASTE1	asteroid homolog 1 (Drosophila)
B2M	beta-2-microglobulin
B4GALT1	UDP-Gal:betaGlcNAc beta 1,4-galactosyltransferase, polypeptide 1
BAIAP2	BAI1-associated protein 2
BECN1	beclin 1 (coiled-coil, myosin-like BCL2 interacting protein)
BFSP1	beaded filament structural protein 1, filensin
BNIP3L	BCL2/adenovirus E1B 19kDa interacting protein 3-like
BRD2	bromodomain containing 2
BRD9	bromodomain containing 9
BRMS1	breast cancer metastasis suppressor 1
BSDC1	BSD domain containing 1
BTF3	basic transcription factor 3
BTN3A3	butyrophilin, subfamily 3, member A3
BUB1	BUB1 budding uninhibited by benzimidazoles 1 homolog (yeast)
BZW1	basic leucine zipper and W2 domains 1
C14orf118	chromosome 14 open reading frame 118
C15orf39	chromosome 15 open reading frame 39
C16orf34	chromosome 16 open reading frame 34
C16orf5	chromosome 16 open reading frame 5
C17orf70	chromosome 17

111

	open reading frame 70	CCNJ	cyclin J
C1orf108	chromosome 1 open reading frame 108	CCNT2	cyclin T2
		CDCA8	cell division cycle associated 8
C1orf121	chromosome 1 open reading frame 121	CDH11	cadherin 11, type 2, OB-cadherin (osteoblast)
C1orf166	chromosome 1 open reading frame 166	CDK10	cyclin-dependent kinase (CDC2-like) 10
C1QDC1	C1q domain containing 1	CDKAL1	CDK5 regulatory subunit associated protein 1-like 1
C20orf18	chromosome 20 open reading frame 18	CDS2	CDP-diacylglycerol synthase (phosphatidate cytidylyltransferase) 2
C20orf3	chromosome 20 open reading frame 3		
C21orf55	chromosome 21 open reading frame 55	CDV3	CDV3 homolog (mouse)
C2orf24	chromosome 2 open reading frame 24	CERK	ceramide kinase
		CES2	carboxylesterase 2 (intestine, liver)
C2orf56	chromosome 2 open reading frame 56	CFLAR	CASP8 and FADD-like apoptosis regulator
C4orf16	chromosome 4 open reading frame 16	CH25H	cholesterol 25-hydroxylase
C6orf62	chromosome 6 open reading frame 62	CHCHD3	coiled-coil-helix-coiled-coil-helix domain containing 3
C6orf68	chromosome 6 open reading frame 68	CHST4	carbohydrate (N-acetylglucosamine 6-O) sulfotransferase 4
C7orf25	chromosome 7 open reading frame 25	CLK1	CDC-like kinase 1
C8orf41	chromosome 8 open reading frame 41	CLN8	ceroid-lipofuscinosis, neuronal 8 (epilepsy, progressive with mental retardation)
CANT1	calcium activated nucleotidase 1		
CASP10	caspase 10, apoptosis-related cysteine peptidase	COG5	component of oligomeric golgi complex 5
CBX3	chromobox homolog 3 (HP1 gamma homolog, Drosophila)	COL1A1	collagen, type I, alpha 1
		COX15	COX15 homolog, cytochrome c oxidase assembly protein (yeast)
CCDC59	coiled-coil domain containing 59		
CCNG2	cyclin G2	CRBN	cereblon

112

CREM	cAMP responsive element modulator
CRKL	v-crk sarcoma virus CT10 oncogene homolog (avian)-like
CSGlcA-T	chondroitin sulfate glucuronyltransferase
CSNK1E	casein kinase 1, epsilon
CTAGE5	CTAGE family, member 5
CTBP1	C-terminal binding protein 1
CTSO	cathepsin O
CUL1	cullin 1
CXorf34	chromosome X open reading frame 34
CXorf45	chromosome X open reading frame 45
CYB561	cytochrome b-561
CYP26B1	cytochrome P450, family 26, subfamily B, polypeptide 1
CYP2R1	cytochrome P450, family 2, subfamily R, polypeptide 1
CYP51A1	cytochrome P450, family 51, subfamily A, polypeptide 1
DARS2	aspartyl-tRNA synthetase 2 (mitochondrial)
DBF4	DBF4 homolog (S. cerevisiae)
DCUN1D2	DCN1, defective in cullin neddylation 1, domain containing 2 (S. cerevisiae)
DCUN1D4	DCN1, defective in cullin neddylation 1, domain containing 4 (S. cerevisiae)
DDX17	DEAD (Asp-Glu-Ala-Asp) box polypeptide 17
DHODH	dihydroorotate dehydrogenase
DHRS7	dehydrogenase/reductase (SDR family) member 7
DKFZP564O0523	hypothetical protein DKFZp564O0523
DLG1	discs, large homolog 1 (Drosophila)
DLX4	distal-less homeobox 4
DNAJB4	DnaJ (Hsp40) homolog, subfamily B, member 4
DNAJC10	DnaJ (Hsp40) homolog, subfamily C, member 10
DRAM	damage-regulated autophagy modulator
DYRK3	dual-specificity tyrosine-(Y)-phosphorylation regulated kinase 3
ECHDC1	enoyl Coenzyme A hydratase domain containing 1
EDIL3	EGF-like repeats and discoidin I-like domains 3
EGFR	Epidermal growth factor receptor (EGFR)
EIF2AK1	eukaryotic translation initiation factor 2-alpha kinase 1
EIF4E2	eukaryotic translation initiation factor 4E family member 2
ELAVL1	ELAV (embryonic lethal, abnormal vision, Drosophila)-like 1 (Hu antigen R)
EPB41L4B	erythrocyte membrane protein band 4.1 like 4B
EPN2	epsin 2
ETFDH	electron-transferring-

113

	flavoprotein dehydrogenase		catalytic, 3
EVA1	epithelial V-like antigen 1	GALNT1	UDP-N-acetyl-alpha-D-galactosamine:poly peptide N-acetylgalactosamin yltransferase 1 (GalNAc-T1)
EXOC7	exocyst complex component 7		
EXTL2	exostoses (multiple)-like 2		
EXTL3	exostoses (multiple)-like 3	GAPDH	glyceraldehyde-3-phosphate dehydrogenase
FAIM	Fas apoptotic inhibitory molecule	GCAT	glycine C-acetyltransferase (2-amino-3-ketobutyrate coenzyme A ligase)
FAM32A	family with sequence similarity 32, member A		
FAM46C	family with sequence similarity 46, member C	GCLC	glutamate-cysteine ligase, catalytic subunit
FAM69A	Family with sequence similarity 69, member A	GCNT1	glucosaminyl (N-acetyl) transferase 1, core 2 (beta-1,6-N-acetylglucosaminyl transferase)
FANCC	Fanconi anemia, complementation group C		
FARP1	FERM, RhoGEF (ARHGEF) and pleckstrin domain protein 1 (chondrocyte-derived)	GDAP2	ganglioside induced differentiation associated protein 2
FBXL2	F-box and leucine-rich repeat protein 2	GLB1L	galactosidase, beta 1-like
FBXL5	F-box and leucine-rich repeat protein 5	GLMN	glomulin, FKBP associated protein
		GLO1	glyoxalase I
FEZ2	fasciculation and elongation protein zeta 2 (zygin II)	GMFB	glia maturation factor, beta
		GNA11	guanine nucleotide binding protein (G protein), alpha 11 (Gq class)
FKBP14	FK506 binding protein 14, 22 kDa		
FLJ1118 4	hypothetical protein FLJ11184	GNL1	guanine nucleotide binding protein-like 1
FNBP3	formin binding protein 3		
FOXK2	forkhead box K2	GOLGA1	golgi autoantigen, golgin subfamily a, 1
FRAT1	frequently rearranged in advanced T-cell lymphomas	GRB2	growth factor receptor-bound protein 2
FZD6	frizzled homolog 6 (Drosophila)	GTF2F2	general transcription factor IIF, polypeptide 2, 30kDa
G6PC3	glucose 6 phosphatase,		

114

GTF2H1	general transcription factor IIH, polypeptide 1, 62kDa
GTF3C4	general transcription factor IIIC, polypeptide 4, 90kDa
H2AFY	H2A histone family, member Y
H3F3A	H3 histone, family 3A
HADHB	hydroxyacyl-Coenzyme A dehydrogenase/3-ketoacyl-Coenzyme A thiolase/enoyl-Coenzyme A hydratase (trifunctional protein), beta subunit
HERC4	hect domain and RLD 4
HFE	hemochromatosis
HIP2	huntingtin interacting protein 2
HIST2H2BE	histone 2, H2be
HLA-DPA1	major histocompatibility complex, class II, DP alpha 1
HMGA1	high mobility group AT-hook 1
HMGN4	high mobility group nucleosomal binding domain 4
HNRPDL	heterogeneous nuclear ribonucleoprotein D-like
HTATSF1	HIV TAT specific factor 1
HUS1	HUS1 checkpoint homolog (S. pombe)
HYPK	Huntingtin interacting protein K
IDH3A	isocitrate dehydrogenase 3 (NAD+) alpha

IDS	iduronate 2-sulfatase (Hunter syndrome)
IFIT3	interferon-induced protein with tetratricopeptide repeats 3
IFNAR1	interferon (alpha, beta and omega) receptor 1
IGFBP3	insulin-like growth factor binding protein 3
IL27RA	interleukin 27 receptor, alpha
IMPDH2	IMP (inosine monophosphate) dehydrogenase 2
IQCB1	IQ motif containing B1
IRAK4	interleukin-1 receptor-associated kinase 4
ITCH	itchy homolog E3 ubiquitin protein ligase (mouse)
ITM2B	integral membrane protein 2B
ITPK1	inositol 1,3,4-triphosphate 5/6 kinase
JMJD4	jumonji domain containing 4
KATNB1	katanin p80 (WD repeat containing) subunit B 1
KCNS3	potassium voltage-gated channel, delayed-rectifier, subfamily S, member 3
KCTD2	potassium channel tetramerisation domain containing 2
KIAA0494	KIAA0494
KIAA0495	KIAA0495
KIAA0652	KIAA0652
KIAA0892	KIAA0892
KIAA0974	KIAA0974 mRNA
KIAA112	KIAA1128

115

8			binding domain protein 4
KIAA2010	KIAA2010	MCM4	MCM4 minichromosome maintenance deficient 4 (S. cerevisiae)
KLHL12	kelch-like 12 (Drosophila)		
KRIT1	KRIT1, ankyrin repeat containing	MDH2	malate dehydrogenase 2, NAD (mitochondrial)
LAP3	leucine aminopeptidase 3		
LBH	limb bud and heart development homolog (mouse)	MELK	maternal embryonic leucine zipper kinase
LDLRAP1	low density lipoprotein receptor adaptor protein 1	MGAT2	mannosyl (alpha-1,6-)-glycoprotein beta-1,2-N-acetylglucosaminyl transferase
LEPR	leptin receptor		
LEPROT	leptin receptor overlapping transcript	MGC12760	hypothetical protein MGC12760
LEPROTL1	leptin receptor overlapping transcript-like 1	MGC3262	hypothetical protein MGC3262
LIF	leukemia inhibitory factor (cholinergic differentiation factor)	MIPEP	mitochondrial intermediate peptidase
		MKRN1	makorin, ring finger protein, 1
LMF2	lipase maturation factor 2	MMP24	matrix metalloproteinase 24 (membrane-inserted)
LOC127406	similar to laminin receptor 1 (ribosomal protein SA)		
		MNS1	meiosis-specific nuclear structural 1
LOC145387	LOC145387	MON1B	MON1 homolog B (yeast)
LOC63920	transposon-derived Buster3 transposase-like	MOSPD1	motile sperm domain containing 1
LOC92249	hypothetical protein LOC92249	MRP63	mitochondrial ribosomal protein 63
LPXN	leupaxin		
M6PR	mannose-6-phosphate receptor (cation dependent)	MSRB2	methionine sulfoxide reductase B2
		MSTO1	misato homolog 1 (Drosophila)
MAEA	macrophage erythroblast attacher	MTCH1	mitochondrial carrier homolog 1 (C. elegans)
MAP2K3	mitogen-activated protein kinase kinase 3	MTHFD2	methylenetetrahydrofolate dehydrogenase (NADP+ dependent) 2,
MAP3K7	mitogen-activated protein kinase kinase kinase 7		
MBD4	methyl-CpG		

116

	methenyltetrahydro folate cyclohydrolase
MTUS1	mitochondrial tumor suppressor 1
MUM1	melanoma associated antigen (mutated) 1
MXD4	MAX dimerization protein 4
NDRG3	NDRG family member 3
NET1	neuroepithelial cell transforming gene 1
NFIC	nuclear factor I/C (CCAAT-binding transcription factor)
NFIL3	nuclear factor, interleukin 3 regulated
NFKBIA	nuclear factor of kappa light polypeptide gene enhancer in B-cells inhibitor, alpha
NFYA	nuclear transcription factor Y, alpha
NR2C1	nuclear receptor subfamily 2, group C, member 1
NR2C2	nuclear receptor subfamily 2, group C, member 2
NR2F6	nuclear receptor subfamily 2, group F, member 6
NRF1	nuclear respiratory factor 1
NUDT13	nudix (nucleoside diphosphate linked moiety X)-type motif 13
OSR2	odd-skipped related 2 (Drosophila)
PACS2	phosphofurin acidic cluster sorting protein 2

PAICS	phosphoribosylami noimidazole carboxylase, phosphoribosylami noimidazole succinocarboxamid e synthetase
PAK4	p21(CDKN1A)-activated kinase 4
PAM	peptidylglycine alpha-amidating monooxygenase
PARP16	poly (ADP-ribose) polymerase family, member 16
PARVA	parvin, alpha
PBLD	phenazine biosynthesis-like protein domain containing
PDCD4	programmed cell death 4 (neoplastic transformation inhibitor)
PDE8A	phosphodiesterase 8A
PDGFA	platelet-derived growth factor alpha polypeptide
PDLIM5	PDZ and LIM domain 5
PHLDA1	pleckstrin homology-like domain, family A, member 1
PIGO	phosphatidylinosit ol glycan, class O
PIP5K2A	phosphatidylinosit ol-4-phosphate 5-kinase, type II, alpha
PIP5K2B	phosphatidylinosit ol-4-phosphate 5-kinase, type II, beta
PKP3	plakophilin 3
PLA2G6	phospholipase A2, group VI (cytosolic, calcium-independent)
PLK4	polo-like kinase 4 (Drosophila)
POLR2D	polymerase (RNA) II (DNA directed)

117

	polypeptide D		PTEN	phosphatase and tensin homolog (mutated in multiple advanced cancers 1)
PPCS	phosphopantothenoylcysteine synthetase		PTENP1	phosphatase and tensin homolog (mutated in multiple advanced cancers 1), pseudogene 1
PPIC	peptidylprolyl isomerase C (cyclophilin C)			
PPM1G	protein phosphatase 1G (formerly 2C), magnesium-dependent, gamma isoform		PTN	pleiotrophin (heparin binding growth factor 8, neurite growth-promoting factor 1)
PPP2CB	protein phosphatase 2 (formerly 2A), catalytic subunit, beta isoform		PTTG1IP	pituitary tumor-transforming 1 interacting protein
PRDM2	PR domain containing 2, with ZNF domain		PUS3	pseudouridylate synthase 3
PRDX3	peroxiredoxin 3		PYGO1	pygopus homolog 1 (Drosophila)
PREI3	preimplantation protein 3		RAB11A	RAB11A, member RAS oncogene family
PRKACB	protein kinase, cAMP-dependent, catalytic, beta		RAB27B	RAB27B, member RAS oncogene family
PRPS1	phosphoribosyl pyrophosphate synthetase 1		RAB8A	RAB8A, member RAS oncogene family
PRR14	proline rich 14		RABIF	RAB interacting factor
PRSS3	protease, serine, 3 (mesotrypsin)		RAD51L3	RAD51-like 3 (S. cerevisiae)
PSMC3	proteasome (prosome, macropain) 26S subunit, ATPase, 3		RAP1GDS1	RAP1, GTP-GDP dissociation stimulator 1
PSMC3IP	PSMC3 interacting protein		RBMS3	RNA binding motif, single stranded interacting protein
PSMD14	proteasome (prosome, macropain) 26S subunit, non-ATPase, 14		RCC1	regulator of chromosome condensation 1
PSPC1	paraspeckle component 1		REXO2	REX2, RNA exonuclease 2 homolog (S. cerevisiae)
PSTPIP2	proline-serine-threonine phosphatase interacting protein 2		RGL2	ral guanine nucleotide dissociation stimulator-like 2
PTDSS1	phosphatidylserine synthase 1		RGS10	regulator of G-protein signalling

	10		RPS28	ribosomal protein S28
RINT1	RAD50 interactor 1		RPS6	ribosomal protein S6
RIOK3	RIO kinase 3 (yeast)		RTF1	Rtf1, Paf1/RNA polymerase II complex component, homolog (S. cerevisiae)
RIPK1	receptor (TNFRSF)-interacting serine-threonine kinase 1			
RNF11	ring finger protein 11		SAP18	sin3-associated polypeptide, 18kDa
RNF13	ring finger protein 13		SC4MOL	sterol-C4-methyl oxidase-like
RNF139	ring finger protein 139		SCAMP1	secretory carrier membrane protein 1
RNF216	ring finger protein 216		SCAMP5	secretory carrier membrane protein 5
RNF24	ring finger protein 24		SCML1	sex comb on midleg-like 1 (Drosophila)
RNF4	ring finger protein 4			
RNF44	ring finger protein 44		SCRN3	secernin 3
RP4-692D3.1	hypothetical protein LOC728621		SCYE1	small inducible cytokine subfamily E, member 1 (endothelial monocyte-activating)
RPL12	ribosomal protein L12			
RPL13A	ribosomal protein L13a		SCYL3	SCY1-like 3 (S. cerevisiae)
RPL15	ribosomal protein L15		SDC2	syndecan 2 (heparan sulfate proteoglycan 1, cell surface-associated, fibroglycan)
RPL18A	ribosomal protein L18a			
RPL21	ribosomal protein L21			
RPL22	ribosomal protein L22			
RPL28	ribosomal protein L28		SDC4	syndecan 4 (amphiglycan, ryudocan)
RPL31	ribosomal protein L31			
RPL38	ribosomal protein L38		SDFR1	stromal cell derived factor receptor 1
RPL5	ribosomal protein L5			
RPN1	ribophorin I		SEC11L1	SEC11-like 1 (S. cerevisiae)
RPS12	ribosomal protein S12		SEMA4F	sema domain, immunoglobulin domain (Ig), transmembrane domain (TM) and short cytoplasmic domain, (semaphorin) 4F
RPS19	ribosomal protein S19			
RPS21	ribosomal protein S21			
RPS27A	ribosomal protein S27a			

119

SEPT11	septin 11		SPATA2 L	spermatogenesis associated 2-like
SERINC 3	serine incorporator 3		SRR	serine racemase
SF3A1	splicing factor 3a, subunit 1, 120kDa		SSRP1	structure specific recognition protein 1
SFN	stratifin		ST13	suppression of tumorigenicity 13 (colon carcinoma) (Hsp70 interacting protein)
SFRS14	splicing factor, arginine/serine-rich 14			
SFXN3	sideroflexin 3		STC1	stanniocalcin 1
SHOX2	short stature homeobox 2		STCH	stress 70 protein chaperone, microsome-associated, 60kDa
SIRT5	sirtuin (silent mating type information regulation 2 homolog) 5 (S. cerevisiae)		STK24	serine/threonine kinase 24 (STE20 homolog, yeast)
			STOML1	stomatin (EPB72)-like 1
SIX1	sine oculis homeobox homolog 1 (Drosophila)		STX12	syntaxin 12
			STX6	syntaxin 6
			STX7	syntaxin 7
SKP1A	S-phase kinase-associated protein 1A (p19A)		STYK1	serine/threonine/tyr osine kinase 1
			SVIL	supervillin
SLC25A 37	solute carrier family 25, member 37		SYBL1	synaptobrevin-like 1
SLC26A 4	solute carrier family 26, member 4		TACSTD 2	tumor-associated calcium signal transducer 2
SLC35E1	solute carrier family 35, member E1		TAF1A	TATA box binding protein (TBP)-associated factor, RNA polymerase I, A, 48kDa
SMAD5	SMAD, mothers against DPP homolog 5 (Drosophila)			
SMARC D3	SWI/SNF related, matrix associated, actin dependent regulator of chromatin, subfamily d, member 3		TBXA2R	thromboxane A2 receptor
			TDP1	tyrosyl-DNA phosphodiesterase 1
			TERF1	telomeric repeat binding factor (NIMA-interacting) 1
SMS	spermine synthase			
SNN	stannin		TES	testis derived transcript (3 LIM domains)
SOD2	superoxide dismutase 2, mitochondrial			
			TEX261	testis expressed sequence 261
SP110	SP110 nuclear body protein		TGFBR2	transforming growth factor, beta receptor II
SP2	Sp2 transcription factor			

120

	(70/80kDa)
TGIF2	TGFB-induced factor 2 (TALE family homeobox)
THAP1	THAP domain containing, apoptosis associated protein 1
TIMM44	translocase of inner mitochondrial membrane 44 homolog (yeast)
TIMP3	TIMP metallopeptidase inhibitor 3 (Sorsby fundus dystrophy, pseudoinflammatory)
TM7SF1	transmembrane 7 superfamily member 1 (upregulated in kidney)
TMEFF1	transmembrane protein with EGF-like and two follistatin-like domains 1
TNFRSF1A	tumor necrosis factor receptor superfamily, member 1A
TOB1	transducer of ERBB2, 1
TOM1L1	target of myb1-like 1 (chicken)
TPI1	triosephosphate isomerase 1
TPK1	thiamin pyrophosphokinase 1
TPM1	tropomyosin 1 (alpha)
TTC4	tetratricopeptide repeat domain 4
TULP3	tubby like protein 3
TWISTNB	TWIST neighbor
TXK	TXK tyrosine kinase
TXNDC	thioredoxin domain containing

UBE2NL	ubiquitin-conjugating enzyme E2N-like
UFM1	ubiquitin-fold modifier 1
UIMC1	ubiquitin interaction motif containing 1
UQCRB	ubiquinol-cytochrome c reductase binding protein
VAMP3	vesicle-associated membrane protein 3 (cellubrevin)
VAPA	VAMP (vesicle-associated membrane protein)-associated protein A, 33kDa
VPS24	vacuolar protein sorting 24 (yeast)
WDR46	WD repeat domain 46
WDR48	WD repeat domain 48
XPO6	exportin 6
XPO7	exportin 7
YRDC	yrdC domain containing (E.coli)
YWHAZ	tyrosine 3-monooxygenase/tryptophan 5-monooxygenase activation protein, zeta polypeptide
ZBED1	zinc finger, BED-type containing 1
ZCCHC10	zinc finger, CCHC domain containing 10
ZCCHC4	zinc finger, CCHC domain containing 4
ZFAND1	zinc finger, AN1-type domain 1
ZFP37	zinc finger protein 37 homolog (mouse)
ZNF177	zinc finger protein 177
ZNF227	zinc finger protein 227
ZNF230	zinc finger protein 230

ZNF306	zinc finger protein 306	ZNF675	zinc finger protein 675
ZNF330	zinc finger protein 330	ZWINT	ZW10 interactor
ZNF505	zinc finger protein 505	ZXDC	ZXD family zinc finger C
ZNF557	zinc finger protein 557		